



marine technology SOCIETY

Journal

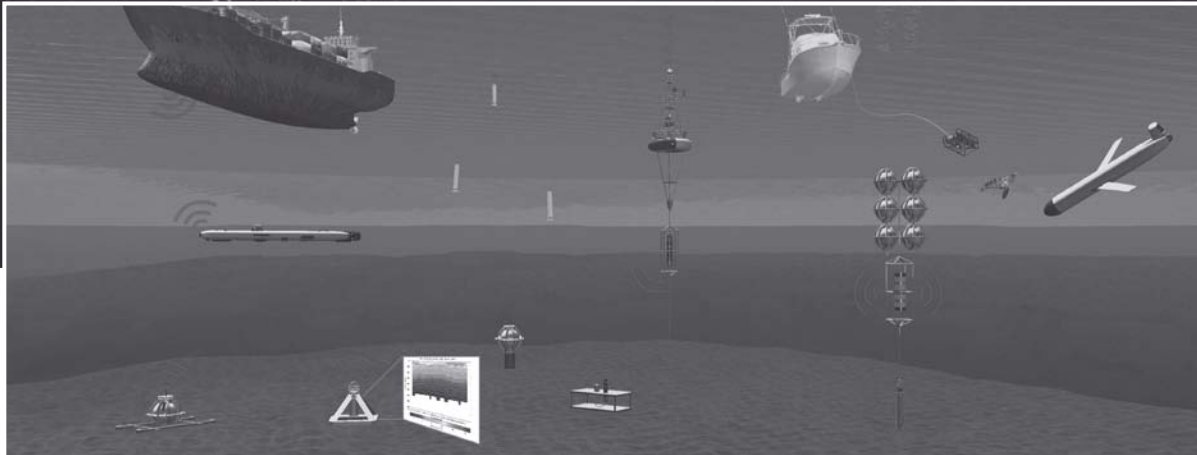
The International, Interdisciplinary Society Devoted to Ocean and Marine Engineering, Science, and Policy

Volume 47 Number 6 November/December 2013

**Diving Technologies
and Techniques for
the 21st Century**



High Performance, Low Logistics ... Unmanned Vehicles and Subsea Infrastructure



Leveraging our combined expertise to meet your challenges in ocean research, monitoring, and fisheries

- Habitat mapping
- Marine life monitoring
- Undersea positioning
- Meteorology and oceanography (METOC)
- Ocean observing systems
- Deepsea instrument housings



TELEDYNE MARINE SYSTEMS
Everywhere you look™

www.teledynemarinesystems.com

UPCOMING EVENTS

February 11-13..... **UI** Booth 722
March 3-6 **Buoy Workshop**
March 11-13..... **OI** Booth D100
April 14-17..... **Nat'l Hurricane Conf.** Booth 101
May 5-8 **OTC** Booth 1333
May 12-15 **AUVSI**



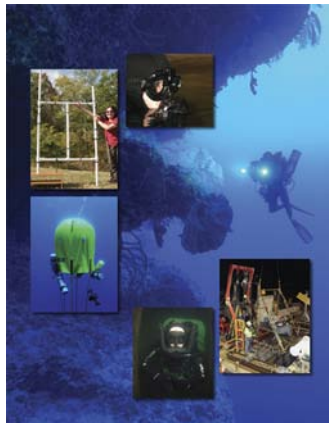
marine technology SOCIETY Journal

Volume 47, Number 6, November/December 2013

Diving Technologies and Techniques for the 21st Century Guest Editor: Michael Lombardi

Front Cover: J.F. White Contracting Company diver test pilots the Exosuit Atmospheric Diving System (photo by M. Lombardi).

Back Cover: Background image—Scientific diver Jeff Godfrey (UConn) explores the vertical Mesophotic coral ecosystem using a mixed-gas rebreather (photo by M. Lombardi, courtesy of National Geographic Society/Waite Grants Program). Thumbnail images, clockwise from top left: PVC structure for mounting camera for benthic surveys (photo by Barrett Brooks); HUD system from Sieber et al. paper, this issue; Figure 4 from Clark paper, this issue; Rebreather prototype from Sieber et al. paper, this issue; Portable inflatable habitat deployed to augment lengthy decompression (photo by M. Lombardi, courtesy National Geographic Society/Waite Grants Program).



Text: SPI
Cover and Graphics:
Michele A. Danoff, Graphics By Design

The Marine Technology Society Journal (ISSN 0025-3324) is published by the Marine Technology Society, Inc., 1100 H Street NW, Suite LL-100 Washington, DC 20005

Subscription Prices (all prices include shipping): MTS members can purchase the printed *Journal* for \$32 domestic and \$110 international. Non-members and library subscriptions are \$435 **online only** (includes 13 years of archives); \$460 for **online with print** (includes 13 years of archives); \$135 **print only** within the U.S. and Canada, \$200 **print only** international. Single-issue (hardcopy) is \$20 plus \$7.50 S&H (domestic), \$24.50 S&H (international); Pay-per-view (worldwide): \$15/article. Postage for periodicals is paid at Washington, DC and additional mailing offices.

POSTMASTER:
Please send address changes to:

Marine Technology Society Journal
1100 H Street NW, Suite LL-100
Washington, DC 20005
Tel: (202) 717-8705; Fax: (202) 347-4305

Copyright © 2013 Marine Technology Society, Inc.

In This Issue

5
Guest Editor's Introduction
Michael Lombardi

7
Long-Term Methods for High-Definition Image Maps of Benthic Surveys
Laurie Penland, Barrett Brooks, Edgardo Ochoa

16
A Diver's Automatic Buoyancy Control Device and Its Prototype Development
Darko Valenko, Zdenko Mezgec, Martin Pec, Marjan Golob

27
Compact Recreational Rebreather with Innovative Gas Sensing Concept and Low Work of Breathing Loop Design
Arne Sieber, Andreas Schuster, Sebastian Reif, Michael Kessler, Thomas Lucyshyn, Peter Buzzacott, Peter Enoksson

42
Head-Up Display System for Closed-Circuit Rebreathers With Antimagnetic Wireless Data Transmission
Arne Sieber, Andreas Schuster, Sebastian Reif, Dennis Madden, Peter Enoksson

52
An Experimental Deployment of a Portable Inflatable Habitat in Open Water to Augment Lengthy In-Water Decompression by Scientific Divers
Michael Lombardi, Winslow Bursleson, Jeff Godfrey, Richard Fryburg

64
Manufacturing Imperfection Sensitivity Analysis of Spherical Pressure Hull for Manned Submersible
Bhaskaran Pranes, Dharmaraj Sathianarayanan, Sethuraman Ramesh, Gidugu Ananda Ramadass

73
A New Generation of ADS Capabilities
James F. Clark

80
Take Me Back Down: The Best "Over the Counter" Remedy for DCIs
Joseph Dituri

83
Book Review

Index to Volume 47

84
Author Index

86
Subject Index

93
2013 Reviewers for MTS Journal

Marine Technology Society Officers

BOARD OF DIRECTORS

President

Drew Michael
ROV Technologies, Inc.

President-elect

Richard W. Spinrad
Oregon State University

Immediate Past President

Jerry Boatman
QinetiQ North America – Technology Solutions Group

VP—Section Affairs

Lisa Medeiros
Geospace Offshore Cables

VP—Education and Research

Jill Zande
MATE Center

VP—Industry and Technology

Raymond Toll
Computer Sciences Corporation

VP—Publications

Donna Kocak
HARRIS Corporation

Treasurer and VP—Budget and Finance

Debra Kill
International Submarine Engineering

VP—Government and Public Affairs

Justin Manley
Teledyne Benthos

SECTIONS

Canadian Maritime

Vacant

Great Lakes

TBD

Gulf Coast

Laurie Jugan
Consultant

Hampton Roads

Raymond Toll
Old Dominion University

Hawaii

Stu Burley
Strategic Theories Unlimited

Houston

Brian Bearden
Zephyr Salvo

Japan

Prof. Toshitsugu Sakou
Tokai University

Mid-Gulf Coast-Florida

Erica Moulton
MATE

Monterey

Jill Zande
MATE Center

New England

Chris Jakubiak
UMASS Dartmouth-SMAST

Norway

TBD

Newfoundland and Labrador

Gary Dinn
Memorial University

Oregon

Jeremy Childress
Oregon State University
College of Oceanic & Atmospheric Sciences

Puget Sound

Fritz Stahr
University of Washington

San Diego

Brian Smallwood
Teledyne Impulse

South Korea

Dr. Byung-Gul Lee
Jeju Sea Grant Center

Washington, D.C.

Capt. Dennis “Mike” Egan, P.E.
EESS LLC

PROFESSIONAL COMMITTEES

Industry and Technology

Buoy Technology
Dr. Walter Paul
Woods Hole Oceanographic Institution

Cables and Connectors

Jennifer Snyder
Leidos

Deepwater Field Development Technology

Dr. Benton Baugh
Radoil, Inc.

Diving

Michael Lombardi
Ocean Opportunity

Michael Max

Hydrate Energy International LLC

Dynamic Positioning

Howard Shatto
Shatto Engineering

Manned Underwater Vehicles

William Kohnen
HYDROSPACE Group

Moorings

Jack Rowley
Leidos

Oceanographic Instrumentation

Dr. Carol Janzen
Sea-Bird Electronics, Inc.

Offshore Structures

Dr. Peter W. Marshall
MHP Systems Engineering

Remotely Operated Vehicles

Chuck Richards
C.A. Richards and Associates, Inc.

Ropes and Tension Members

Evan Zimmerman
Delmar Systems, Inc.

Seafloor Engineering

Craig Etka
Scorpio Ventures, LLC

Underwater Imaging

Dr. Fraser Dalgleish
Harbor Branch Oceanographic Institute

Unmanned Maritime Vehicles

Rafael Mandujano
Vehicle Control Technologies, Inc.

Education and Research

Marine Archaeology

Dan Warren
C & C Technologies

Marine Education

Erica Moulton
MATE Center

Marine Geodetic Information Systems

Dave Zilkoski
NOAA

Marine Materials

Capt. Dennis “Mike” Egan
EESS, LLC

Ocean Exploration

Erika Montague
OceanGate, Inc.

Physical Oceanography/Meteorology

Dr. Richard L. Crout
Naval Research Laboratory

Remote Sensing

Ryan Vandermeulen
University of Southern Mississippi

Government and Public Affairs

Marine Law and Policy

Vacant

Marine Mineral Resources

Dr. John C. Wiltshire
University of Hawaii

Marine Security

Dallas Meggitt
Sound & Sea Technology

Ocean Economic Potential

James Marsh
University of Hawaii

Ocean Observing Systems

Donna Kocak
HARRIS Corporation

Ocean Pollution

Ryan Morton
Anadarko Petroleum

Renewable Energy

Maggie L. Merrill
Marine Marketing Services and New England
MREC at UMass Dartmouth

Kenneth Baldwin

University of New Hampshire

STUDENT SECTIONS

Alpena Community College

Counselor: TBD

Brigham Young University

Counselor: TBD

College of William & Mary

Counselor: Heather MacDonald

Dalhousie University

Counselor: Tejana Ross, Ph.D.

Duke University

Counselor: Douglas Nowacek, Ph.D.

Florida Atlantic University

Counselor: Douglas A. Briggs, Ph.D.

Florida Institute of Technology

Counselor: Stephen Wood, Ph.D., P.E.

Long Beach City College

Counselor: Scott Fraser

Marine Institute (MI)

Counselor: Kevin Strowbridge

Massachusetts Institute of Technology

Counselor: Alexandra Techet, Ph.D.

Memorial University (MUN)

Counselor: TBD

Monterey Peninsula College/Hartnell College

Counselor: Jeremy R. Hertzberg

Northeastern University

Counselor: Joseph Ayers, Ph.D.

Oregon State University

Counselor: R. Kipp Shearman

Texas A&M University—College Station

Counselor: Robert Randall, Ph.D.

Texas A&M—Corpus Christi

Counselor: Dugan Um, Ph.D.

Texas A&M University—Galveston

Counselor: David Talent, Ph.D.

United States Naval Academy

Counselor: Cmdr. David J. Robillard

University of Hawaii

Counselor: Dr. Reza Ghorbani

University of Houston

Counselors: Rares Pascali, P.E.,
Chuck Richards

University of North Carolina—Charlotte

Counselor: James Conrad, Ph.D.

University of Southern Mississippi

Counselor: Stephen Howden, Ph.D.

University of Washington

Counselor: Rick Rupan

Webb Institute

Counselor: Matthew Werner

HONORARY MEMBERS

†Robert B. Abel

†Charles H. Bussmann

John C. Calhoun, Jr.

John P. Craven

†Paul M. Fye

David S. Potter

†Athelstan Spilhaus

†E. C. Stephan

†Allyn C. Vine

†James H. Wakelin, Jr.

†deceased

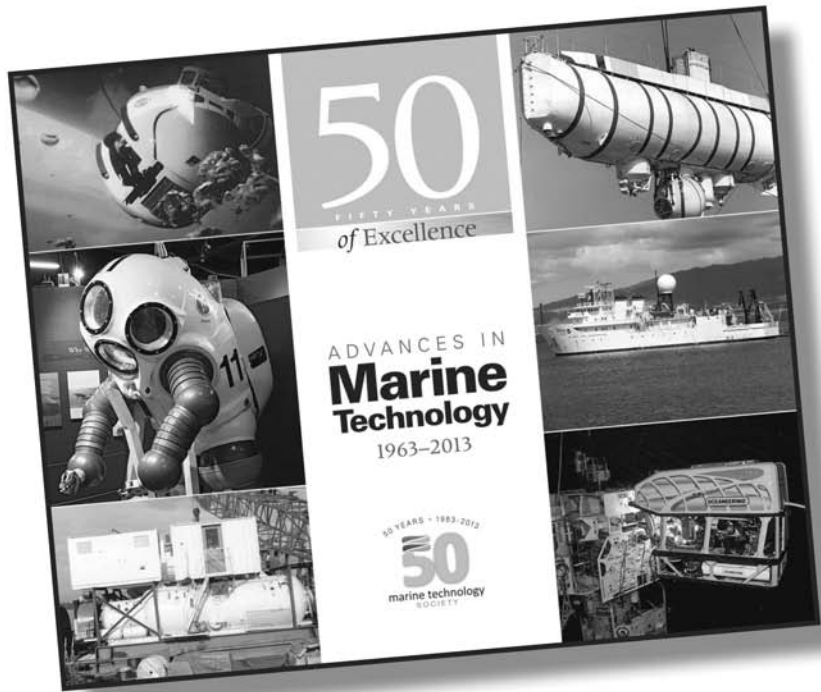
50 YEARS • 1963-2013

50

marine technology
SOCIETY

NOW
AVAILABLE!

The Marine Technology
Society is proud to offer:



50 Years of Excellence: Advances in Marine Technology, 1963—2013

This 128-page, fully illustrated book provides an overview of the advances in technology and many of the people who made these advancements possible.

50 Years of Excellence offers a look at the early days of the *Trieste* dive through James Cameron’s repeat dive in 2012, dynamic positioning, manned submersibles, ROVs and AUVs, buoys and sensor advances, communications, underwater photography, vessels, and much more.

Featured are many of the pioneers of our industry. The book concludes with a short history of the Marine Technology Society.

This limited edition publication is a must for everyone in the industry or with a desire to learn more about “how it all happened.”

Order your copy today for your own library or as a gift. **Hardbound copies are \$60 and quality paperback is \$45. (Please add \$5.00 for shipping and handling.)**

Call 202-717-8705, ext. 102 or use the coupon on right.

Please send me _____copy(ies) of *50 Years of Excellence: Advances in Marine Technology, 1963—2013*.

Name _____
Street _____
City _____
State _____ Zip _____

hardbound (\$60/ea.) quality paperback (\$45/ea)
(Please add \$5 each for shipping/handing.)

check enclosed (amount) _____

Visa MasterCard Discover American Express

Card number: _____

CVV: _____

Expiration: _____

Signature: _____

Fax to: 202-347-4302 or **mail to:** MTS Fulfillment, 1100 H Street NW, LL-100, Washington, DC 20005

Editorial Board

Ann E. Jochens, Ph.D.

Editor

Texas A&M University

Brian Bingham, Ph.D.

University of Hawaii at Manoa

Donna Kocak

HARRIS Corporation

Scott Kraus, Ph.D.

New England Aquarium

Dhugal Lindsay, Ph.D.

Japan Agency for Marine-Earth Science
& Technology

Justin Manley

Teledyne Benthos

Eugene Massion

Monterey Bay Aquarium Research Institute

Jill Zande

MATE Center

Editorial

Donna Kocak

VP of Publications

Ann E. Jochens, Ph.D.

Editor

Amy Morgante

Managing Editor

Administration

Drew Michel

President

Richard Lawson

Executive Director

Chris Barrett

Director of Professional Development
and Meetings

Jeanne Glover

Membership and Marketing Manager

Allan Gray

Financial Operations Manager

Jacob Sobin

Member Groups and Student
Outreach Manager

Suzanne Voelker

Subscription Manager

The Marine Technology Society is a not-for-profit, international professional society. Established in 1963, the Society's mission is to promote the exchange of information in ocean and marine engineering, technology, science, and policy.

Please send all correspondence to:

The Marine Technology Society
1100 H Street NW, Suite LL-100

Washington, DC 20005

(202) 717-8705 Tel.

(202) 347-4305 Fax

MTS Journal: morganteeditorial@verizon.net

Publications: publications@mtsociety.org

Membership: Jeanne.Glover@mtsociety.org

Programs: Jake.Sobin@mtsociety.org

Director: Rich.Lawson@mtsociety.org

Online: www.mtsociety.org

MEMBERSHIP INFORMATION

may be obtained by contacting the Marine Technology Society. Benefits include:

- Free subscription to the online *Marine Technology Society Journal*, with highly reduced rates for the paper version
- Free subscription to the bimonthly newsletter, *Currents*, covering events, business news, science and technology, and people in marine technology
- Member discounts on all MTS publications
- Reduced registration rates to all MTS and MTS-sponsored conferences and workshops
- Member-only access to an expansive Job Bank and Member Directory
- Reduced advertising rates in MTS publications
- National recognition through our Awards Program

Individual dues are \$75 per year. Life membership is available for a one-time fee of \$1,000. Patron, Student, Emeritus, Institutional, Business, and Corporate memberships are also available.

ADVERTISING

Advertising is accepted by the *Marine Technology Society Journal*. For more information on MTS advertising and policy, please contact Mary Beth Loutinsky, mbloutinsky@gmail.com

COPYRIGHT

Copyright © 2013 by the Marine Technology Society, Inc. Authorization to photocopy items for internal or personal use, or the internal or personal use of specific clients, is granted by the Marine Technology Society, provided that the base fee of \$1.00 per copy, plus .20 per page is paid directly to Copyright Clearance Center, 222 Rosewood Dr., Danvers, MA 01923.

For those organizations that have been granted a photocopy license by CCC, a separate system of payment has been arranged. The fee code for users of the Transactional Reporting Service is 0025-3324/89 \$1.00 + .20. Papers by U.S Government employees are declared works of the U.S. Government and are therefore in the public domain.

The Marine Technology Society cannot be held responsible for the opinions given and the statements made in any of the articles published.

ABSTRACTS

MTS Journal article abstracts, if available, can be accessed for free at <http://www.ingentaconnect.com/content/mts/mts.j>.

Print and electronic abstracts of *MTS Journal* articles are also available through *GeoRef* <<http://www.agiweb.org/georef/>>, *Aquatic Sciences and Fisheries Abstracts*, published by Cambridge Scientific Abstracts <<http://www.csa.com/factsheets/aquclust-set-c.php>>, and *Geobase's Oceanbase* published by Elsevier Science.

CONTRIBUTORS

Contributors can obtain an information and style sheet by contacting the managing editor. Submissions that are relevant to the concerns of the Society are welcome. All papers are subjected to a stringent review procedure directed by the editor and the editorial board. The *Journal* focuses on technical material that may not otherwise be available, and thus technical papers and notes that have not been published previously are given priority. General commentaries are also accepted and are subject to review and approval by the editorial board.

Diving Technologies and Techniques for the 21st Century

Michael Lombardi

J. F. White Contracting Company
American Museum of Natural History
MTS Diving Committee Co-Chair

The art and science of placing people underwater to live, work, and play has been at work for centuries. Those of us entrenched in the trade are humbled at that moment when our [humans'] role here on the Blue Planet becomes distinctly evident—to take strides towards an improved interaction with and within the ocean. It's a hard thing, to bear the cold, the darkness; but to see the light in that there is so much work to be done, keeps us evolving. Each of us that ventures beneath the waves with a mission in mind finds solace in knowing that we are one among a common brotherhood.

We are divers.

The 20th century in particular gave rise to unprecedented accessibility. The advent of SCUBA afforded any person with an inquisitive mind the opportunity to visit the underwater world. This sole pursuit of setting foot in *oceana incognita*—an unknown ocean—has since opened countless opportunities in industry and academia, for defense strategies and for recreation and entertainment.

While short-duration diving has become a mainstream and popular activity, the pursuit of human permanence on the seafloor rose and largely fell with various “life in the sea” programs throughout the 1960s and 1970s. Numerous resulting technologies and techniques found a home in the offshore industry and in the military; however, a focused human presence for advancing the humanities—the arts, the sciences, and technology—has yet found a sustainable niche here on our Blue Planet.

Today, the start of the 21st century is marred with a crippled global economy—a flawed system not lending itself to the massive private and government investments needed to revisit a human permanence on the seafloor. This, coupled with increased pressures to acquire massive bulk data sets and mitigate human risks, has shifted industry focus to robotics and underwater vehicles. For the working diver, it is understood among our brotherhood that there will always be a task requiring the human hand, and the inherent need to explore, to satisfy our species' curiosities, and to make progress.

This curiosity has led to vastly improved technology and techniques over the past 50 years by individuals who seek to improve humans' interpersonal relationship with the ocean. This

innovation has come from all industry sectors, is affording unsurpassed access to new ocean frontiers, and is allowing humans to again consider taking bold steps in reconsidering a direction for humanity at new frontier limits. Fifty years ago, a diver left the surface and was forced to return within an hour. Today, a self-contained diver can remain submerged for 8 h or more—totally changing the paradigm for living, working, and exploring underwater.

With a world view of taking humanity to a new frontier to foster a new beginning, a literal mile-high perspective of our planet would lead us to rethink our relationship with the single most overwhelming earthly environment—the ocean. Divers, the citizens of the sea, are those getting their feet wet each and every day, taking bold strides for themselves and for all of us.

This special issue of *MTS Journal* brings just a glimpse of today’s very wet world into view—from the perspective of divers. The issue examines topics from new survey methods as a diving scientist to improvements of well-established, commodity-style technology; from radical improvements of emerging rebreather technologies to forward-looking approaches to colonize the ocean with semipermanence; and from new mathematical models for improved human vehicles to charting a new course in cross-sector exploration with the absolute latest generation diving systems. The journal concludes with a commentary that recognizes our very real human limitations and a book review that fosters new curiosity in our next generation to keep us pressing forward, as this Blue Planet, *our* Blue Planet, depends on our continued evolution and improved symbiosis to continue to turn, arrive at a sustainable future, and chart a course for “a new life in the sea.”

I welcome you to dive in, lurk around, and enjoy.

Long-Term Methods for High-Definition Image Maps of Benthic Surveys

AUTHORS

Laurie Penland
Scientific Diving Program,
Smithsonian Institution,
Washington, DC

Barrett Brooks
National Museum of Natural
History, Smithsonian Institution,
Washington, DC

Edgardo Ochoa
Smithsonian Tropical Research
Institute, Smithsonian Institution,
Panama City, Panama

Introduction

Studies at varying measurements of both time and space are necessary to understand the dynamic mechanisms that influence coral reefs (Connell et al., 1997). However, there are inherent difficulties in maintaining long-term research in marine environments. Access time is limited in marine field-work with both scuba and free diving constraints. Fatigue, cold, dehydration, weather, water conditions, and tides—all may limit survey time. If scuba diving is required, gas supply, depth, and allowable bottom time may become limiting factors as well (Jones et al., 1971; Ohlhorst et al., 1988).

Photography and videography monitoring techniques increase data capture time (Lirman et al., 2007) and allow scientists to gather more field information in the same time necessary to perform a reliable estimate. Often these methods require considerably higher analysis time and technical

ABSTRACT

Coral reef health assessment has relied on benthic photographic surveys as an essential measurement tool for decades. The emergence of gigapixel image (1 billion pixels) stitching technologies makes possible the creation of high-definition benthic image map surveys (HDBIMS). These image maps provide the traditional overall percentage coverage data. In addition, they allow zoom capabilities in such detail that scientists can, for example, count the polyps on a coral head. While the image maps are easily viewed over the Internet, they are challenging to produce. Numerous previous studies have contributed to the advancement of high-definition benthic survey methods. This ongoing HDBIMS study is focused on production methods that (1) produce the best image quality for the lowest cost, (2) provide accurate and repeatable results at any depth over time, and (3) utilize off-the-shelf (OTS) stitching software that allows accurate results that can be reviewed in the field. This structured approach to image acquisition, integrated with the OTS grid-oriented stitching software, produces highly accurate benthic image maps.

Keywords: benthic survey, image maps, photo mosaic, coral monitoring, high definition

or computer expertise and equipment in the field and laboratory (Weinberg, 1981; Uychiaoco et al., 1992). Even so, photography and videography data are so valuable that these mediums have been used for decades as a nondestructive sampling method that can create a permanent record for long-term analysis (Littler and Littler, 1985; Rodgers et al., 1994; Aronson and Swanson, 1997; Roelfsema et al., 2006).

The earliest scientific publications referencing underwater image stitching for documentation of benthic research sites date back to Dr. Dimitri Rebikoff's work on Mediterranean shipwrecks (Rebikoff, 1952). Over a decade later, Dr. Mendel Peterson described a system for documenting shipwrecks using piano wire and a large camera stand (Peterson, 1965).

By June of 1966, Rebikoff presented further findings of this technique (Rebikoff, 1966), specifically referring to "The Scanning Principle," where he described rules to follow; particularly pertinent to this study is his first rule, "First, it is not acceptable to snap thousands of uncontrolled photos along random curved tracks, the result of using manned or unmanned underwater vehicles or swimmers which have no dynamic stability and travel along random sinusoids." Other publications described methods of underwater archaeological excavations that include techniques for creating photomosaics of sites as seen before and after excavation (Bass, 1967). Clearly, these documentation methods were being utilized in both archaeological and biological studies around the globe by the 1970s (Rebikoff, 1972).

Until the advent of the digital revolution, photo acquisition was accomplished using underwater film cameras. Photomosaics were constructed by hand, combining the resulting hard prints through cut-and-paste methods. With the invention of electronic imagery, digital manipulation of images became possible. Adobe Photoshop provided new ways to view and combine images. Even so, the basic concept of cut and paste had not changed (Martin & Martin, 2002).

With the emergence of image stitching technologies, when applied to familiar underwater photomosaic techniques, it is now possible to create high-definition benthic image map surveys (HDBIMS). HDBIMS are an emerging high-resolution photographic underwater documentation technique that will broaden access, enrich data collection, and enhance outreach for benthic research. These image map surveys provide traditional overall percentage coverage data while simultaneously allowing highly detailed zoom capabilities. Once combined with panorama viewing technologies, such as Google Maps, Zoomify, and GigaMacro, these extremely high-resolution images become easily viewed throughout the world.

Contemporary studies have supported the effectiveness of data extraction from HDBIMS (aka photo/video mosaics) for use in a variety of research. Deep water surveys using underwater vehicles (Woods Hole Oceanographic Institution, 2012; Ludvigsen et al., 2007) for underwater mapping is highly successful for scientific surveys of marine structures as well as archaeology research. These images are scientifically useful as well as visually stunning and therefore used effectively in public outreach (National Oceanic & Atmospheric Administration, 2006).

Video mosaic survey data have been compared to other methods (Jokiel et al., 2005; Lirman et al., 2007). Advances in camera technology have improved image resolution over time, incrementally improving results (Gintert et al., 2008, 2012). A variety of image capture methods have been tested such as georeferencing (Siwiec et al., 2008; Stetson et al., 2008), creating 3-D photo surface bathymetry maps (Park et al., 2011), and various image alignment methods (Elibol et al., 2011; Lirman et al., 2010). Furthermore, image map surveys are increasingly a key element in scientific studies (Ludvigsen et al., 2007; Lirman et al., 2010).

The purpose of this ongoing study is to create a standardized method for generating high-definition benthic image map surveys of permanent research sites for long-term monitoring. With the overarching concern of cost and simplicity, the concept is to provide a specific image acquisition and stitching protocol that will deliver consistent results when immersed in the inconsistent conditions of the underwater environment across the globe.

This specific study focuses on methods that produce the best image map quality with off-the-shelf (OTS) stitching software. In this paper, we describe a highly structured image acquisition method and provide the results of tested localized image stitching software options.

Materials and Methods

Photography Acquisition

Photographic acquisition and image stitching tests previously completed in this study resulted in drift issues, which hindered proper “side-lap” (overlap of side-by-side columns;

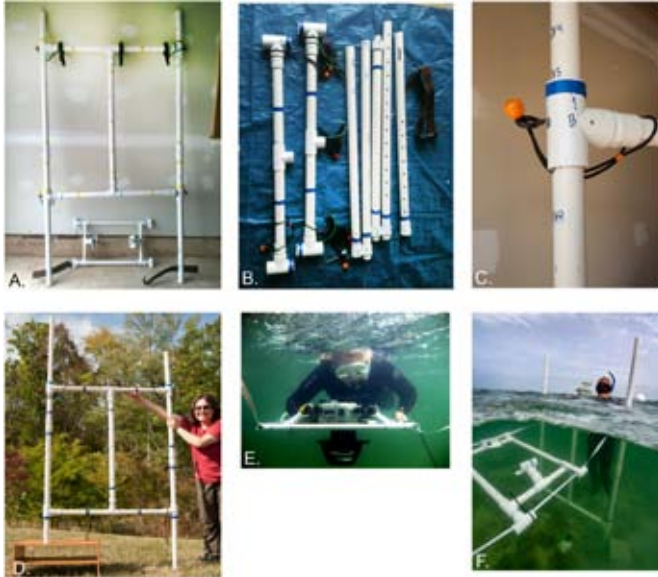
Ludvigsen et al., 2007); therefore, a more structured approach was developed and tested. Utilizing 1.25 inch PVC pipes, two 1 × 2 m structures were constructed (Figure 1A) to provide a strong and steady apparatus for maintaining a track on which to guide the camera in a consistent pattern across the site of study. The structures were designed to meet specific requirements so that they must be (1) easy to break down for travel (Figure 1B), (2) simple to reassemble on site, (3) easily adaptable on multiple terrains (Figure 1D), and (4) flexible enough to work on a variety of transect formats. Terrain flexibility was achieved through structure design by mounting the mid-bars to the vertical bars with sliders that not only allow for a variety of midbar heights but also allow the vertical bars to adjust individually to heights that will accommodate the various topography of the reef (Figures 1C and 1D). A camera mount was created with 1-inch PVC pipe to seat the camera on the track (Figures 1E and 1F).

To prepare the study site for image acquisition, four buoys attached to cinderblocks marked each corner of the 5 × 5 m site. A weighted rope was placed around the area to create an outline of the study site. Transect tapes, running east to west, were placed across the north end and south end of the site. Labeled slates were placed at the south end to mark the photographic columns of the grid, and one slate, labeled “N” for north, was placed along the north end and relocated with the movement of the camera track across the site. The PVC structures described above were held at the north and south ends of the site.

This test was photographed using a Canon 7D SLR in a Subal housing. For the final image map of this test, a focal length of approximately 22 mm

FIGURE 1

Photographs of PVC structures at construction and during in-water use. Shown here is a fully assembled 1×2 m PVC structure (A) with camera mount beneath; a PVC structure broken down for travel (B); detail of slider, pin, and numbered pin holes (C); the structure adapted to floor variance (D); the camera in mount while shooting* (E); and one PVC structure with camera mounted on the track (F). *Photograph by Barrett Brooks, Smithsonian Institution.



was used to maximize overlap with the lens distortion minimalized effectively within Adobe Bridge and Photoshop. The camera mode was set to time value with the shutter speed at 200, an aperture of f11, and ISO of 400. Image capture resolution was set for two images, RAW and jpeg small fine. Camera focus mode was set to AI servo with the center zone active. Total elapsed time for photographing one complete 5×5 m² was 62 min.

Two transect tapes were run across from the south PVC structure to the north PVC structure, which created a track for guiding the camera along a controlled grid (Figure 1F). The camera mount, attached to this track, assisted in keeping the camera level and in a down-facing position (Figure 1E). Transect tapes were used for this track as a guide to control the camera firing rate (one picture at every 10 cm) and to

obtain a minimum overlap of 75% (Gintert et al., 2012).

This system of documentation required a three-person team. One person was on the north end of the study site and one person was on the south end. Each held and moved the PVC structure along the site in half-meter increments as the photographing of each column was completed. A third person guided the camera across the track while shooting photographs. The OTS image stitching software does not make use of the double lawnmower pattern method (Lirman et al., 2007); therefore, a single lawnmower pattern was used. The location for this test was a Living Laboratory Community Assessment Monitoring Program site at the Keys Marine Lab on the bayside of Long Key, Florida, and was at a depth of approximately 1 m.

OTS Image Stitching

Precise stitching of images is essential for repeatable and accurate results capable of providing direct comparisons over time. Coral reefs are complex, three dimensional, and heterogeneous, which proves challenging for the image stitching process. Low-cost or no-cost photo-stitching software options are available. Through discussions with professionals in the photographic industry, five stitching programs were considered (Table 1). The image composite used for this test consisted of 500 images. The images were photographed in a grid of 10 columns (50 images per column), creating 50 rows. Each column consisted of a sidelap of 94%, and the images inside each of the columns overlapped by 92%. While in the field, the laptop used for this project was a Dell Precision running Windows 7 with 8-GB RAM and a 300-GB hard drive. All images were downloaded off the camera, and onto a 2-TB passport drive after each dive. The 5-mg jpeg small fine images were used for in-field stitching tests.

The image-stitching software comparison tests were run after field tests. All tests were run with the same set of RAW file images that were preadjusted in a batch using Adobe Bridge, Adobe Photoshop, and Adobe Camera Raw image converter. Using the image preset function, the same image sharpen, lens profile, and exposure correction adjustments were made to all 500 images (Table 2).

Further comparison tests were completed to determine if repeat stitching within the OTS software produced similar results. From the same image set, three separate stitching sessions were completed with the three grid-import OTS software. Viewed in Photoshop, with each stitched image on a separate layer, the three stitching

TABLE 1

Comparison of OTS stitching software considered for this study.

Developer	Software	Cost	500 Images Stitched	Grid Import	Error Count	Repeated Stitching	Limits	Benefits
Adobe	Photoshop CS6	\$20 per month	No, stitched only columns.	No	N/A	N/A	No grid import.	Minimal learning curve.
GigaPan	Stitch 2.2.0375	\$149	Yes	Yes	10	Precise repeat stitching	Not as accurate.	Easy to use. Ran on laptop. Good in-field check.
Kolor	Autopano Giga 3.0	199€	Yes	Yes GigaPan plugin	0	Minimal position variance	Large learning curve.	Most accurate. Good for final image. Did not run entire image set on laptop.
Microsoft	Image CompositeEditor 1.4.4.0	Free	Yes	Yes	7	Precise repeat stitching	Final image too small.	Easy to use. Ran on laptop. Good for in-field check.
SourceForge	Hugin 2012.0.0	Free	No, found no control points.	No	N/A	N/A	No grid import.	Easy to use.

TABLE 2

Images were batch-adjusted with Adobe Camera Raw 7.0 Image Converter.

All images were first reviewed in Adobe Bridge to assure that exposures were similar.

1. Using Bridge, we opened one RAW file image.
2. Within Camera Raw, lens profile correction was enabled.
3. Sharpening was set to 40.
4. Adjusted exposure appropriately.

We then saved these settings into a preset to apply the adjustments to the rest of the images.

5. Clicked on the pull down menu just above the slider bar on the right and selected "SAVE SETTINGS", then selected "SAVE."
6. Named this file something memorable as it became the preset.
7. Clicked "CANCEL."
8. Back in Bridge, we selected all 500 of the raw images.
9. Double-clicked to open the images.

One image was large, and the rest were viewed as thumbnails in a column on the left.

10. Clicked "SELECT ALL" in the upper left corner.
11. Back to the small pull down above the scroll on the right, we clicked "APPLY PRESET."
12. Selected the preset we just created.
13. All of the thumbnails were modified to the preset adjustments.
14. Clicked the link directly below the large image to adjust the saved file size.
15. Clicked "SAVE IMAGES" below the thumbnails and save all of the adjusted images.

test images were compared to ascertain repeat stitching capabilities. The resulting layered images were viewed at 100% with opacity reductions to allow for direct alignment and artifact comparisons.

Results

Photography Acquisition

The camera track method for documenting benthic research sites created a reliable and highly structured method of shooting, which was reflected in the results. The final images directly aligned in a 10 × 50 square grid. Providing a measured structure for image capture aided in the completion of these highly predictable results. While there will be minor changes of the PVC structures and camera track

system for the next round of tests, overall the system produced usable results.

Once broken down, the structures traveled easily through airport checked-in luggage inside a golf travel bag. On-site reassembly and use were straightforward. The system adapted well to our unexpectedly shallow study site, even though it was designed to work at deeper depths. Transect tapes worked for a measured camera firing rate, although they tended to drag in a current. Having these tapes fully tended seemed to overcome this difficulty. In the future, an incrementally marked dive line would be stronger and more precise. This most recent site was accomplished while snorkeling; no scuba was used at any time during the production of these images.

OTS Stitching Software

The images captured by the camera track easily fit into the grid import method of panorama stitching (Kolor, 2012; GigaPan Systems, 2012) or the "structured panorama" mode in Microsoft Image Composite Editor (Uyttendaele et al., 2010). This import method requires the user to enter the number of columns or rows and the percentage of overlap. Using the images selected to import the software then builds a grid, which if photographed correctly will resemble the study site, which is used as a guide for the stitching process. This predetermination of individual image location within the composite image assisted the software application's outcome by providing it with a starting point. Stitching software that did not utilize a structured method

were tested and resulted in image maps that had high occurrences of artifacts and deemed unsuccessful. This failure is possibly due to the exceedingly monotonous nature of the study site. Various applications provide useful statistics, such as the notes in GigaPan Stitch, where the actual horizontal and vertical percentage overlap of the completed composite image is provided.

Photographing in the RAW/jpeg small fine setting allowed for simultaneous capture of both resolutions. The low-resolution jpeg files provided a means for a quick in-field alignment, overlap, and exposure check on our field laptop, which is less powerful than our office desktop computers. The RAW images were useful for pre-production in a multitude of ways. Using Adobe Bridge and Photoshop, these images were adjusted for sharpness and contrast consistently as a group (Table 2), then resaved at various resolutions and formats, while retaining the RAW data of the original images.

The OTS stitching software considered in this study produced varied results. Success was determined by considering (1) ability to stitch the 500 images into a single image, (2) to maintain a high level of accuracy, and (3) ease of use.

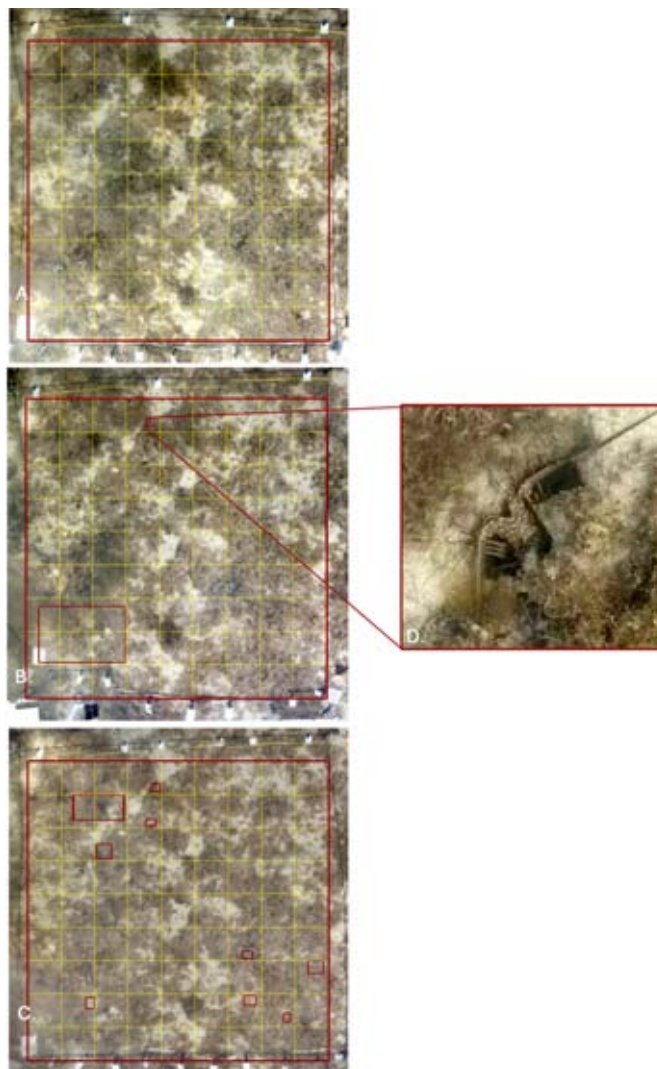
Five software applications were evaluated, Photoshop, Stitch, Autopano Giga, Image Composite Editor, and Hugin. Two of the five, Photoshop and Hugin, were unable to find enough control points, which identify overlapping features for alignment, to stitch the images into a proper square. To measure the accuracy of alignment, a quantifying method that takes into consideration the size of an artifact and integrates it into the total number of artifacts

was used. This method was calculated by searching for visible artifacts while viewing the complete composite at 100%. Each artifact was noted with a red square. A yellow grid was placed over the composite image. Each square within the yellow grid was counted as one “error” if it contained any part of a red square (Figure 2). Therefore, the larger artifacts

are weighted more than the smaller artifacts in the final “error count” (Table 1). Of the repeat stitching tests of the same images within the same software, Stitch and Image Composite Editor yielded precise repeat stitching results. Autopano Giga produced results that differed slightly in alignment and viewpoints, although overall content was the same.

FIGURE 2

Three benthic image maps of Keys Marine Lab Living Laboratory site, bayside off Long Key, Florida. Autopano Giga (A), Microsoft ICE (B), and GigaPan (C) stitched the image maps. Red shapes outline the known artifacts. Shown above (D) is a detail from the image map of a lobster with an artifact distorting the shape of the lobster hole.



Discussion

Photography Acquisition

The camera track method created a controlled photographic setting, which produced images that were easily imported into a grid format. We found this acquisition method to be manageable. Utilizing a camera track provided a thorough documentation of the site and was therefore worthwhile.

Future changes will include a shortening of the PVC structure width. It had not yet been determined that half-meter columns were necessary; therefore, the structure was constructed at a width of 1 m. After one field session using this structure it was quickly determined that the 1-m width was cumbersome in the boat and not necessary in the water. A PVC structure of a half meter could still be used to shoot columns at a width of 1 m by using the transect tapes along the perimeter to measure distance.

Due to permit issues, our study site was shallower than anticipated. The flexibility of the PVC structure proved valuable in this unexpected situation. The midbars were lowered to their lowest point (Figure 1F), which placed the guidelines close to the surface. We concluded that shallow research sites are an option with this method of image acquisition. In a water depth of 1 m, a fully stitched image map of a 5 × 5 m site was created.

OTS Stitching Software

Certain OTS stitching programs are a viable option for stitching of HDBIMS. Multiple OTS software options exist for in-field testing of image acquisition. These applications can be run on robust laptops in combination with imaging software such as Adobe Photoshop and Bridge. A lack of detail within the study site can prove challenging for OTS software. The flat,

sandy bottom of our study site was covered in algae with an occasional small sponge, which provided minimal relief. While there was adequate contrast between the algae and the sand, the algae were so similar throughout the site that the OTS software could not determine which tiles should go where without the additional help of the grid import method. The only acceptable results were produced by the stitching software that uses the grid method of image selection. Therefore, we conclude that the grid import method of OTS stitching software provides more control over mosaic results and may be necessary for some locations where highly identifiable organisms are lacking. Of the five OTS stitching software that were tested in this situation, Autopano Giga allowed for more control than the others and was consistently more accurate. However, Autopano Giga requires more computing power and would not run the entire image set on the laptop. All Autopano Giga tests were run on a Power Mac v. 10.7.5 3.33-GHz 6 core Intel processor and 20-GB ram.

Further Research

Our main intention for this study is to determine if a clearly defined and specific image acquisition and stitching protocol will return consistent and comparable results for every participating research site across the globe over time. To meet this goal, more trials are necessary. This study covered an area of 25 m², which is minimal if compared to other studies (Gintert et al., 2012); however, for the purpose of the research sites that will utilize these methods, linear and square areas of 25 m are desirable. Equally important will be the ability to document the exact location and orientation of each

site, year after year. Therefore permanent markers will become an essential part of the protocol. Potential studies may include merging bathymetric maps (Stetson et al., 2008; Park et al., 2011) with image maps to monitor structural changes in the reef. We will need answers to additional questions: What are the exact distances for photographing with the underwater track that will provide the necessary overlap while minimizing the photographic acquisition time? What are the best methods that will provide the most effective use of strobe lighting? We will then develop a best practices manual (Abdo et al., 2004) to assist in implementing these methods into reef monitoring programs. Over time, we will definitively learn the answer to our larger question: Will the consistent use of best practices across the globe under varying conditions and situations produce consistent results?

Acknowledgments

Funding of this project was provided by the Smithsonian Institution's Office of the Undersecretary for Science and the Smithsonian Scientific Diving Program. Team members include Barrett Brooks, Bill Ferrell, Amanda Feuerstein, Nancy Knowlton, Matt Leray, Edgardo Ochoa, Alex Penland, and Dane Penland. Logistical support provided by Keys Marine Lab, Smithsonian Caribbean Coral Reef Ecosystems, and NOAA Florida Keys National Marine Sanctuary. All photographs are by Laurie Penland unless otherwise noted.

Corresponding Author:

Laurie Penland
Scientific Diving Program, Smithsonian Institution, Washington DC
Email: penlandl@si.edu
Website: www.si.edu/dive

References

- Abdo, D., Burgess, S., Coleman, G., & Osborne, K.** 2004. Surveys of Benthic Reef Communities Using Underwater Video. Townsville: Australian Institute of Marine Science.
- Aronson, R., & Swanson, D.** 1997. Video Surveys of Coral Reefs: Uni- and Multivariate Applications. pp. 1441-6.
- Bass, G., Throckmorton, P., Du Plat Taylor, J., Hennessy, J., Shulman, A., & Buchholz, H.** 1967. Cape Gelidonya: A Bronze Age Shipwreck. Philadelphia: The American Philosophical Society.
- Connell, J., Hughes, T., & Wallace, C.** 1997. A 30 year study of coral abundance, recruitment, and disturbance at several scales in space and time. *Ecol Monogr.* November. 67(4):461-88.
- Elibol, A., Garcia, R., & Gracias, N.** 2011. A new global alignment approach for underwater optical mapping. *Ocean Eng.* 38:1207-19.
- GigaPan Systems.** 2012. Stitch 2.0, Stitch. Efx, and Upload [Online]. Available at: <http://gigapan.com/cms/manual/pdf/stitch-efx-upload-manual.pdf> (accessed September 11, 2013).
- Gintert, B., Gracias, N., Gleason, A., Lirman, D., Dick, M., Kramer, P., & Reid, R.** 2008. Second-Generation Landscape Mosaics of Coral Reefs. Ft. Lauderdale: National Coral Reef Institute. 577-81.
- Gintert, B., Gleason, A., Cantwell, K., Gracias, N., Gonzalez, M., & Pamela Reid, R.** 2012. Third-Generation Underwater Landscape Mosaics for Coral Reef Mapping and Monitoring. Cairns: James Cook University.
- Jokiel, P., Rodger, K., Brown, E., Kenyon, J., Aeby, G., Smith, W., & Farrell, F.** 2005. Comparison of Methods Used to Estimate Coral Cover. Honolulu: NOAA/NOS NWHI Coral Reef Ecosystem Reserve.
- Jones, N. S.** 1971. Diving. In: Holme, N. A., & McIntyre, A. D. (eds). *Methods for the study of marine benthos*. Oxford, Blackwell: Science Publications. pp. 71-9.
- Kolor,** 2012. Autopano Pro - Import... - Gigapan [Online]. Available at: http://www.autopano.net/wiki-en/action/view/Autopano_Pro_-_Import/4_-_Gigapan (accessed September 11, 2013).
- Lirman, D., Gracias, N., Gintert, B., Gleason, A., Reid, R., Negahdaripour, S., & Kramer, P.** 2007. Development and application of a video-mosaic survey. *Environ Monit Assess.* 125:59-73.
- Lirman, D., Gracias, N., Gintert, B., Gleason, A., Deangelo, G., Dick, M., Martinez, E., & Reid, R.** 2010. Damage and recovery assessment of vessel grounding injuries on coral reef habitats by use of georeferenced landscape video mosaics. *Limnol Oceanogr-Meth.* 8:88-97.
- Littler, M., & Littler, D.** 1985. *Handbook of Phycological Methods Ecological Field Methods: Macroalgae 8. Nondestructive sampling*. Washington, DC: Cambridge University Press.
- Ludvigsen, M., Sortland, B., Johnsen, G., & Singh, H.** 2007. Applications of geo-referenced underwater photo mosaics in marine biology and archaeology. *Oceanography.* 20(4):141-9.
- Martin, C.J., & Martin, E.A.** 2002. An underwater photomosaic technique using Adobe Photoshop. *Int J Naut Archaeol.* 31:137-47.
- National Oceanic & Atmospheric Administration.** 2006. National Marine Sanctuaries Photo-Mosaic Gallery [Online]. Available at: <http://sanctuaries.noaa.gov/missions/2006fknms/photomosaicgallery.html> (accessed September 24, 2013).
- Oelaorst, S. L., Liddell, W. D., Taylor, R. J., & Taylor, J. M.** 1988. Proceedings of the 6th International Coral Reef Symposium. Evaluation of Reef Census Techniques. Australia. 2:319-24.
- Park, J. Y., Choi, J. Y., & Jeong, E. Y.** 2011. Applying an underwater photography technique to nearshore benthic mapping: A Case Study in a rocky shore environment Proceedings from 11th International Coastal Symposium. *J Coastal Res.* 1764-8.
- Peterson, M.** 1965. *History Under the Sea; a Handbook for Underwater Exploration*. Washington DC: Smithsonian Institution.
- Rebikoff, D.** 1952. *Exploration sous-marine; ouvrage illustré de 21 héliogravures et de 6 photos en couleurs, reproduites d'après clichés Kodachrome et de 6 photographies en couleurs*. Paris: B. Arthaud.
- Rebikoff, D.** 1966. Mosaic and Strip Scanning Photogrammetry of Large Areas Underwater Regardless of Transparency Limitations. Santa Barbara, Proc. SPIE 0007. 7:105.
- Rebikoff, D.** 1972. Precision underwater photomosaic techniques for archaeological mapping. *Int J Naut Archaeol Underw Explor.* 1:184-6.
- Rogers, C., Garrison, G., Grober, R., Hillis, Z., & Franke, M.** 1994. *Coral Reef Monitoring Manual for the Caribbean and Western Atlantic Virgin Islands National Park*: National Park Service.
- Roelfsema, C., Phinn, S., & Joyce, K.** 2006. Proceedings of the 10th International Coral Reefs Symposium. Evaluation of Benthic Survey Techniques for Validating Remotely Sensed Images of Coral Reefs. Okinawa: Japanese Coral Reef Society. 1:10-5.
- Siwiec, T., Sheldrake, S., Hess, A., Thompson, D., Macchio, L., & Duncan, P. B.** 2008. Survey Technique for Underwater Digital Photography with Integrated GPS Location Data. San Diego: American Academy of Underwater Sciences.
- Stetson, P., Shank, B., & Lobel, P.** 2008. Proceedings of the 11th International Coral Reef Symposium. Mapping Reef Structure and Bathymetry in Belize Using Cobra-Tac. Ft. Lauderdale. 1:510-4.
- Uychiaoco, A. J., Alino, P. M., & Atrigenio, M. P.** 1992. Video and Other Monitoring Techniques for Coral Reef Communities. Singapore. 6:471.
- Uyttendaele, M., Stollnitz, E., & Good, H.** 2010. Stitching and viewing panoramas [Online]. Available at: <http://hdview.wordpress.com/2010/03/18/ice-is-now-synthy/> (accessed September 11, 2013).
- Weinberg, S.** 1981. *Bijdragen tot de Dierkunde. A Comparison of Coral Reef Survey Methods*.

Amsterdam: Society Natura Artis Magistra.
51:199-218.

Woods Hole Oceanographic Institution.

2012. WHOI Team Uses Advanced Imaging Data to Bring a New View of Titanic to the World [Online]. Available at: <http://www.whoi.edu/page.do?pid=83577&tid=3622&cid=133629&c=2> (accessed 24 September 2013).

A Diver's Automatic Buoyancy Control Device and Its Prototype Development

AUTHORS

Darko Valenko

Zdenko Mezgec

Martin Pec

Emsiso, Maribor, Slovenia

Marjan Golob

University of Maribor, Slovenia

Introduction

Buoyancy control device (BCD; Figure 1) is an accessory used by divers for buoyancy control, thus resulting in depth control. BCD is equipped with pneumatic valves for inflating and deflating. Added released air to or from the BCD increases/decreases a diver's buoyancy. Consequently, the diver will rise or sink.

The BCD's main components are jacket, activation buttons, inflate (inside the actuating button's housing), deflate, and overpressure valves.

Since the BCD was invented, several people have tried to upgrade it so that it could automatically change or maintain a diver's depth. The first automated BCD was patented in the early 1970s, filed by Brecht (1970). Research has continued, and several subsequent patents have been submitted. The more important patents are as follows: Bohmrich et al. (1978), Harrah (1982), Courtney (1988), Tolksdorf and Tolksdorf (1996), Egan (1996), Leonard (1998), Kromp (1998), Leonard and Engel (2004), Donahue (2005), Roseborough (2006), and Adams (2008).

Divers, submarines, and submarine-like vessels (hereinafter referred to

ABSTRACT

Maintaining depth is a diver's essential task, and that is why he/she uses a buoyancy vest for maintaining and changing depth [the so-called buoyancy control device (BCD)]. Changing depth is controlled by manually actuating pneumatic valves, which causes the BCD volume to expand or shrink and consequently change its buoyancy.

Divers' desires for devices that automatically change or maintain depth have been present since the first arrival of modern diving using a buoyancy vest. This need has arisen, particularly when diving, in regard to the following: where poor visibility is present; when both hands are needed for the job in amateur diving; where decompression procedures are needed; during safety stop procedures; during automatic ascending when a diver's life functions are critical; and also when using the same technology for changing depth in small modern submarines and submarine-like vessels.

The presented prototype device has been developed for automatic buoyancy control using flexible BCD. This device can limit ascending and descending velocities, allow a diving diver to request a depth at a requested velocity and hold that requested depth, ensure a diver's requested depth and velocity are controlled, minimize any depth and velocity errors in relation to disturbances from the environment, and record all captured data for dive analyses. Controlling velocity is important for proper decompression.

This paper presents a mathematical model of a diver's buoyancy, the prototype development of an automatic BCD, and simulation and actual diving results. The prototype device has been fully tested by one of the leading manufacturers of diving equipment.

Keywords: buoyancy vest, control, mathematical model, dive simulation

submarines) use the same principle of depth control when changing buoyancy. However, there is a major difference; submarines use tanks for buoyancy control, which are not compressible. Divers mostly use a BCD, which is flexible and thus compressible according to depth. Controlling a diver's depth is more complex than a submarine's. Within scientific literature, many contributions can be found within the field of developing, modeling, and controlling submarines. A few more interesting articles within

this area are as follows: Akkizidis et al. (2003), Bagheri and Moghaddam (2009), Bambang et al. (2008), Bessa et al. (2008), Lea et al. (1999), Min and Smith (1994), Petrich and Stilwell (2010, 2011), and Tangirala and Dzielski (2007). A submersible drogue was presented by Han et al. (2010). There are two major differences. The first is that the pressure source is generated by compressed CO₂ gas with constant output pressure, and the second is that it has variable volume under an elastic membrane.

FIGURE 1

Modern BCD with pneumatic valves.



The elastic membrane is stiff, and pressure builds up with volume.

Despite many patents, there are still presently no devices within the scuba diving market field that are able to automatically change or maintain a diver's depth and velocity. There have also been no contributions in scientific literature regarding the field of mathematically modeling diver's buoyancy with BCD and pneumatic valves. Very few prototype devices can be found on the Internet for divers' automatic buoyancy control. One is from author Robert J. Dyer (2001), another is called SUBA: Cruise Control for Your Dive (Pandora Underwater Equipment SA, Switzerland), and the third is Aquapilot GFT (Gesellschaft für Tauchtechnik mbH & Co., Bochum, Germany). None of these devices is on the market, and there is no contribution in the scientific literature regarding any of these devices.

Air source pressure is higher than its surrounding water pressure. Water pressure changes with depth, and absolute air source pressure also changes

with water depth. Therefore, inflate and deflate valves' volume flows also change with depth. Knowing how the inflation and deflation valves' volumes' flow and the BCD's volume changes with depth is essential for optimal diver's depth and velocity control.

Firstly, this paper describes the pneumatic valves' volume flows' dependencies and their consequences. Secondly, it presents the physical background and mathematical modeling of a diver's buoyancy, BCD's volume, and the pneumatic valves' volume flows. Next, it describes a prototype device's development using electronics, software, and mechanical design. The dive measurements and simulations are then presented, and finally, our future work on an automatic BCD is presented.

Pneumatic Valves' Volume Flows' Dependencies

Divers use an air source from a compressed air tank through a mounted first-stage pressure regulator. There is also a second-stage pressure regulator for breathing. It is used for inflating BCD air from the first-stage pressure regulator and is approximately 10 bar higher than the surrounding ambient pressure. The ambient pressure increases with depth, and vice versa. This means that the inlet absolute air pressure of the inflate valve varies according to the ambient pressure. The inflate valve's outlet air pressure equals the BCD's pressure. The BCD's pressure depends on its volume and ambient pressure. It is because of this that the inflate valve's air volume flow changes with water depth. The deflate valve's inlet air pressure equals the BCD's pressure, and its outlet pressure equals the surrounding ambient pressure. In view of this, the deflate

valve's volume flow depends on the surrounding ambient pressure and the BCD's volume. When a diver's depth is increased/decreased, the surrounding ambient pressure also increases/decreases; consequently, the air volume inside the BCD decreases/increases.

These are the main factors as to why maintaining a constant diver's depth and/or velocity is difficult. When considering that a diver's breathing constantly changes the diver's buoyancy, controlling the depth becomes even more complex. This task is additionally more difficult when there is low visibility in the water. In this case, the diver does not have any visible surrounding area, which is important for guessing the current velocity and depth.

Buoyancy control, in practice, is a skill that divers have to learn and master when diving. Most problems with buoyancy control are by occasional divers and beginners. Until a diver masters buoyancy control, he/she is consuming lots of air, which he/she also needs for breathing, and therefore, diving time is shortened. What is more important, he/she cannot perform decompression properly.

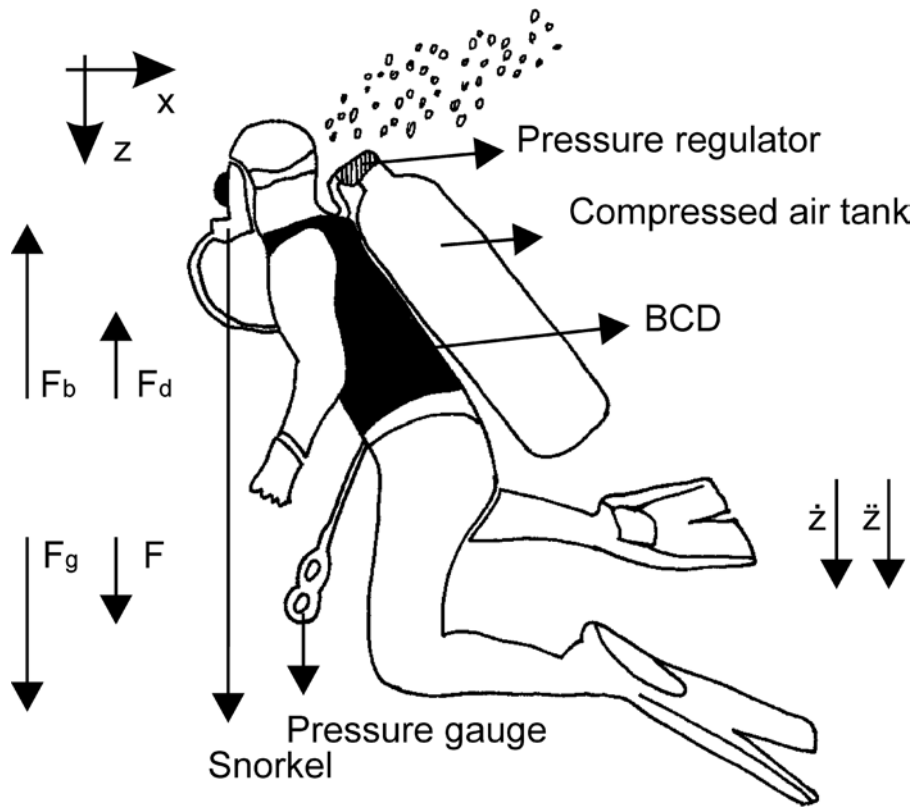
Physical Background and Mathematical Modeling

A prerequisite for successful control of the system is fundamental knowledge that can be derived from mathematical modeling. This article only presents the derived mathematical model equations of a diver's buoyancy, derived from physical laws, as shown in Figure 2.

The arrows represent the directions of the acting forces, velocity $\dot{z}(t)$ and acceleration $\ddot{z}(t)$. The mass force F_g always acts in a descending direction,

FIGURE 2

Acting forces on a submerged diver in the water.



while the buoyancy force $F_b(t)$ acts in an ascending direction. When the diver is moving at velocity $\dot{z}(t)$, then the drag force $F_d(t)$ occurs and is always pointing in the opposite direction to the diver's movement. The sum of all forces is force $F(t)$, and it is

$$F(t) = F_g - (F_b(t) + F_d(t)), \text{ sum of all forces [N]}, \quad (1)$$

Where the corresponding forces are

$$F_b(t) = \rho_w \cdot (V_{\text{BCD}}(t) + V_d) \cdot g, \text{ buoyancy force [N]}, \quad (2)$$

where ρ_w is water density, $V_{\text{BCD}}(t)$ is air volume inside of the buoyancy device, V_d is diver's volume, and g is the acceleration of gravity.

$$F_d(t) = \frac{1}{2} \cdot \rho_w \cdot (S_{\text{BCD}} + S_d) \cdot c_d \cdot |\dot{z}(t)| \cdot \dot{z}(t), \text{ drag force at a low Reynolds number [N]}, \quad (3)$$

where S_{BCD} is buoyancy device frontal aerial surface, S_d is diver's frontal aerial surface, and c_d drag coefficient.

$$F_g = m_d \cdot g, \text{ mass or gravitational force [N]}, \quad (4)$$

where m_d is diver's mass with equipment.

When the diver is stationary, acceleration $\ddot{z}(t)$ and velocity $\dot{z}(t)$ are equal to zero. In this case, the drag force $F_d(t)$ and the summing force $F(t)$ are also equal to zero. The remaining forces are the mass force F_g and the buoyancy force $F_b(t)$, which are equal by size and opposite in directions.

$$F_g = F_b(t). \quad (5)$$

As soon as the buoyancy force $F_b(t)$ is higher/lower than the mass force F_g , the diver will start to rise/sink without stopping. This means the diver's depth $z(t)$ has become unstable as a result of compressible BCD and changing water pressure $p_z(t)$ with water depth $z(t)$.

When combining equations (1) to (4), Newton's first law and the written variables for the diver provide the diver's motion.

$$m_d \cdot \ddot{z}(t) = m_d \cdot g - \rho_w \cdot g \cdot [V_{\text{BCD}}(t) + V_d] - \frac{1}{2} \cdot \rho_w \cdot c_d \cdot |\dot{z}(t)| \cdot \dot{z}(t) \cdot [S_{\text{BCD}} + S_d]. \quad (6)$$

The diver's neutral buoyancy, at all depths, can be derived from (6) under the initial conditions that velocity $\dot{z}(t)$ and acceleration $\ddot{z}(t)$ are equal to zero. The initial BCD's volume $V_{\text{BCD}}(0)$ is

$$V_{\text{BCD}}((\ddot{z}(t), \dot{z}(t)) = 0) = \frac{m_d}{\rho_w} - V_d. \quad (7)$$

A diver's mass m_d and diver's volume V_d should be appropriate so as to provide a wide range of BCD's volume $V_{\text{BCD}}(t) > 0$ for buoyancy control.

BCD's volume $V_{\text{BCD}}(t)$ is controlled using two pneumatic valves. These pneumatic valves are controlled by an electric signal u using the on/off mode and have three states: *add*, *none*, or *deduct*. According to the control signal u , the inflated/deflated volume $\psi(t)$ is

$$\psi(t) = \begin{cases} \frac{1}{T_{\text{al}}(t)} \int_{\tau=0}^t q_{\text{VI}}(\tau) \cdot d\tau & u = 1 \quad \text{add} \\ 0 & u = 0 \quad \text{none} \\ -\frac{1}{T_{\text{aD}}(t)} \int_{\tau=0}^t q_{\text{VD}}(\tau) \cdot d\tau & u = -1 \quad \text{deduct} \end{cases} \quad (8)$$

The surrounding's ambient pressure $p_z(t)$ changes from the pressure at the water's surface p_0 , up to the pressure of the water at depth $z(t)$,

$$p_z(t) = \rho_w \cdot g \cdot z(t) + p_0. \quad (9)$$

The initial pressure $p_z(0)$ is

$$p_z(0) = \rho_w \cdot g \cdot z(0) + p_0. \quad (10)$$

BCD's volume $V_{\text{BCD}}(t)$ with an inflated/deflated volume $\psi(t)$ is (Hicks, 2003; U.S. Environmental Protection Agency et al. 1989)

$$V_{\text{BCD}}(t) = T_z(t) \cdot \left[\frac{1}{T_z(0)} \frac{(\rho_w \cdot g \cdot z(0) + p_0) \cdot V_{\text{BCD}}(0)}{\rho_w \cdot g \cdot z(t) + p_0} + \psi(t) \right] \quad (11)$$

where the added valve volume air flow $q_{VI}(t)$ is

$$q_{VI}(t) = \frac{\alpha_I \cdot A_I \cdot (\rho_w \cdot g \cdot z(t) + p_0 + p_r) \cdot \sqrt{R_a \cdot T_{aI}(t) \cdot \kappa \cdot [2/(\kappa + 1)]^{(\kappa+1)/(\kappa-1)}}}{\rho_w \cdot g \cdot z(t) + p_0} \quad (12)$$

where variables are as follows: α_I = add valve discharge coefficient, A_I = add valve orifice surface, p_r = regulator pressure, R_a = gas constant for air, $T_{aI}(t)$ = absolute inflated air temperature, and κ = ratio of specific heat constants for dry air.

And the deducted valve air volume flow $q_{VD}(t)$ is

$$q_{VD}(t) = \alpha_D \cdot A_D \cdot \sqrt{\frac{2 \cdot R_a \cdot T_{aD}(t) \cdot \rho_w \cdot g \cdot \left(\frac{V_{BCD}(t)}{S_{BCD}}\right)}{\rho_w \cdot g \cdot z(t) + p_0}} \quad (13)$$

where variables are as follows: α_D = deduct valve discharge coefficient, A_D = deduct valve orifice surface, and $T_{aD}(t)$ = absolute deflated air temperature.

Simplifications and Assumptions

For the sake of simplicity, the diver's mass, water density, water temperature, the cross section of BCD and the diver, the diver's volume, and the air temperature are considered to be constant. It is assumed that all other variables are measurable. Only the diver's vertical motion is modeled and simulated.

Prototype's Development

Experimental measurements were needed for mathematical model verification. It was necessary to develop an embedded electronic device for data acquisition and pneumatic valve control. The development of the electronic device was divided into three correlated stages, which were electronic (HW), software (SW), and mechanical design.

Electronic Device

Figure 3 shows a block diagram of the electronic device.

The electronic device has an internal battery power supply. The deflation valve is a small pneumatic pilot valve used for triggering the BCD's deflate valve, while the inflation pneumatic valve is a directly acting valve with 1.2 mm orifice size. CPUs' main tasks are data acquisition regarding the pressure sensors and the 3D accelerometer, controlling the pneumatic valves according to the control algorithm, and data recording and sending the data to the computer. The used microprocessor is from the STMF32 F4 series. The RS232 interface is implemented for communication using a personal computer (PC) for software update and recorded data downloading. The Data flash and EEPROM are used for data recording and configuring the parameters. The 3D accelerometer is used for capturing accelerations along all three axes: x , y , and z . One pressure sensor is used for capturing the first stage pressure and one for capturing the water pressure. The more crit-

ical components within the circuit are the water pressure sensor and the external analog-digital (A/D) converter. The water pressure has to be measured very precisely and during low noise. It is used for depth measuring and velocity estimation, and so for these reasons, low noise is essential. In regard to the external A/D converter and analog water pressure sensor, the depth can be measured at a resolution of 1.068 mm. The depth measuring range covers up to 70 m. The main electronics is connected to a graphical user interface (GUI) by a cable. This cable provides the power supply and communication. Four function buttons are integrated within the GUI for entering the desired depths, thus optionally triggering the manual pneumatic valves and mode selection. The LED diodes display the actuated pneumatic valve and mode status. LCD (liquid crystal display) is used for displaying the parameters, which are the battery voltage, current depth, desired depth, current velocity, and the log's status.

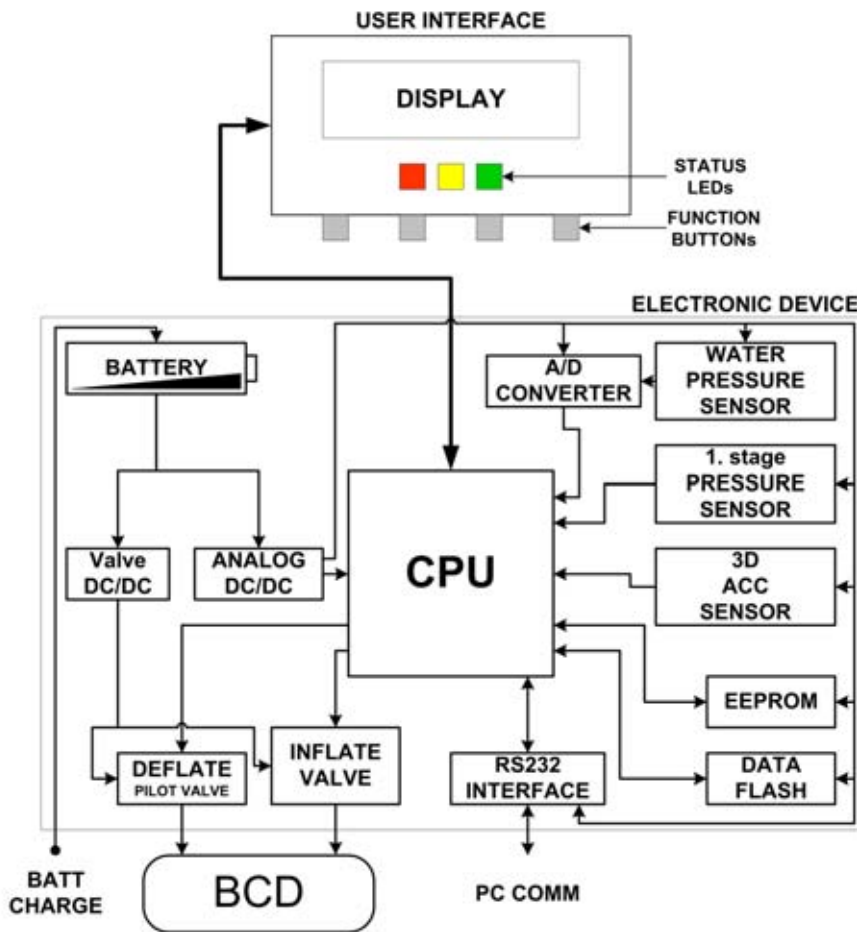
Software Architecture

Embedded electronic software was developed and the software architecture is explained in Figure 4.

The diver enters toward the desired depth via the user interface. The device descends/ascends the diver to the desired depth using predefined (limited) and controlled velocity. At the entered depth the diver can choose between three modes: *Off*, *Hold*, and *Swim*. The *Hold* mode holds the diver at an entered depth within a range of ± 0.5 m, while the *Swim* mode has an adaptive limit and increases with depth. The *Off* mode device does not control the pneumatic valves, and so they can be manually actuated via the keyboard. The minimum *Swim* limit is ± 0.5 m or a depth of $\pm 10\%$.

FIGURE 3

Electronic device block diagram.



Mechanical Assembly

Main mechanical requirements are pressure withstanding 8 bar, waterproofing, a small device, simple design, and easy to produce. The mechanical design was developed in the 3D CAD software SolidWorks. All the mechanical components were drawn and then assembled within a custom-designed housing (Figure 5).

The housing was designed to be milled from an aluminum block with a PMMA (poly-methyl methacrylate, shorter acrylic glass) cover. There is an O-type rubber gasket within the joint. The aluminum block and cover are screwed together for disassembling, if necessary.

The Prototype

Figure 6 shows the actual prototype device with GUI attached to BCD.

When diving, safety comes first. It is for this reason that the prototype device was designed to operate in parallel with manual pneumatic valves. The device has its own air pressure source fitted, which can be disconnected at any time if necessary. The pressure source can be realized with separate small (for example, 4 L) air tanks. So there is no consumption/waste of air for breathing. The power switch is crafted with a reed switch and magnet. The magnet has locks at the *On* and *Off* positions. The diving depth is limited to 40 m for safety reasons.

Measurements and Simulations

Measurements

Before the prototype device was developed, measurements were performed using a Matlab XPC target within a water tower. The water tower's depth was 10 m. The pressure sensor measurement accuracy and the adequacies of the pneumatic valves were tested. The pressure sensor and pneumatic valves were properly selected.

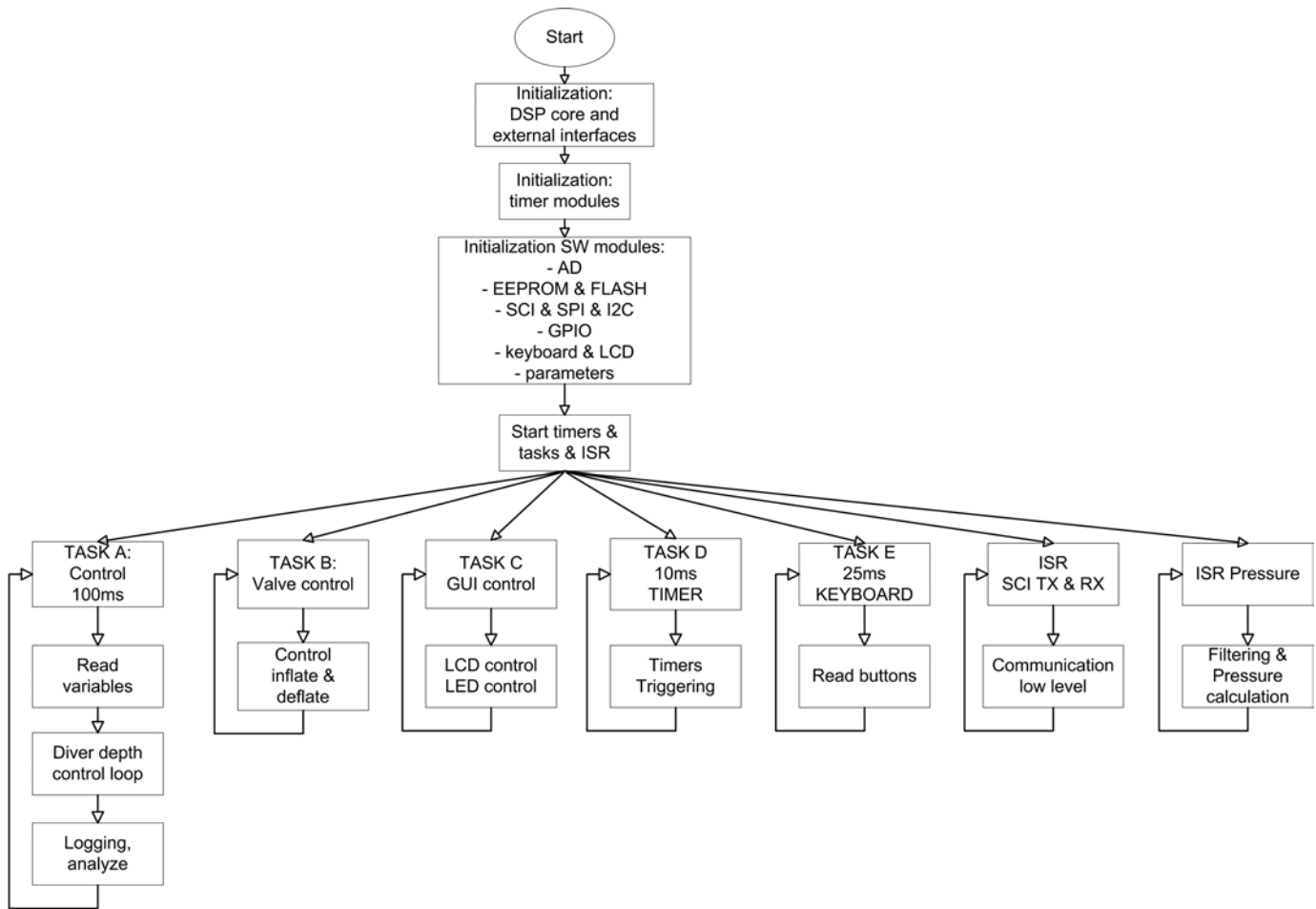
When the prototype device had been produced, functional tests were carried out in the laboratory. Finally, functional tests were done within the water tower at up to 10 m of water depth. Waterproof testing was done within a pressure chamber at 8 bar pressure.

The primary measurements and regulator testing were done within the water tower, and the secondary ones were done in the sea at up to 30 m water depth. Figure 7 shows the recorded data from the sea diving.

The first graph shows the desired and actual depths, and the control mode is illustrated in the second graph. The diving preparation time took 84 s after the device was turned on. The actual depth had an offset of -0.6 m. This was because the atmospheric air pressure changed during the day and the diver had not set zero depth on the boat. After 84 s, a small snag occurred at the actual depth, this being when the diver had jumped into the water. After 140 s the diver had started to enter the requested depth and had activated the device control after 143 s, which can be seen from the control graph, and the device had started transporting the diver toward the requested depth. It was because the diving velocity was limited that the controlled diver had not reached the first requested depth. While descending, the diver had reached a newly requested

FIGURE 4

Software block diagram.



depth. He then reached all the other requested depths. The diver had disabled the control mode between 844 and 1,598 s, and took control at

1,127 s. After that point in time, the diver was diving manually, and because of that, the actual and requested depths differed.

Some fluctuations in the actual depths can be seen within the whole graph. This was because the depth measurement had a resolution of

FIGURE 5

Electronic device's mechanical design.

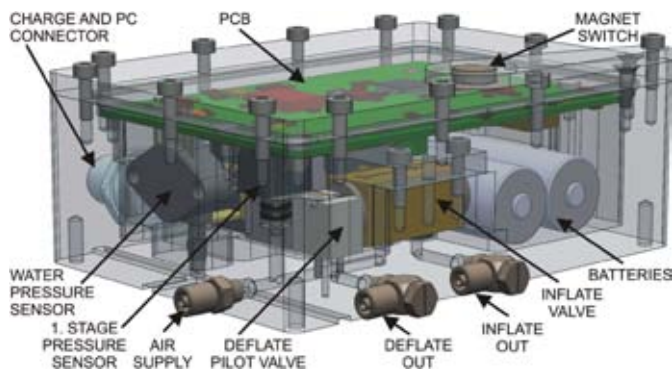


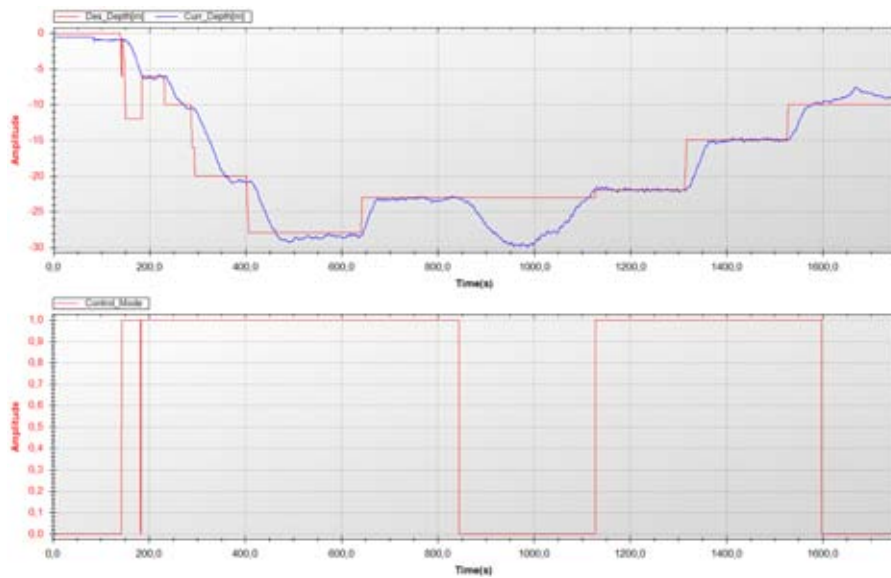
FIGURE 6

Finished prototype device attached to BCD.



FIGURE 7

Recorded sea diving.



1.068 mm, and the diver’s breathing and movement thus resulted in these fluctuations. Another reason for the fluctuations was the regulator. This was the first developed regulator for measurement and verification purposes and was not optimally tuned.

Matlab-Simulink Model

The Matlab-Simulink model (Figure 8) consists of diver’s buoy-

ancy mathematical model and control part.

This model is assembled with inflate and deflate valves, BCD’s volume and mass buoyancy drag and a summing force. The depths and velocities are calculated from the sum of all forces. The reference signal “Depth trajectory” is generated by a signal generator. The regulator consists of P depth and PD velocity regulators. Figure 9 shows simulated results for a

similar dive reference signal to those for actual sea dives (Figure 7).

Figure 9 shows the depth set value, simulated depth, and simulated velocity. The simulated results are very close to those of the actual dive. The main difference is that the fluctuations for the simulated results are minimal. This is because the diver’s breathing and movements were not simulated. The diver’s maximum velocity was limited to ± 0.2 m/s. A maximum velocity of ± 0.23 m/s was reached during simulation, which was the consequence of a nonoptimal regulator. The regulator’s oscillations were a consequence of an unstable system, as the diver’s buoyancy and regulator were not optimal.

Future Work

First, we would publish detailed derivations of the mathematical model regarding the diver’s buoyancy using pneumatic valves. Next a linear model of the diver’s buoyancy would be derived at when using pneumatic valves. The linear model would then be used for system stability analysis and optimal regulator design. The optimal

FIGURE 8

Matlab-Simulink model.

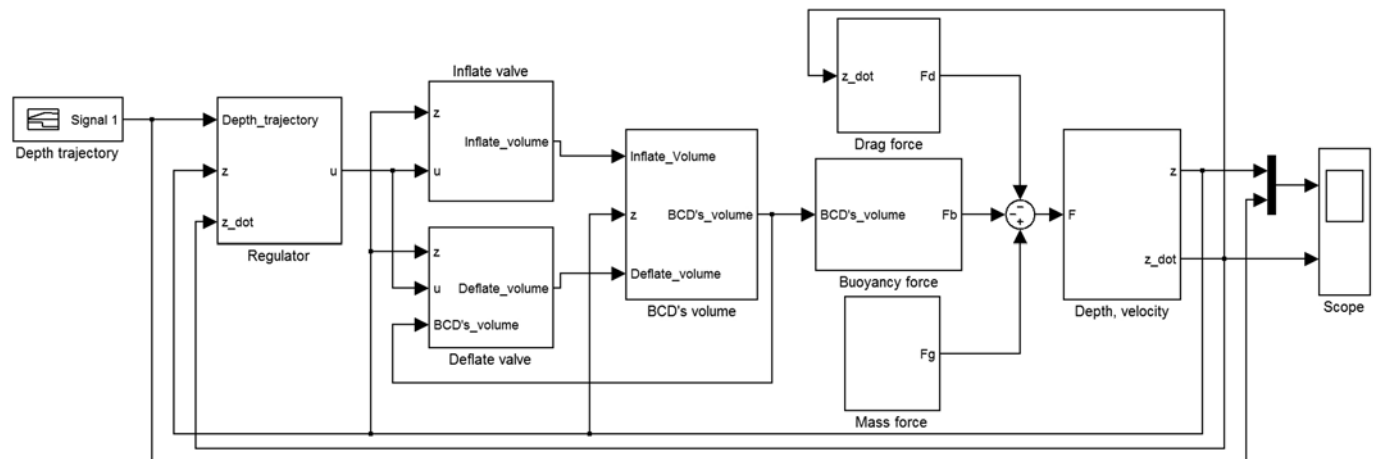
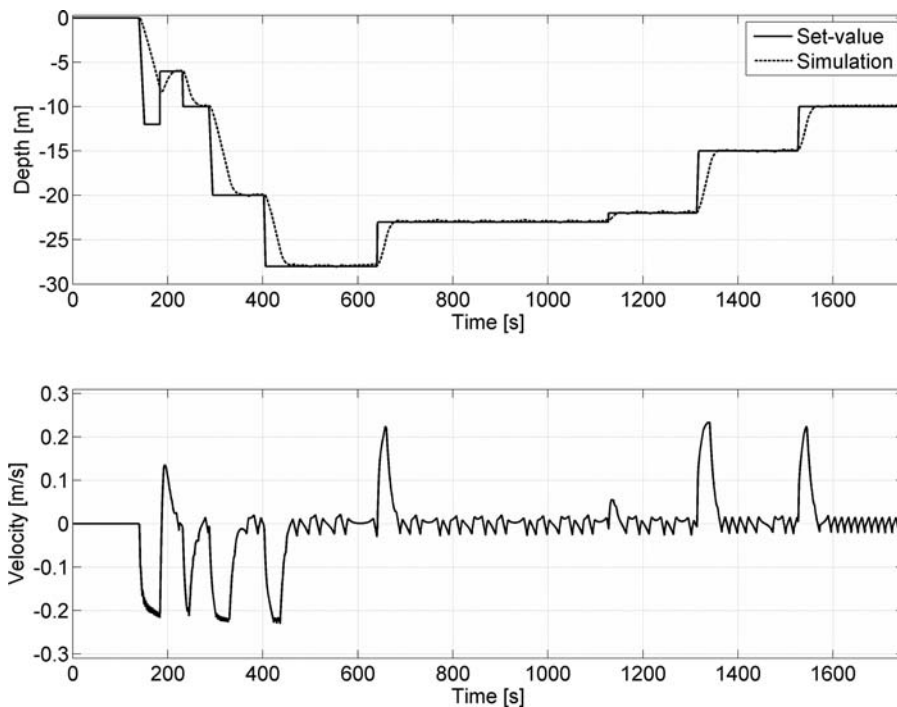


FIGURE 9

Matlab-Simulink simulation.



regulator would be a regulator that would consume the least air using satisfactory depth and velocity control. Algorithms would be developed for estimating the BCD's and divers' inhaled volumes for air consumption improvement. A 3D accelerometer and first-stage air pressure algorithms for a diver's state would be developed from the captured data. This device would identify whether a diver was breathing or not and would automatically ascend him/her to the surface.

Conclusion

Maintaining a diver's depth and also controlling the velocity is quite a difficult task in reality. Major obstacles are the nonlinearities of the BCD's volume and the pneumatic valves' volume flows that change with the depth. Nonlinearities are probably one of the main reasons why within the div-

ing market field there is still no device for automatic buoyancy control.

This paper described those nonlinearities and their influences on divers' depth controls. This paper also presented a mathematical model for a diver's buoyancy using BCD and pneumatic valves. It then explained the prototype device development used for data acquisition and the first testing of the regulator. The initial correlations between the real dives' and the simulated dive' results were satisfactory. In the future, a derived mathematical model of diver's buoyancy will be used for developing depth control algorithms and air consumption optimization.

Acknowledgments

Operations were financed by the European Union, European Social Fund. Operations implemented in the framework of the Operational

Programme for Human Resources Development for the Period 2007–2013, Priority axis 1: Promoting entrepreneurship and adaptability, Main type of activity 1.1.: Experts and researchers for competitive enterprises.

The authors would like to thank the Mares Company for contributed diving equipment and technical advice.

Corresponding Author:

Darko Valenko

Emsiso d. o. o., Zagrebska cesta 20,
SI-2000 Maribor, Slovenia

Email: darko.valenko@emsiso.com

References

Adams, P.M. 2008. Buoyancy-based, underwater propulsion system and method. U.S. Patent. Patent number 7,328,669.

Akkizidis, I.S., Roberts, G.N., Ridao, P., & Batlle, J. 2003. Designing a fuzzy-like PD controller for an underwater robot. *Control Eng Pract.* 11(4):471-80. [http://dx.doi.org/10.1016/S0967-0661\(02\)00055-2](http://dx.doi.org/10.1016/S0967-0661(02)00055-2).

Bagheri, A., & Moghaddam, J.J. 2009. Simulation and tracking control based on neural-network strategy and sliding-mode control for an underwater remotely-operated vehicle. *Neurocomputing.* 72(7-9):1934-50. <http://dx.doi.org/10.1016/j.neucom.2008.06.008>.

Bambang, S., Karsiti, M.N., & Agustawan, H. 2008. Development of a Variable Ballast Mechanism for the Depth Positioning of a Spherical URV. *Information Technology ITSIm 2008. International Symposium (Kuala Lumpur, Malaysia).* pp. 1-6.

Bessa, W.M., Dutra, M.S., & Kreuzer, E. 2008. Depth control of remotely operated underwater vehicles using an adaptive fuzzy sliding mode controller. *Robot Auton Syst.* 56(8):670-7. <http://dx.doi.org/10.1016/j.robot.2007.11.004>.

Bohmrich, J.L., Bowden, W.A. Jr., & Pedersen, V.G. 1978. Constant-volume buoyancy

- compensator. U.S. Patent. Patent number 4,114,389.
- Brecht**, W.F. Jr. 1970. Buoyancy control for scuba diving. U.S. Patent. Patent number 3,487,647.
- Courtney**, W.L. 1988. Rigid diver backpack with internal buoyancy compensator and ballast compartment. U.S. Patent. Patent number 4,779,554.
- Donahue**, C.A. 2005. Diving tank pocket buoyancy compensator with adjustable pressure valve. U.S. Patent. Patent number US 2005/0158124 A1.
- Dyer**, R.J. 2001, January. Development of an Automatic Buoyancy Device for Application in Scuba Diving. Submitted to the Department of Mechanical Engineering in Partial Fulfillment of the Requirements for the Degree of Bachelor of Science at the Massachusetts Institute of Technology.
- Egan**, M.P. 1996. Automatic buoyancy compensator with electronic vertical motion. U.S. Patent. Patent number 5,496,136.
- Han**, Y., Callafon, R.A.D., Cortés, J., & Jaffe, J. 2010. Dynamic Modeling and Pneumatic Switching Control of a Submersible Drogue. Proc 7th Int. Conference on Informatics in Control, Automation, and Robotics. 2:89-97.
- Harrah**, S. 1982. Automatically-controlled buoyancy vest. U.S. Patent. Patent number 4,324,507.
- Hicks**, T.G. 2003. Gas Laws. In Mechanical engineering formulas: pocket guide, Eds. Hager, L.S., Fogarty, D.E., & Pelton, P.A., 184-5. New York: McGraw-Hill.
- Kromp**, T. 1998. Method and device for letting out gas from life jackets of divers. U.S. Patent. Patent number 5,749,679.
- Lea**, R.K., Allen, R., & Merry, S.L. 1999. A comparative study of control techniques for an underwater flight vehicle. Int J Syst Sci. 30(9):947-64. <http://dx.doi.org/10.1080/002077299291831>.
- Leonard**, K.J. 1998. Volume control module for use in diving. U.S. Patent. Patent number 5,746,543.
- Leonard**, K.J., & Engel, J. 2004. Variable buoyancy apparatus for controlling the movement of an object in water. U.S. Patent. Patent number 6,772,705.
- Min**, X., & Smith, S.M. 1994. Adaptive fuzzy logic depth controller for variable buoyancy system of autonomous underwater vehicles. Proceedings of the Third IEEE Conference on Fuzzy Systems, IEEE World Congress on Computational Intelligence. (Orlando, FL, USA) 2:1191-6.
- Petrich**, J., & Stilwell, D.J. 2010. Model simplification for AUV pitch-axis control design. Ocean Eng. 37(7):638-51. <http://dx.doi.org/10.1016/j.oceaneng.2009.11.007>.
- Petrich**, J., & Stilwell, D.J. 2011. Robust control for an autonomous underwater vehicle that suppresses pitch and yaw coupling. Ocean Eng. 38(1):197-204. <http://dx.doi.org/10.1016/j.oceaneng.2010.10.007>.
- Roseborough**, T.E. 2006. Controlled volume buoyancy compensating device. U.S. Patent. Patent number US 2006/0120808 A1.
- Tangirala**, S., & Dzielski, J. 2007. A Variable Buoyancy Control System for a Large AUV. IEEE J Oceanic Eng. 32(4):762-71. <http://dx.doi.org/10.1109/JOE.2007.911596>.
- Tolksdorf**, M., & Tolksdorf, T. 1996. Counterbalancing device for divers. U.S. Patent. Patent number 5,482,405.
- U.S. Environmental Protection Agency, U.S. Federal Emergency Management Agency, & U.S. Department of Transportation.** 1989. Liquid Discharge Models. In. Handbook of Chemical Hazard Analysis Procedures. Appendix B2-B3. Washington, DC: Federal Emergency Management Agency.

Appendix

Summary of symbolic parameters and simulation values.

Symbol	Meaning	Simulation values
$z(t)$	diver's depth	
$z(0)$	initial diver's depth	0 m
$\dot{z}(t)$	velocity	
$\ddot{z}(t)$	acceleration	
$F_b(t)$	buoyancy force	
$F_d(t)$	drag force	
F_g	gravitational force	
$F(t)$	resulting force	
c_d	drag coefficient	1.2
g	gravitational constant	9.81 m/s ²
m_d	diver's mass with equipment	85 kg
ρ_w	water density	1025 kg/m ³
$V_{BCD}(t)$	air volume inside of buoyancy device	
$V_{BCD}(0)$	initial air volume inside of buoyancy device	0.005 m ³
V_d	diver's volume	0.08 m ³
S_{BCD}	buoyancy device frontal aerial surface	0.0283 m ²
S_d	diver's frontal aerial surface	0.2 m ²
$p_z(t)$	surrounding ambient pressure	
p_0	atmospheric pressure at water level	97.574 kPa
$T_z(t)$	absolute surrounding water temperature	304.5 K
$T_z(0)$	initial absolute water temperature	304.5 K
$T_{al}(t)$	absolute inflated air temperature	304.5 K
$T_{aD}(t)$	absolute deflated air temperature	304.5 K
$q_{VI}(t)$	added valve volume flow	
$q_{VD}(t)$	deducted valve volume flow	
p_r	regulator pressure	857.426 kPa
R_a	gas constant for air	287
u	control signal	
κ	ratio of specific heat constants for dry air	1.4
A_I	add valve orifice surface	1.31 mm ²
α_I	add valve discharge coefficient	0.744
A_D	deduct valve orifice surface	11.34 mm ²
α_D	deduct valve discharge coefficient	0.68

Compact Recreational Rebreather With Innovative Gas Sensing Concept and Low Work of Breathing Design

AUTHORS

Arne Sieber

SEABEAR Diving Technology,
Leoben, Austria

Chalmers University of Technology,
Gothenburg, Sweden

Andreas Schuster

SEABEAR Diving Technology,
Leoben, Austria

ACREO AB, Gothenburg, Sweden

Sebastian Reif

SEABEAR Diving Technology,
Leoben, Austria

Michael Kessler

Thomas Lucyshyn

University of Leoben, Austria

Peter Buzzacott

University of Western Brittany,
Brest, France

Peter Enoksson

Chalmers University of Technology,
Gothenburg, Sweden

Introduction

In recreational diving, autonomous open circuit (OC) breathing systems are dominant. Breathing gas is most often carried in a single high-pressure cylinder on the back of the diver. The diver inhales through an on-demand regulator, which delivers gas at ambient pressure. The exhaled gas is expelled into the surrounding water. Breathing gases in recreational diving are mainly compressed air but also oxygen (O₂)-enriched air, usually

ABSTRACT

Recreational rebreathers are increasingly popular, and recreational diver training organizations now routinely offer training for rebreather diving. Few rebreathers on the market, however, fulfill the criteria of a dedicated recreational rebreather. These remain based on traditional sensor technology, which may be linked to rebreather use having an estimated 10 times the risk of mortality while diving compared with open circuit breathing systems. In the present work, a new recreational rebreather based on two innovative approaches is described. Firstly, the rebreather uses a novel sensor system including voltammetric and spectroscopic validation of galvanic pO₂ sensor cells, a redundant optical pO₂ sensor, and a two-wavelength infrared pCO₂ sensor. Secondly, a new breathing loop design is introduced, which reduces failure points, improves work of breathing, and can be mass fabricated at a comparatively low cost. Two prototypes were assembled and tested in the laboratory at a notified body for personal protective equipment before both pool and sea water diving trials. Work of breathing was well below the maximum allowed by the European Normative. These trials also demonstrated that optical pO₂ sensors can be successfully employed in rebreathers. The pCO₂ sensor detected pCO₂ from 0.0004 to 0.0024 bar. These new approaches, which include a new concept for simplified mechanical design as well as improved electronic control, may prove useful in future recreational diving apparatus.

Keywords: rebreather, pO₂ control system, O₂ sensor, CO₂ sensor, counterlung

referred to as NITROX. For deeper diving, a proportion of the nitrogen (N₂) in the breathing gas is substituted with helium (He) and the resultant blend known as TRIMIX.

Compared with alternative breathing systems, OC diving faces several disadvantages. The breathing gas is dry and cold and produces expelled bubbles that disturb the environment. The main disadvantage though is the relatively poor gas efficiency, which only worsens with increasing depth. Just a fraction of O₂ from the breathing gas is used in any system before it is exhaled by the diver, and in the case of

OC, it is then expelled into the environment. Therefore, a typical recreational dive with one 12-L cylinder filled with air compressed to 200 bar and thus containing 500 L of oxygen may not last more than 40–45 min at 20-m depth; although with, for example, an O₂ metabolism of 0.8 L/min, the O₂ content in the cylinder should suffice for more than 10 h of diving.

In contrast to OC diving apparatus, diving with a closed circuit rebreather (CCR) more efficiently uses the available breathing gas and is less disruptive to the environment (Shreeves & Richardson, 2006). The exhaled gas

is not expelled into the surrounding water but is returned back into a breathing bag—the so-called *counterlung*. Carbon dioxide (CO₂) is chemically turned into insoluble carbonate and removed from the gas while passing through a scrubber. Metabolized O₂ is replaced by oxygen from a small high-pressure supply cylinder. The simplest form of a CCR uses pure oxygen as the breathing gas. However, oxygen becomes increasingly toxic at partial pressures exceeding approximately 1.6 bar, so the operational depth limit of such devices at sea level is 6 msw.

For deeper diving with CCR, the partial pressure of oxygen (pO₂) must be maintained at less than 1.6 bar to minimize the risk of oxygen toxicity and yet also as high as can be safely tolerated to reduce both the uptake of inert gas into the diver's tissues and the concomitant risk of decompression sickness. This is achieved by diluting the gas in the breathing bag with a mixture containing inert gas such as air, NITORX, TRIMIX, or HELIOX (a blend of O₂ and He). This mixture is known as the diluent. While O₂ CCRs are relatively uncomplicated mechanical devices, CCRs using blends of gas containing only a proportion of oxygen use oxygen sensors for monitoring pO₂ in the breathing gas and an electronic system for maintenance of the pO₂ within acceptable limits.

The earliest recreational rebreathers date back to 1996 when Dräger launched the Atlantis and later the Ray and Dolphin. The Dräger Ray came with a price tag that offered a realistic alternative to OC equipment. However, those units were semiclosed rebreather (SCR) systems where gas was still expelled into the environment and the systems were not as silent as CCRs. Their gas efficiency was much greater

compared with OC systems, even though a significant portion of the breathing gas was still wasted.

More advanced CCRs for deep “technical” divers have been available since approximately 1995. A common attribute among currently available models is that they are relatively more complex to operate than either OC or SCR, they require practice and regular training, and they take longer to prepare (including manual checklists) before any dive and longer maintenance after diving. Such systems are not well suited to recreational divers who perform a relatively low number of dives per year—for example, during holidays only—since only a high level of training and more regular diving assures an acceptably low level of risk.

The first electronically controlled CCR specifically intended for sport divers was introduced in 2009 (Shreeves, 2009). For the first time, pre-dive tests and operation under water were automated. For rebreather novices with an OC diving certification, this reduced the initial learning demand. When CCRs became available specifically for recreational divers, then large recreational diver training agencies launched rebreather training programs, also specifically for recreational divers.

Meanwhile, the mere availability of rebreathers and training is not enough for a market success, as Mark Caney, Head of the Professional Association of Diving Instructors TecRec Division, explained in his 3T (Training/Technology/Travel) concept (Caney, 2010). Many recreational divers devote themselves to diving on vacation only, and many also do this at a place far from home. To become a market success, the rebreather not only has to be transportable but also usable at the diving site. Therefore, diving locations that accept rebreather divers are

required to provide O₂ filling equipment and should be able to supply CO₂ filters used to “scrub” the exhaled gas of CO₂.

We believe that there are other important factors conditioning the commercial success of recreational rebreathers:

- Safety: The risk of mortality while diving a CCR is estimated to be approximately 4–10 times greater than OC diving (Fock, 2013). Rebreather features that may help reduce rebreather accidents include the following:

- full automation to avoid user errors,
- reliable O₂ sensor system to avoid a hypoxic or hyperoxic breathing gas composition,
- O₂ sensor system that can detect sensor failures: current O₂ sensor technology is known to be failure prone and O₂ sensor failures happen frequently,
- CO₂ sensor to detect a scrubber failure, and
- low work of breathing

- Price: To be successful in the recreational rebreather market, the price of a recreational rebreather should be comparable to a price of an upper-end OC technical diving configuration. The CCRs currently available on the market are complex systems with more relatively expensive parts and higher production costs than OC system components. Thus, it is unlikely that the current systems will become available at prices comparable to OC systems. Therefore, new approaches in mechanical design as well as electronic and sensor technology are required.

- Shorter pre- and post-dive preparation of the rebreather: While OC diving systems can be assembled

in short order and require only a minimum of maintenance (rinsing in fresh water after a dive is usually enough), CCRs require that the breathing loop is disassembled, cleaned, disinfected, and dried.

The current paper addresses these three factors with two fresh approaches. Firstly, a novel gas control system is introduced that uses, for the first time in CCR technology, voltammetric galvanic pO_2 sensor validation and optical pO_2 sensors as backup systems in combination with a highly automated user interface. Secondly, lower manufacturing costs, short pre- and postdive preparation/maintenance of the unit as well as low work of breathing are addressed with a simplified breathing loop concept.

State of the Art of Rebreather Design: Breathing Loop

There are two dominant counterlung positions found in today's recreational and technical rebreathers (Kellon, 1998). Over-the-shoulder counterlungs provide acceptably low work of breathing, are accessible by the diver during the dive, and can be easily equipped with manual O_2 and diluent injection buttons. However, a proportion of divers report that they prefer a free chest and avoid such front-mounted counterlungs. In contrast, back-mounted counterlungs have a greater work of breathing and/or a hydrostatic imbalance that may even fall outside of limits set by the European standard for rebreathers (EN14143:2003), and yet they provide a higher degree of convenience for certain types of sport diving (e.g., cave exploration).

The breathing loop mouthpiece, counterlungs, and scrubber are usually connected with corrugated hoses and appropriate connectors. For example, in rebreathers detailed by Shreeves in 2009, a total of four corrugated hoses were used to connect the components. Breathing hoses typically have a connector at each end with one o-ring in each connector. Every additional part increases the risk of system failure, especially when they are connected in series (Fock, 2013). Additionally, the overall work of breathing also depends on the amount of connectors, gas resistance in the loop, length of hoses, etc. Therefore, many rebreathers hardly meet the limits for the work of breathing defined in the European Normative EN14143:2003, especially at high respiratory minute volumes.

State-of-the-art mouthpieces for recreational rebreather diving can be switched between two modes: In the closed circuit mode, the diver breathes from the breathing loop of the rebreather. If the rebreather fails, then the diver can switch the mouthpiece to OC mode using gas from either the diluent cylinder or a separate cylinder carried specifically for such an emergency. Such mouthpieces are known as "bail out valve mouthpieces."

Some manufacturers also integrate an automatic loop diluent valve into the mouthpiece by using the valve of the OC mode. To function correctly, this requires that the cracking pressure (to initiate gas injection) is adjusted accordingly to the mode. While in OC mode, the cracking pressure should be adjusted to a value between 1 and 3 mbar; in closed circuit mode, the cracking pressure should be set to 25–35 mbar, otherwise the hydrostatic pressure equivalent to the difference in depth between the mouthpiece and the counterlung may lead to a free

flow of diluent into the counterlung. This is a particular problem when a diver uses a CCR with back-mounted counterlungs, as in the horizontal diving position there is a constant negative inspiratory pressure, primarily caused by the rebreather's hydrostatic imbalance (Kellon, 1998).

O_2 Sensor System

CCR systems that use a gas other than 100% O_2 cannot be purely mechanical since they require pO_2 monitoring and control. Galvanic pO_2 sensors are uniformly used in CCRs to measure pO_2 . The pO_2 in the breathing loop is held within a tolerable range by replacing metabolized O_2 either manually or automatically with fresh O_2 from a supply cylinder. In an electronic CCR, a solenoid gas injector for adding O_2 is incorporated (Shreeves & Richardson, 2006).

It is imperative that oxygen sensors measure pO_2 correctly because the safe range for breathing is fairly narrow. Incorrect pO_2 readings from faulty pO_2 sensors can lead to too little O_2 (hypoxia) or too much O_2 (hyperoxia or "oxygen toxicity"). Either condition is life threatening. Indeed, unsustainable breathing gas composition in the rebreather loop is believed to be the primary cause of many fatalities (Vann et al., 2007; Buzzacott et al., 2009).

Galvanic oxygen sensors in rebreathers essentially operate in similar fashion to a metal/air battery (Chang et al., 1993; Sieber, 2012). Oxygen is dissociated and reduced at the cathode to hydroxyl ions. These pass through the electrolyte and oxidize the metal anode (Pb). When the cathode and anode are electrically loaded with a resistor (typically between 50 and 300 Ω), a current proportional to the rate of oxygen consumption is generated.

A diffusion barrier (sensor membrane) is mounted in front of the cathode. This limits the volume of molecules able to reach the cathode during any particular period. All O₂ molecules at the cathode get reduced. The amount of molecules reaching the cathode follows Fick's First Law of Diffusion and is proportional to the pO₂ in front of the sensor membrane. Thus, the current of the (ideal) sensor is dependent only on the pO₂ in front of the sensor membrane.

Each sensor changes its output over time due to consumption of the cathode. While new sensors may typically achieve an output of up to 14 or 15 mV in air, after 1 year of usage the output may have decreased to below 8 mV. Therefore, sensors in rebreathers are usually calibrated before each dive by exposing them to air or 100% O₂.

The current produced by a sensor increases with temperature (about 2–3% per 1 K) as the diffusion is temperature dependent. Galvanic cells used in rebreathers are typically equipped with a small electronic board on their underside. These include a load resistor; thus, on the terminals of the sensor, one terminal does not relate to current but voltage. Additionally, a small resistor network with a negative temperature coefficient is used for temperature compensation.

Failure modes of galvanic sensors include the following:

- Nonlinearity: Functional pO₂ sensors usually have a linear output and a constant slope of about 40–60 mV/bar. In a nonlinear sensor, this slope is not constant but dependent on environmental factors such as, for example, ambient pressure, temperature (defective temperature compensation) or pO₂.
- Current limitation is a special case of nonlinearity, where the sensor

fails to provide a linear output above a certain pO₂.

- Slow sensor signal response: While a typical sensor response time is about 6–10 s, water condensation on the sensor membrane or low temperature can result in response times of 30 s to several minutes.
- Other mechanical failures (electrical connections broken, cell housing damaged, etc.).

In all failure modes, the sensor no longer produces an electronic signal corresponding to the pO₂ in front of the sensor membrane. As a consequence, the control loop may inject too little or too much O₂, and either case may quickly lead to an unsustainable breathing gas mixture.

Whereas electronic O₂ injectors are robust and failures are unlikely during a dive, sensor failures happen relatively more frequently. Rebreather manufacturers commonly address this problem by using three pO₂ sensors instead of merely one, together with a voting algorithm. Here the sensor signals are continuously compared with each other. If one sensor signal differs from the others, then that sensor signal is “voted out.” Such voting algorithms will fail, however, if two or more sensors concurrently malfunction.

The basis for such an approach is the assumption that sensors fail independently. This is, however, not always the case. O₂ sensors in a CCR are subjected to a common environment. If sensors are installed together in a rebreather, then they will also have the same “diving history.” Therefore, having three or possibly even more O₂ sensors may not provide triple or higher redundancy in the event of every type of sensor failure (Jones, 2012).

An alternative to the voting algorithm is true sensor signal validation

(Sieber et al., 2008), commonly used in medical analyzers. In the case of a CCR galvanic sensor cell readings are validated by flushing them with gas of a known O₂ fraction at regular intervals, for example, every 2 min. This differs to the voting algorithm because true sensor validation gives real-time feedback on sensor operation as the sensor is checked for linearity, current limitation, and response time.

A current, limiting disadvantage of true sensor validation is the additional hardware effort, which includes two additional solenoid gas injectors. This results in both additional manufacturing costs and also additional failure points. A slightly leaking solenoid gas injector may continuously flush the sensors with gas. In such an eventuality, the sensor signal may not only correspond to the pO₂ in the loop but might also be influenced by the leaking gas stream.

An alternate approach to galvanic pO₂ sensor validation has been described (Sieber et al., 2012), where the analog electronic board of pO₂ sensors was substituted with low-cost microprocessor-based multifunctional sensor electronics. This allowed on-board signal processing including digital temperature compensation. In addition, by using the internal digital-to-analog converter of the microcontroller, it was possible to perform voltammetry and impedance spectroscopy of the sensor. These measurements indicated the electrochemical constitution of a sensor (including the cathode, anode and the electrolyte). If the characteristics of any sensor differ significantly from its baseline values, then this indicates sensor malfunction and/or changed electrochemistry, which may soon lead to a sensor failure. An advantage of this technology is that additional hardware costs were

very low in comparison with the true sensor validation approach.

One alternative to galvanic pO_2 sensors are solid state ceramic sensors. Solid state pO_2 sensors are based mainly on the ionic conductivity of ceramic materials (Park et al., 2009). For many years, this technology has been deployed in cars for combustion control (i.e., lambda probes). At present, only yttria-doped zirconium dioxide (Zirconia, YDZ) is applied in commercial transducers as a conducting solid state electrolyte. Conductivity in YDZ requires high temperatures. Therefore, the transducer is heated by an electrical resistance to reach an operating temperature of about 650°C , which demands considerable energy. Micromanufacturing allows miniaturization of such sensors, which results in reduced power consumption for heating. An overview of micro-solid state gas sensors can be found elsewhere (Dubbe, 2003; Bogha et al., 2007). Solid state electrolyte sensors can also be designed for other gases, for example, NASICON is a suitable ionic conductor for a solid state CO_2 transducer. A rebreather sensor module has been developed consisting of one solid state sensor for pO_2 and one for pCO_2 (Sieber et al., 2011a, 2011b). Preliminary results are promising, but no serial production process has commenced; therefore, existing results are purely academic. It may be expected to take several years before such sensors could be used in commercially available CCRs.

Another possible alternative for galvanic pO_2 sensors are optodes, which are optical pO_2 sensors. To our knowledge, such sensors have not previously been tested in CCRs. These optical pO_2 sensors consist of a chemical layer with illuminated color pigments. The color pigments start to fluoresce at a corresponding wavelength. Optical

filters are used to separate the illumination light and the fluorescence signal. In the presence of O_2 , the fluorescence is quenched; thus, the output signal is reduced. Such sensors are most sensitive when no or only traces of O_2 are present. The sensitivity decreases with increasing pO_2 . Recently, new fluorescence pigments have been developed (Borisov et al., 2008), which may also allow reliable measurements of pO_2 above 1 bar. Alternatively to measuring the absolute sensor signal, one can also measure the decay time. As the time constant is only a few microseconds for measurements at 0.21 bar pO_2 and even shorter at higher pO_2 , time measurement is difficult. However, decay time offers a unique advantage in that factory calibration becomes possible, as decay time does not change over the lifetime of the sensor.

CO₂ Sensors and Scrubber Monitoring

A malfunction of the scrubber or even the absence of a scrubber leads to a rapid increase of pCO_2 in the breathing loop. This is known to account for numerous CCR fatalities. Today, two methods of scrubber function monitoring are available. The first approach examines the heat generated in the scrubber to give a prognosis on the remaining scrubber lifetime (Warkander, 2003). Secondly, direct gaseous pCO_2 measurement can be done with optical absorption spectroscopy, as CO_2 absorbs infrared light at $4.3\ \mu\text{m}$. One sensor used in rebreathers is the OEM CO_2 sensor module from Gas Sensing solution (Glasgow, UK). It is a one wavelength optical sensor measuring the absorption of infrared light at $4.3\ \mu\text{m}$. The advantages include a relatively small size, low power consumption, and commercial

availability. However, as this sensor is based on a single wavelength measurement, contamination of the sensor or condensation of water on the internal components may lead to a falsely increased output signal.

Two academic research results, both of which are still far from commercial availability, may in the future provide alternative pCO_2 measurement technology; pCO_2 sensors based on ionic solid state sensor technology described above (Sieber et al., 2011b) and optical films that change color in the presence of CO_2 (Shashidhar & Kane, 2012).

New Recreational CCR Prototype

The purpose of the current project was to develop a rebreather prototype with safer gas management, low manufacturing cost, and simplified loop design to provide a realistic alternative to OC diving systems. In summary, the important key features of it were as follows:

- simplicity and ease of use, assembling, and diving;
- high level of automation to enable simplified training and operation of the rebreather;
- low work of breathing comparable to a high-quality OC regulator;
- compact, low weight, if possible suitable for transport in cabin luggage;
- integrated O_2 sensor validation to detect pO_2 sensor failures;
- CO_2 monitoring;
- bail out valve mouthpiece, with integrated overpressure valve, if possible; and
- price-wise alternative to OC equipment, i.e., designed in a way that allows simple molds and cost-efficient production.

Electronic System Design

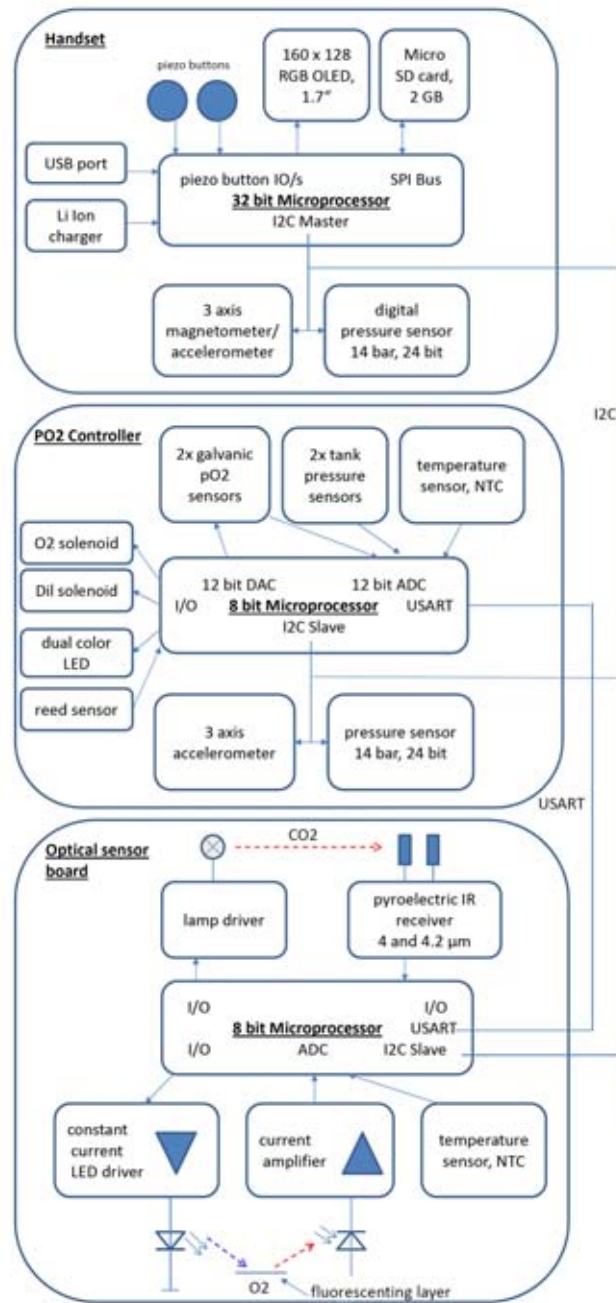
Currently, there are two common electronic solutions used in rebreathers. One is based on having two independent electronics where if one of the electronics fails, then the second can be used. The other approach uses a network of microcontrollers that is designed in such a way that the microcontrollers are able to check each other and detect a failure (Sieber et al., 2011a). In a recreational CCR redundant electronics are not necessary. It is only important that a failure is reliably detected as, by definition, recreational dives do not include decompression obligations and, therefore, bailout and abortion of the dive is the response to any serious system failure. Therefore, a distributed system design with a network of microcontrollers was chosen. Figure 1 details the layout of the electronic system of the rebreather prototype.

Controller Electronics

The core component of the controller board is an 8-bit microcontroller. Even though galvanic sensor cells are failure prone, especially when used in rebreathers, they still provide the most accurate reading. Therefore, two galvanic sensor cells (Figure 2) were incorporated in the design. Instead of using temperature-compensated cells, a galvanic cell with a single load resistor (82 k Ω) and a coaxial gold-plated connector was chosen. Two analog high-pressure sensors (0–300 bar) measured the O₂ and diluent cylinder pressures. One temperature sensor was included in the electronic design for digital temperature compensation of the galvanic pO₂ sensors. Ambient pressure was measured with a 14-bar digital absolute pressure sensor. Two

FIGURE 1

Electronic layout of the rebreather.



solenoid controllers drove two electromagnetic solenoid injectors for O₂ and diluent. The injectors were rated for a maximum differential pressure of 8 bar but were successfully tested up to 15 bar.

The digital to analog converter of the microcontroller was used to apply

voltages across the sensor cell and perform voltammetry and impedance spectroscopy. The concept of using voltammetry with galvanic sensors has been previously detailed (Sieber et al., 2012). By using voltammetry, it is possible to measure the internal impedance of the galvanic pO₂ sensor

FIGURE 2

Sensor compartment of the prototype CCR.



and to create a characteristic plot, which reflects sensor chemistry and state of the electrodes. Changes of this plot indicate that a sensor is at or close to the end of its useful life.

Optical Gas Management Unit

As mentioned earlier, galvanic pO_2 sensors may possibly all fail at the same time, for example, if they hail from the same production lot and share the same history of operation in a CCR. Even though with voltammetry it is possible to detect many types of galvanic sensor failures, alternative pO_2 sensor technology may provide useful additional safety.

Based on promising preliminary laboratory results with optical pO_2 sensors, a new sensor element was designed. The electronic part consisted of a blue LED and a photodiode with a low noise current amplifier. A red gelatin filter separated the blue excitation light from the red fluorescence light. The components were encapsulated in optically clear epoxy resin of 5-mm thickness. The optical layer with color

pigments was glued onto the top of the resin. This layer was prefabricated in the form of self-adhesive stickers; thus, it could easily be replaced by the diver.

Gaseous CO_2 sensing is an important safety feature in a rebreather. To avoid problems associated with single wavelength pCO_2 monitors, a dual wavelength pCO_2 sensor was designed. It consisted of two pyroelectric elements, each equipped with an optical band-pass filter (one at $4.0\ \mu m$, the other at $4.25\ \mu m$). An incandescent light illuminates the sensor through a path of 50 mm. The optimal measurement rate was found to be 1 Hz to achieve the most suitable balance between sensitivity, update rate, and power consumption. A second 8-bit microcontroller was used to read the optical pO_2 sensor as well as the pCO_2 sensor.

Handset

A console diving computer-like handset was developed as the user input device (Figure 3). It featured a 160×128 pixel color OLED screen

and two piezo input buttons. The core component is a powerful 32-bit microcontroller operated at 12 MHz and optionally at 60 MHz. A 32-bit processor was chosen in order to be able to provide sufficient processing power to calculate advanced decompression algorithms such as the Variable Permeability Model (Yount & Hoffman, 1986; Yount & Strauss, 1976; Kuch et al., 2011) or the Reduced Gradient Bubble Model (Wienke, 1990) in real time and while also driving the OLED display with an update rate of at least 2 Hz. The handset also includes a 2-GB flash memory, a 14-bit digital pressure sensor, a three-axis magnetometer, and a three-axis accelerometer.

Communication Protocol

Connecting devices underwater usually requires expensive cables and connectors so a wireless solution was desirable. Unfortunately, wireless links traditionally used in diving computers are only capable of transmitting a few bytes per second. Faster transmitters such as those used in consumer electronics do not work well underwater (Lloret et al., 2012). Therefore, with current technology, the electronic components of this rebreather prototype were connected with cables. Several interfaces exist that can be used for communication between the microcontrollers. Controller Area Network (CAN) Bus, for example, is fast, well proven in safety critical systems and is insensitive to electrical interferences. From this point of view, it would be suitable for rebreathers. Unfortunately, CAN requires additional electronic components and hardware CAN interfaces are only available on automotive microcontrollers. As the diver and all cables are surrounded by water,

FIGURE 3

Handset of the rebreather.



external electrical interferences are reduced. Therefore, it was convenient to use an interface based on ground referenced single-ended voltage inputs, rather than a differential pair of CAN.

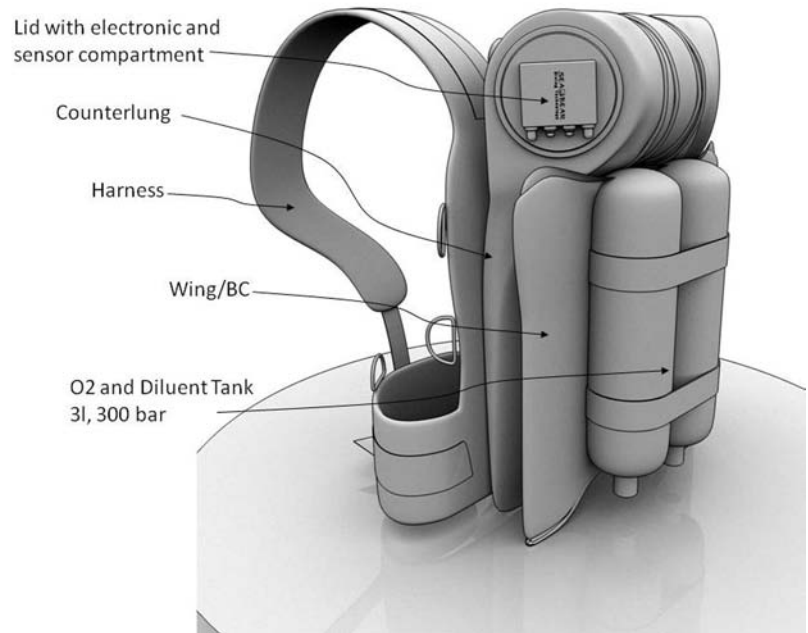
Serial peripheral interface is an interface implemented in nearly all microcontrollers on the market. This interface uses three communication lines plus one chip select line for each slave connected to the master. It allows high data transmission rates. I2C is an interface that requires only two communication lines but operates at lower speed. Previous research demonstrated that the operation speed of I2C is sufficient for rebreathers (Sieber et al., 2011a). For these two reasons, I2C was implemented in the current project with only a single master system utilized to increase the stability of the communication. Additionally, the controller electronics communicated with the microcontroller of the optical sensors via a separate Universal Synchronous/Asynchronous Receiver/Transmitter (USART) interface.

Novel Loop Design

The main idea for the loop design of the rebreather prototype detailed in this paper was to use a single piece counterlung into which a CO₂ filter cartridge could be inserted (Figure 4).

FIGURE 4

Rebreather design with novel counterlung concept.



In this way, a separate filter housing and otherwise necessary hose connections could be omitted. The counterlung was equipped with a large opening of diameter of 160 mm through which a filter cartridge was inserted. This diameter was selected so that already commercially available filter cartridges (Poseidon, Sweden or Micropore, USA) could be used. The opening was then closed with a lid, which also housed the electronic components. Figure 5 illustrates how the CO₂ filter was placed between the inhale and exhale section of the counterlung. This novel design allowed a simple manufacturing process where the counterlung could be fabricated from a single piece of high-frequency weldable fabric.

Mouthpiece Design

In addition to the open and closed circuit modes, the specifications of

the mouthpiece of the prototype also included an automatic diluent valve and a loop overpressure valve. The design focused on a simple and cost-efficient production using a low-cost injection molding process. Figure 6 shows the design of the mouthpiece. A barrel could be rotated to switch between open and closed circuit positions. A second stage downstream valve (Scubapro R190) was integrated. A second “dummy” valve was situated in front of the downstream valve for the purpose of applying a force onto the diaphragm to increase the cracking pressure to 30 mbar in the closed circuit position. The loop overpressure valve consisted of a one directional valve and a plate that was held by a spring against a seat. The cracking pressure of the over pressure valve was configured to be about 25 mbar. By rotating the barrel from the closed circuit position to the OC position, the lever of the “dummy” valve was

FIGURE 5

The scrubber cartridge is inserted into the counterlung, where it sits in between inhale and exhale section.

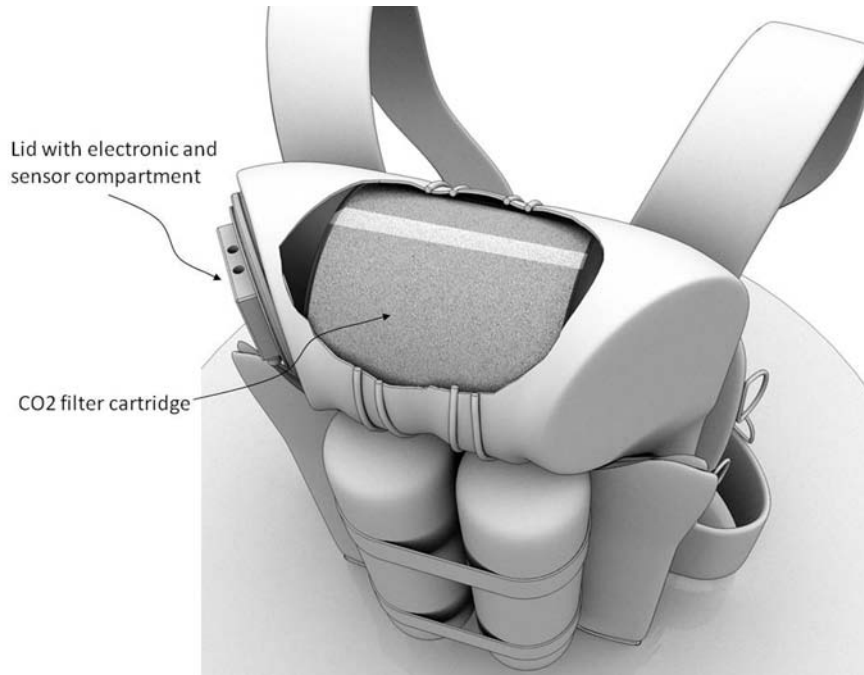
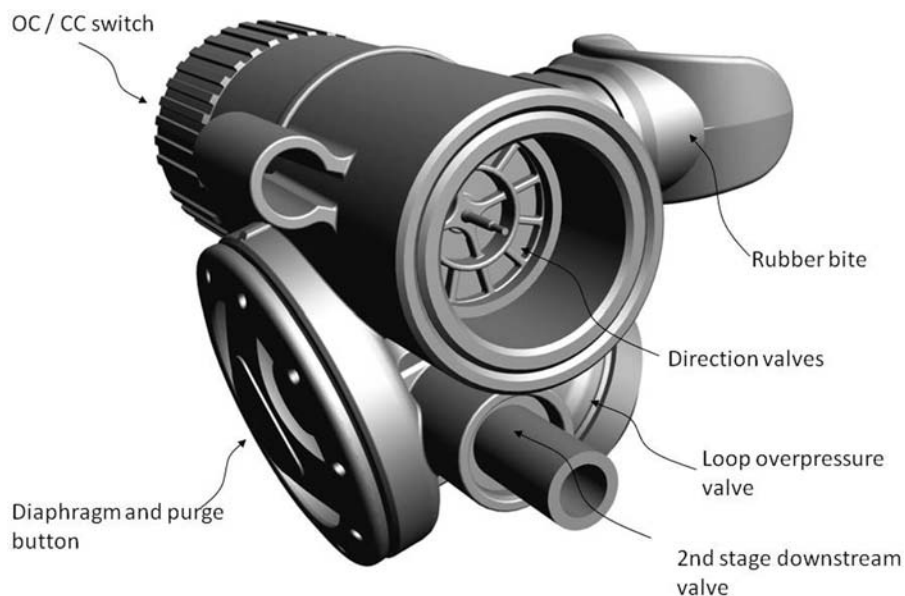


FIGURE 6

Mechanical design of the mouthpiece.



pulled away from the diaphragm and the additional force released. By the same action, the spring of the overpressure valve was also released. This way the diver could exhale with minimum resistance.

Results

Specifications of the CCR Prototype

Two prototypes of the proposed recreational rebreather were manufactured. The specifications are as follows:

- integrated counterlung, maximum capacity 2 times 4 L (restricted to a total volume of 5 L when built into the harness);
- sensor system with two galvanic pO_2 sensors, one optical O_2 sensor, and one optical dual wavelength pCO_2 sensor;
- distributed microcontroller network with three microcontrollers;
- integrated scrubber, 1.8 kg, estimated duration of 120 min;
- two steel cylinders, 3 L, and 300 bar each;
- streamlined design, compact size, low weight (can be carried onto commercial aircraft as hand luggage; the weight of the rebreather excluding cylinders was 4.8 kg);
- counterlungs serve as water traps—in each a sponge is inserted that can absorb up to 0.3 l;
- Li ion rechargeable battery supply, consisting of two pieces Trustfire 16340 type cells, with a capacity of approximately 600 mAh each; and
- average current consumption of 120 mA.

Five counterlung prototypes were manufactured from single sheets of polyurethane-coated fabric. All welding was performed with a 1.5-kW high-frequency welding machine. Ten mouthpieces were produced with

a rapid prototyping silicon mold. The handset (Figure 3) showed all dive-relevant information and was used to initiate the automatic pre-dive tests. Its features were:

- 160 × 128 pixel color OLED display,
- 32-bit microprocessor,
- ZH-L16C decompression algorithm with gradient factors,
- tilt compensated compass,
- 2-GB internal flash memory, and
- USB port.

Operation of the Prototype

Operation of the rebreather was simpler than for currently available CCRs. Pre-dive tests were simplified

by an automatic procedure. First, critical components such as pressure sensors, solenoid valve, and microprocessor were electronically tested. After that the loop was checked (negative and positive overpressure test), and the sensors were calibrated.

All dive and rebreather data were stored in the internal SD card every 5 s. This was done in .csv files, which subsequently allowed simple processing of the data in spreadsheet software such as Microsoft Excel. When the handset was connected to a USB port of a personal computer, it was recognized as mass storage device (like a USB thumbdrive), and the internal flash memory was mounted as a logical drive. All dive data could be downloaded without additional software.

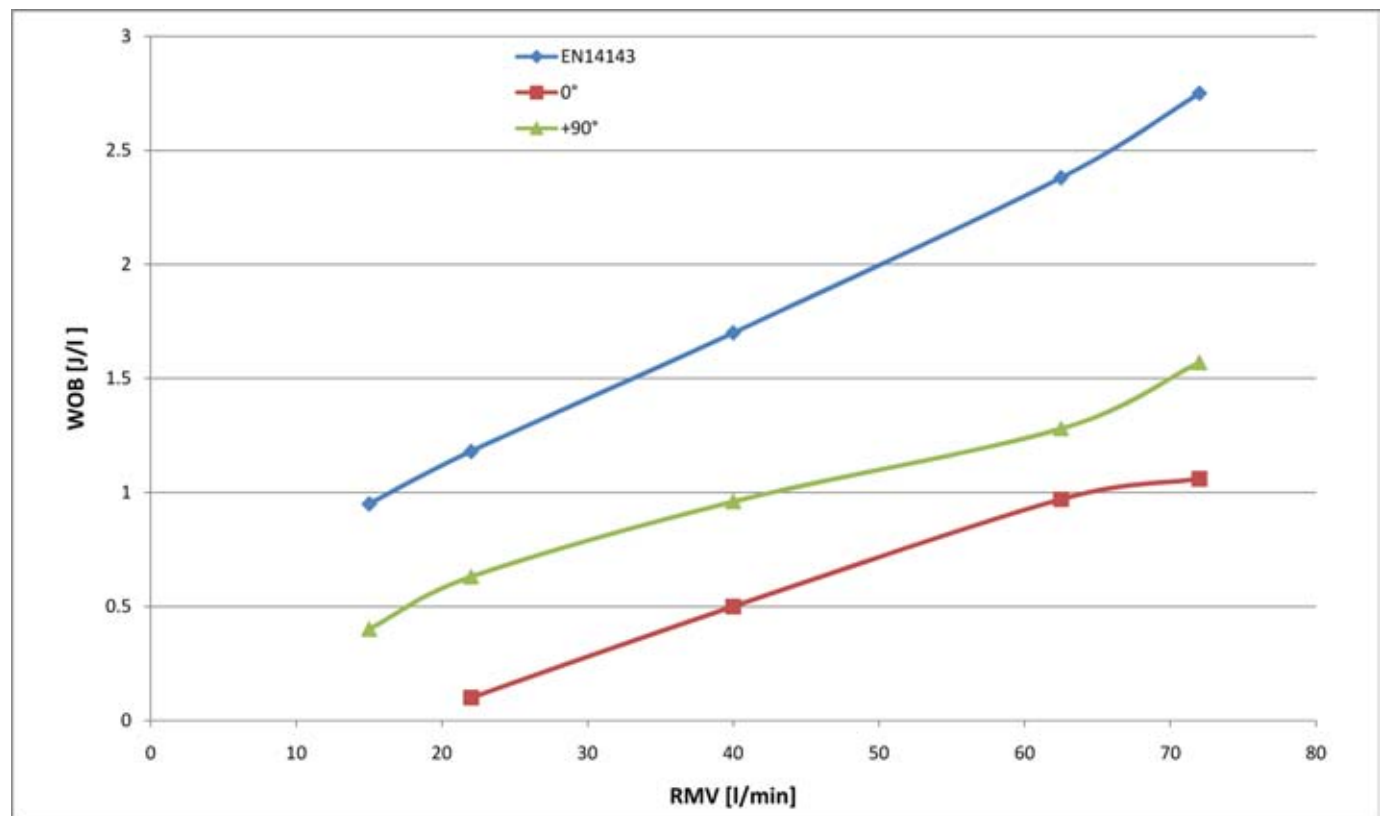
Laboratory Testing of the Prototype

Before in-water trials were carried out, the rebreather was tested at a notified body (DEKRA, Essen, Germany). Figure 6 presents the work of breathing test results. In either horizontal or +90° positions, the work of breathing results was far below limits defined in EN14143:2003 (Figure 7). The main reasons for this were as follows:

- All components were designed to have minimum flow resistance.
- The number of pneumatic parts such as hose connectors, couplers, etc., was reduced by nearly a factor of 2.
- The overall flow resistance and work of breathing were reduced significantly.

FIGURE 7

Results of work of breathing laboratory testing according to EN14143:2003.



Moreover, DEKRA tested and certified the tank pressure sensors for compliance to EN250 and the ambient pressure/depth sensor, real-time clock, and the pressure tolerance of the handset for compliance with EN13319.

The implementation of the decompression algorithm was validated with 70,000 simulated dive profiles.

The optical sensors were characterized in a pressure chamber up to 2 bar pO_2 . Unlike galvanic pO_2 sensors, pO_2 optodes do not produce an output linear to the pO_2 ; therefore, a single calibration point with O_2 or air is not sufficient (Figure 8). Instead, a 3-point calibration was implemented based on the Stern-Volmer equation. Three parameters are calculated during the calibration:

- K (Stern Volmer quenching constant)/sensitivity,
- S_0 (signal at 0 pO_2), and

- X correction factor for nonideal color separation filters and stray light.

The quenching constant as well as S_0 decrease with increasing temperature; therefore, temperature compensation had to be performed. With the first prototype, we were able to achieve an accuracy of 2–5% from 0.2 to 1 bar and 10% above 1 bar pO_2 .

Figure 9 shows a characteristic plot of a galvanic pO_2 sensor obtained with the voltammetry circuit. The second plot is from a faulty cell. Even though this particular sensor could be calibrated on the surface with a normal signal output, it failed during diving. In this case, the reason for the sensor failure was a passivated cathode where, similar to a current limited cell, the output became static above a certain pO_2 . The plot of the faulty cell differs significantly from the working cell in terms of the shape of the rise and fall time of the sig-

nal. In this case, the plot could be used to identify the faulty sensor.

The pCO_2 sensor was characterized in a computer-controlled pressure chamber with a calibration gas containing 5% CO_2 . Figure 10 shows the signal response of the CO_2 channel (4.25 μm wavelength) as well as the reference channel (4 μm wavelength) from air at a pressure of 1–6 bar, corresponding to a pCO_2 of 0.0004–0.0024 bar. The signal intensity of the reference channels was not affected by an increase in pCO_2 . Changes of the supply voltage or condensation inside the measurement chamber affected both measurement and reference signals in the same way; thus, the measurement signal could be corrected.

In-Water Trials

Following the laboratory testing of the rebreather, in-water tests were

FIGURE 8

Raw signals from the optical pO_2 sensor in a hyperbaric chamber. Note: the slope decreases with increasing pO_2 . The sensor signal decreases with increasing temperature; thus, temperature compensation is also required.

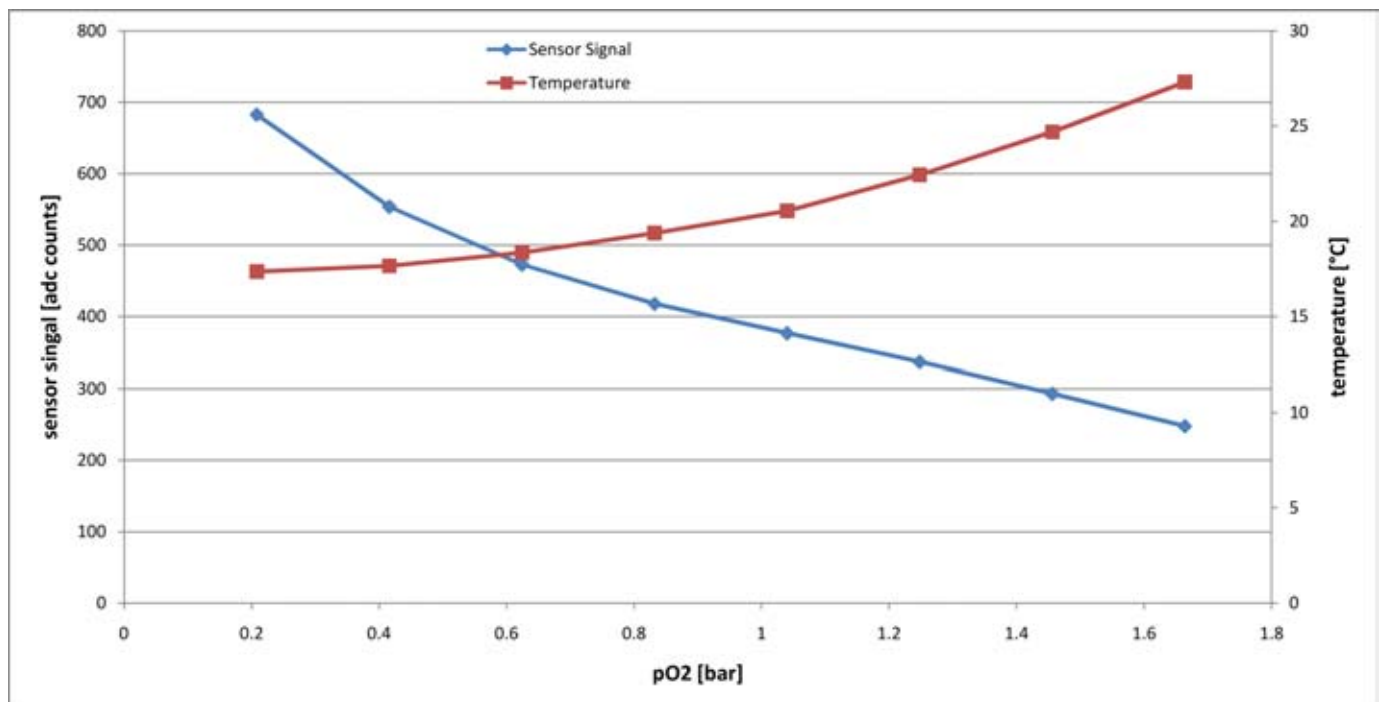
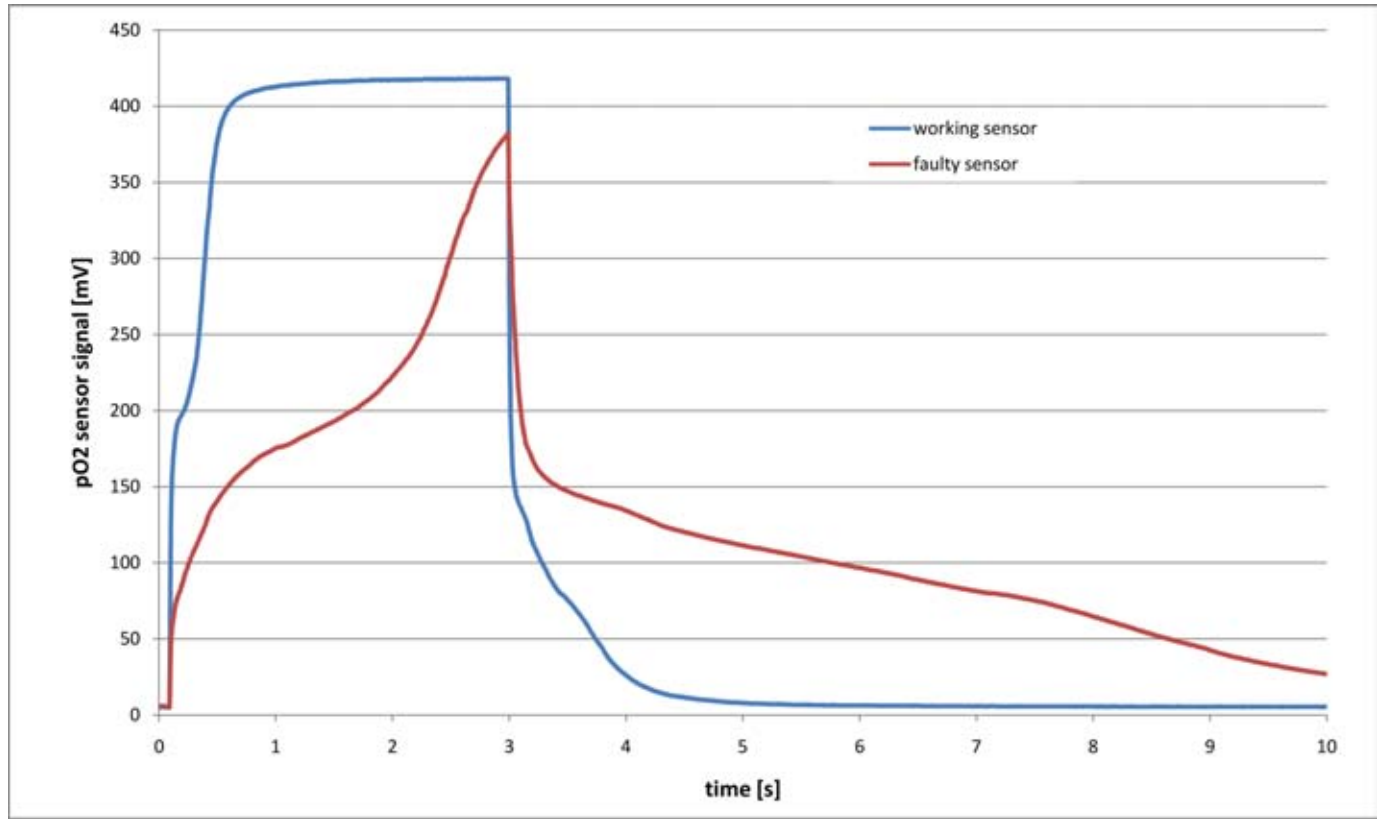


FIGURE 9

Example plots of galvanic pO₂ sensors voltammetry. The plot from the faulty sensor differs significantly from the characteristic plot from a correctly working sensor.



carried out in a 10-m-deep freshwater pool. Initially, the cylinders were mounted with their valves facing downwards. In this position, the rebreather was not well balanced; therefore, the position was reversed and the cylinders were mounted with their valves facing upwards. The immediately apparent disadvantage with this configuration was that the diver was not able to operate the cylinder valves while diving but, since this is not a requirement for a recreational rebreather, it was considered acceptable.

Successful pool dives were then followed by tests in the Mediterranean Sea. Maximum depth was 40 msw, maximum dive time was 70 min, and the water temperature was 12 °C. The

pO₂ setpoint of the controller was programmed to be 0.5 times the ambient pressure till a depth of 10 msw (essentially a constant fraction mix with 50% O₂) and at depth of >10 m constant 1 bar pO₂. All dives were successfully performed without incident. Figure 11 shows depth and pO₂ during a 40-msw test dive in the Mediterranean Sea.

Discussion and Conclusion

An innovative CCR prototype was manufactured (Figure 12). This prototype combined a novel sensor concept and an innovative loop design. The voltammetric validation of the galvanic

pO₂ sensor cells allowed recognition of many sensor failures including aging effects such as cathode passivation or current limitation. For the first time, an optical O₂ sensor has been used in a rebreather. Even though optodes are usually employed to measure traces of O₂, the circuit performed well for pO₂ measurements up to 1.6 bar. These optical pO₂ sensors are extremely robust, insensitive to humidity and may, therefore, be an alternative to traditional galvanic pO₂ sensors used in rebreathers. However, while readout of galvanic pO₂ sensors is rather simple, optode signal processing is more challenging: A 3-point calibration together with complex temperature compensation is necessary. Nonetheless, this research demonstrated that optical

FIGURE 10

CO₂ sensor output in a hyperbaric chamber with air containing 400 ppm CO₂.

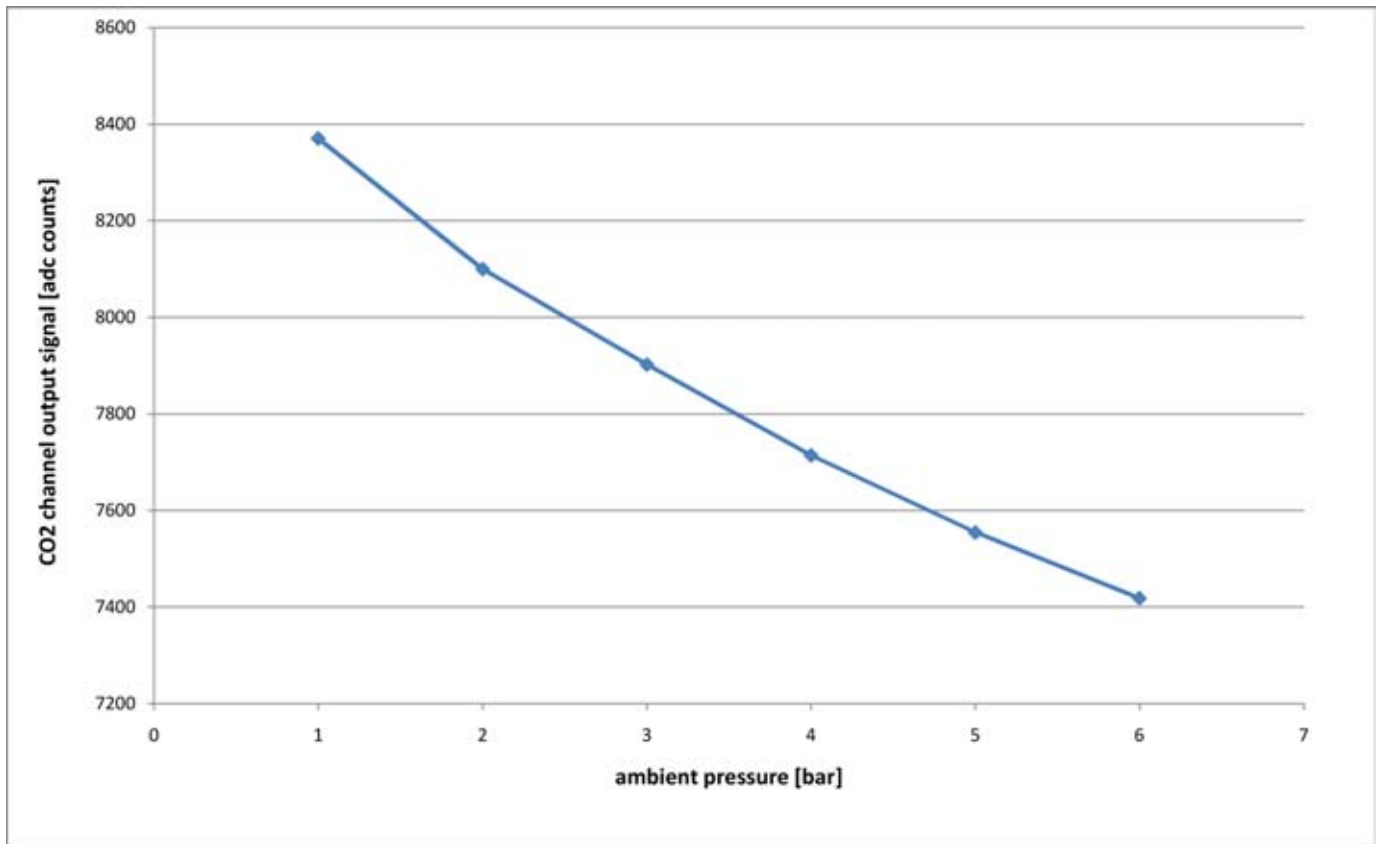
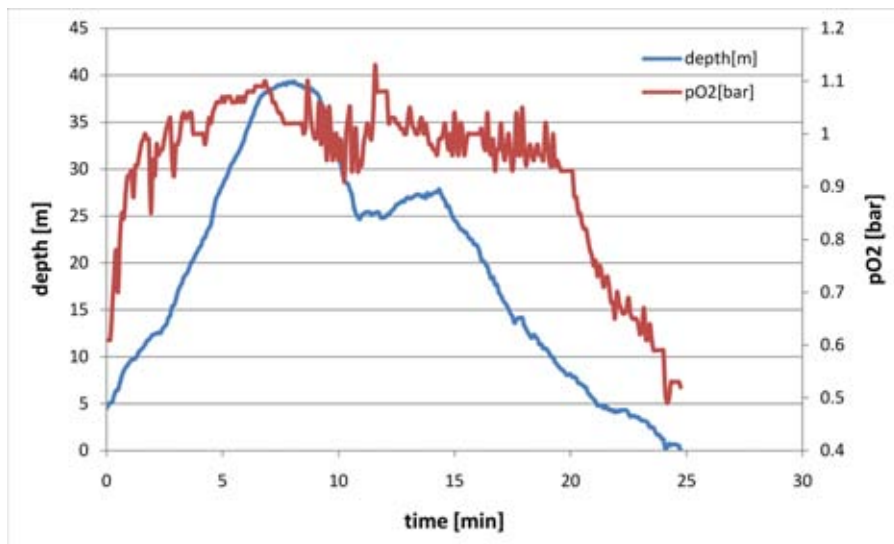


FIGURE 11

Test dive in the Mediterranean Sea to a maximum depth of 40 m. Between surface and 10 m depth, the pO₂ controller was set to maintain a constant fraction of 50% O₂. The pO₂ setpoint was 1 bar for depths deeper than 10 m.



pO₂ sensors can be successfully employed in rebreathers.

Further possibilities to integrate optodes into CCRs exist. For example, fitting them between the mushroom direction valves inside the mouthpiece

FIGURE 12

Diver with the rebreather prototype in a wreck in an Austrian lake.



would allow assessment of inhaled as well as exhaled pO₂. Optodes can be produced as single use parts with a production cost of only cents. The sensor film (the chemical layer) might be mounted on an adhesive and replaced for each dive; thus, any diver could use a new sensor on each dive and the aging of sensors would no longer be of concern. Alternatively, the sensor film might be sprayed or printed onto CO₂ filter cartridges (Fischer et al., 2010). In that way, each time a filter is changed, the O₂ sensor would be concurrently replaced by a new one.

Scrubber monitoring is an important task in rebreather diving. While existing single wavelength infrared CO₂ monitoring is failure prone, dual wavelength measurement has a reference channel, and therefore, erratic readings, caused for example by condensation, can be detected and may even be automatically corrected for.

The second approach of the current paper addressed simplification of the breathing loop. By integration of the scrubber into the counterlung, it was possible to reduce the amount of connectors, bill of materials, and pre- and postdive preparation time. A new mouthpiece with optimized cross sections together with the simplified counterlung scrubber concept has the potential to significantly reduce work of breathing, as demonstrated by the laboratory measurements recorded by a notified body.

The authors are convinced that rebreathers will continue to increase in popularity among recreational divers. However, a rebreather must likely be especially developed according to the needs of recreational divers if it is to become a market success. The current paper has presented several new approaches including a new concept for simplified mechanical design as well

as improved electronic control, which may prove useful in future recreational diving apparatus.

Acknowledgments

This work was partially supported by the Austrian AWS, the Center of Applied Technology in Leoben, Austria, as well as the Austrian FFG. Some of the sensor technology was derived from results obtained within the EU FP7 Marie Curie Project Lifeloop. Andreas Schuster and Peter Buzzacott are currently financed via the EU FP7 Marie Curie Initial Training Network Phypode.

Corresponding Author:

Arne Sieber
SEABEAR Diving Technology,
Leoben, Austria and Chalmers
University of Technology,
Gothenburg, Sweden
Email: Arne.Sieber@seabear-diving.com

References

- Bhoga**, S.S., & Singh, K. 2007. Electrochemical solid state gas sensors: An overview. *Ionics*. 13:417-27. <http://dx.doi.org/10.1007/s11581-007-0150-7>.
- Borisov**, S., Nuss, G., & Klimant, I. 2008. Red light-excitable oxygen sensing materials based on platinum(II) and palladium(II) benzoporphyrins. *Anal Chem*. 80(24):9435-42. <http://dx.doi.org/10.1021/ac801521v>.
- Buzzacott**, P., Zeigler, E., Denoble, P., & Vann, R. 2009. American cave diving fatalities 1969-2007. *Int J Aquat Res Educ*. 3:162-77.
- Caney**, M. 2010. PADI and Rebreathers. In: Eurotek 2010 Advanced Diving Conference. Glasgow, UK. 16-17 October 2010. Available at: <http://www.eurotek.uk.com/presentations2010.html>. (accessed 12 November 2013).

- Chang**, S.C., Stetter, J.R., Cha, C.S. 1993. Amperometric gas sensors. *Talanta*. 40:461. [http://dx.doi.org/10.1016/0039-9140\(93\)80002-9](http://dx.doi.org/10.1016/0039-9140(93)80002-9).
- Dubbe**, A. 2003. Fundamentals of solid state ionic micro gas sensors. *Sensor Actuat B-Chem*. 88:128-48. [http://dx.doi.org/10.1016/S0925-4005\(02\)00317-9](http://dx.doi.org/10.1016/S0925-4005(02)00317-9).
- Fischer**, L.H., Borisov, S., Schaeferling, M., Klimant, I., & Wolfbeis, O.S. 2010. Dual sensing of pO₂ and temperature using a water-based and sprayable fluorescent paint. *Analyst*. 135:1224-9. <http://dx.doi.org/10.1039/b927255k>.
- Fock**, A.W. 2013. Analysis of recreational closed-circuit rebreather deaths 1998-2010. *Diving Hyperb Med*. 43(2):78-85.
- Jones**, A. 2012. Redundant oxygen sensors: Theory and heresy. *Rebreather Forum* 3.0. Orlando, FL. 20 May, 2012.
- Kellon**, J. 1998. The true work of breathing in rebreathers. *Immersed, The International Technical Diving Magazine*. Spring 1998:30-3.
- Kuch**, B., Buttazzo, G., & Sieber, A. 2011. Bubble model based decompression algorithm optimized for implementation on a low power microcontroller. *Soc Underw Technol*. 29(4):1-8.
- Lloret**, J., Sendra, S., Ardid, M., & Rodrigues, J.J.P.C. 2012. Underwater wireless sensor communications in the 2.4 GHz ISM frequency band. *Sensors*. 12:4237-64. <http://dx.doi.org/10.3390/s120404237>.
- Park**, C.O., Fergus, J.W., Miura, N., Park, J., & Choi, A. 2009. Solid-state electrochemical gas transducers. *Ionics*. 15:261-84.
- Shashidhar**, R., & Kane, J. 2012. New real time CO₂ monitor for diver masks. In: *ONR-Navsea Undersea Medicine Program Review Abstracts*, pp. 68-9. Philadelphia, USA: ONR and NAVSEA. August 7-9.
- Shreeves**, K. 2009. Winner: Poseidon discovery. *Spectrum, IEEE*. 46:28-9. <http://dx.doi.org/10.1109/MSPEC.2009.4734307>.
- Shreeves**, K., & Richardson, D. 2006. Mixed-gas closed-circuit rebreathers: an overview of

use in sport diving and application to deep scientific diving. In: Proceedings of Advanced Scientific Diving Workshop, pp. 148-65. Washington, DC, USA. February 2006.

Sieber, A. 2012. O₂ Sensor Technology for Rebreathers. Rebreather Forum 3.0. Orlando, FL. 20 May 2012.

Sieber, A., Baumann, R., Fasoulas, S., & Krozer, A. 2011b. Solid state electrolyte sensors for rebreather applications: preliminary investigation. *Diving Hyperb Med.* 41(2):90-6.

Sieber, A., Enoksson, P., & Krozer, A. 2012. Smart electrochemical oxygen sensor for personal protective equipment. *IEEE Sens J.* 12(6):1846-52. <http://dx.doi.org/10.1109/JSEN.2011.2178593>.

Sieber, A., Jones, N.A., Stone, B., Pyle, R., Koss, B., & Sjöblom, K. 2011a. Embedded Systems in the Poseidon MK6 Rebreather. *Lecture Notes in Electrical Engineering.* 81(3). ISBN: 978-94-007-0637-8.

Sieber, A., L'Abbate, A., & Bedini, R. 2008. Oxygen sensor signal validation for the safety of the rebreather diver. *Diving Hyperb Med.* 38(1):38-45.

Vann, R.D., Pollock, N.W., & Denoble, P.J. 2007. Rebreather fatality investigation. In: *Diving for Science 2007. Proceedings of the American Academy of Underwater Sciences 26th Symposium*, eds. Pollock, N.W., & Godfrey, J.M., pp. 101-10. Dauphin Is., AL: AAUS.

Warkander, D. 2003. Temperature-based estimation of remaining absorptive capacity of a gas absorber. Patent published on April 24, 2003. WO 2003/034252

Wienke, B.R. 1990. Reduced gradient bubble model. *Int J Bio-Med Comput.* 26:237-56. [http://dx.doi.org/10.1016/0020-7101\(90\)90048-Y](http://dx.doi.org/10.1016/0020-7101(90)90048-Y).

Yount, D.E., & Hoffman, D.C. 1986. On the use of a bubble formation model to calculate diving tables. *Aviat Space Envir Md.* 57:149-56.

Yount, D.E., & Strauss, R.H. 1976. Bubble formation in gelatin: A model for decompression sickness. *J Appl Phys.* 47:5081-9. <http://dx.doi.org/10.1063/1.322469>.

Head-Up Display System for Closed Circuit Rebreathers With Antimagnetic Wireless Data Transmission

AUTHORS

Arne Sieber

SEABEAR Diving Technology,
Leoben, Austria, and Chalmers
University of Technology,
Gothenburg, Sweden

Andreas Schuster

SEABEAR Diving Technology,
Leoben, Austria, and ACREO AB,
Gothenburg, Sweden

Sebastian Reif

SEABEAR Diving Technology,
Leoben, Austria

Dennis Madden

University of Split School
of Medicine, Croatia

Peter Enoksson

Chalmers University of Technology,
Gothenburg, Sweden

ABSTRACT

Rebreather divers use LED-based head-up displays (HUD) as a primary display and warning device for the partial pressure of O₂ in the breathing loop. Such devices are usually mounted on the mouthpiece of the rebreather in the field of vision of the diver. LED-based HUDs are simple devices and can be designed so that they are easy to understand but have limited information content. Few alphanumeric or graphical screen-based HUDs have been developed in the past. Connecting such a device to a rebreather requires cable links, which divers dislike, and increases the risk of entanglement. State-of-the-art wireless data transmission uses ultrasonic waves or low-frequency electromagnetic waves; the former is not silent, and the latter achieves only very low data transmission rates of a few bytes per second and does not meet the antimagnetic standards required by military divers. The present paper describes a novel HUD system that incorporates a simple LED-based primary HUD along with an advanced secondary head-up diving computer with a micro organic LED screen. An optical infrared data transmission system is used to transmit all rebreather relevant data from the primary to the secondary device. One prototype of the system was manufactured and successfully tested in the laboratory according to relevant European standards as well as during several dives in fresh and sea water. **Keywords:** head-up display, near eye display rebreather, wireless underwater data transmission

Introduction

Head-up displays (HUDs), or near-eye displays, are mounted directly in close vicinity to the user's eye. In this position, they are always in the field of vision allowing the user to read the display without tilting the head or moving an arm to bring a wrist-worn device into the field of vision. HUDs are currently a hot topic in the media as well as in scientific journals. These discussions focus on the impact they may have on individuals and the society, especially when individuals are continuously updated with e-mails and social media alerts. Google glass,

for instance, is expected to come out later this year (Ackerman, 2013).

Near-eye displays have already been used in professional and military applications for several years, providing the user data about current position, speed, and heading. Displays with a graphical interface may also include a map. These displays provide a hands-free solution and update the user with data in real time, which may be a strategic advantage in professional and military applications.

Recreational divers usually choose where and when they dive. They normally select dive sites with good visibility and are often led by a guide. In

general, they do not perform dives in which they will be required to be continuously updated with navigational data. The need for information is different for professional and military divers, especially for Explosives Ordnance Disposal (EOD), Special Forces, and rescue divers. These divers are expected to dive in the worst conditions. They commonly face visibility close to zero (silt out), where reading a traditional wrist-worn diving computer (DC) may be impossible. In order to follow a predefined profile and course, divers have to be updated continuously with information about heading and depth, along with information

relevant to their breathing apparatus, such as tank pressure and breathing gas composition.

EOD divers use electronically controlled closed circuit rebreathers (ECCRs) as a standard breathing apparatus. In contrast to open circuit systems, most of the time, a failure of such systems is not obvious, and the diver has to rely on electronics and sensors rather than subjective perception. The most critical parameter in an ECCR is the partial pressure of O₂ (pO₂) inside the breathing loop. Failure of the O₂ sensors may quickly lead to a pO₂ above 1.6 bar or below 0.14 bar, a breathing mixture, which is no longer life sustaining. Failure of the pO₂ sensors is believed to be one of the major causes of rebreather fatalities (Vann et al., 2007). Therefore, most modern rebreathers are equipped with an HUD as a primary warning device consisting of one or more LEDs. It is placed on the mouthpiece of the rebreather in a position where it is always in the field of vision of the diver. However, such LED-based systems have limited information content since LEDs may only be switched on or off. More information can be communicated by using blinking and coded sequences; however, the downside of increased information is increased complexity. HUDs must be easy and clear to understand since incorrect breathing gas mixtures, or failure of the rebreather, may influence the mental readiness of the diver.

State-of-the-Art Alphanumeric HUDs for Diving

HUDs with alphanumeric displays for divers do already exist: The commercially available CompuMask (Aeris) and the DataMask (Oceanic) are recre-

ational DCs, which are fully integrated into a traditional diving mask. They are based on a liquid crystal display together with an optical system. These HUDs are based on a closed-system design, and therefore, no add-ons are possible. Although the Data Mask is well designed, it is only available in one size, limiting its use.

Gallagher (1999) and Belcher et al. (2003) developed head-mounted displays for EOD missions. These displays are larger and more expensive to produce, have high power consumption, and require cable connections. Designed and manufactured as military equipment, they are not available to recreational divers.

Previously, we mounted a graphical display with an optical system directly to the mouthpiece of a rebreather (Koss & Sieber, 2011a; Figures 3 and 4). With a carefully positioned device, good visualization of standard dive data was achieved. However, mouthpiece movements resulted in optical misalignments where the display (partially) moved out of sight. Later, we achieved excellent results using the display with a full face mask; in this case, the device was mechanically fixed in a desirable position relative to the eyes.

Following the rebreather display, we developed a technical DC with Trimix (helium, nitrogen, and oxygen breathing gas mixture) capabilities. As an add-on to the primary wrist-worn DC, an HUD was developed. Basically, this HUD showed an identical copy of the screen of the primary DC. As such, it had no microprocessor and was not able to work as a standalone unit without the primary DC. This device featured a unique optical design: The optical path of the system consisted of a solid Polymethylmethacrylate block, which was glued directly onto the visor of a diving mask. The prisma-

shaped lens, which is mounted inside the mask, produces a virtual image equivalent to viewing a 400 × 200 mm² display at a comfortable reading distance of 1 m. More detailed information can be found in our previous work from 2011 (Koss & Sieber, 2011a, 2011b). In general, the system worked well, but mounting the device on a mask turned out to be difficult; once glued onto the visor, the position could no longer be adjusted. Divers also found the cable between the HUD and the primary DC handset disturbing and irritating, especially with rebreathers. Two cable connections were required, one from the DC to the rebreather and another from the computer to the diver's mask.

In our previous work (Sieber et al., 2012), a new HUD system for full face masks was described. Commercially available "AGA style" full face masks were retrofitted with a port into which an HUD was introduced directly in front of the user's eye. To adjust the device, it was possible to rotate the HUD as well as to move it horizontally (left or right).

Several HUD solutions were presented in the past; however, there is no stand-alone device that is specifically developed for a rebreather and can work without a separate handset or controller unit. U.S. Navy EOD divers currently use the MK16 rebreather. These devices are equipped with a simple LED-based HUD. In contrast to LED-based HUDs, graphical or alphanumeric displays have the big advantage of being able to display a large quantity of information but may be more difficult to understand than a simple "red light" warning HUD. Therefore, in a meeting with representatives of the U.S. Navy, it was speculated that the ideal solution could consist of a two-component HUD system. This would include a simple LED-based

primary HUD, located on the rebreather mouthpiece, and a secondary mask worn organic LED (OLED) screen-based HUD, combining the advantages of both HUD design concepts. Ideally, rebreather and dive data should be transmitted to the secondary HUD via a wireless link in order to avoid a disturbing cable link (Koss & Sieber, 2011b). Rather than containing just a simple display, the mask worn device should preferably be a complete computer incorporating a microcontroller, pressure sensor, memory, and tilt-compensated compass—all features that one can also find in an advanced DC. Moreover, the device should also have sufficient processing power to perform decompression calculations in real time. The head-up DC (HUDC) should be a standalone unit with an integrated power supply, preferably rechargeable, and without any cable connections. Another important feature would be a tilt-compensated compass, which should provide heading information on the HUDC directly in the line of sight, facilitating easier navigation. To the best of our knowledge, no commercially available HUDs with an integrated compass exist today.

The current paper details the results of a first feasibility study, which focused on two goals:

- Research and development of a wireless transmission technology for the transmission of rebreather data from the mouthpiece to a mask worn device, with data transmission rates of at least 1 kBit/s. Additionally, a simple mouthpiece worn LED HUD will be developed. This technology should be able to pass antimagnetic requirements due to its intended use by EOD divers.
- Development of a standalone HUDC with a 32-bit microcon-

troller, digital pressure sensor, wireless interface, tilt-compensated compass, high-contrast OLED screen, rechargeable battery, and Universal Serial Bus (USB) port.

Methods Concept

The idea of the current project is a dual HUD, consisting of a primary LED-based HUD, located on the rebreather mouthpiece, and a secondary sophisticated HUDC with an integrated OLED micro screen. While the positioning of the primary LED-based HUD was obvious and well proven in the past by many rebreather manufacturers, one of the main questions remaining was where to mount the secondary HUD. Approaches from the past showed that HUDs mounted on the mask are easy to read. The optical path split design (Koss & Sieber, 2011b) was a good approach, especially when it comes to water and pressure resistance, but the inability to adjust the position was a disadvantage. A potential solution would be a one-piece HUD, mounted on a support from the frame of the mask, where the support could be designed in a way that enables easy tilting and rotation of the device.

The concept is displayed in Figure 1. The primary HUD sits on the mouthpiece of the rebreather and is connected to it via a cable, which can be routed along a breathing hose, so it does not disturb the diver. A secondary HUDC is mounted with a ball joint on the frame of a diving mask. In addition to the adjustment of the HUDC, the ball joint allows it to be tilted up and removed from the line of site completely when it is not required.

After discussions with EOD divers, it became clear that a cable link to a mask-mounted device will not likely

be accepted by divers as it increases the risk of entanglement. Divers would favor a wireless solution.

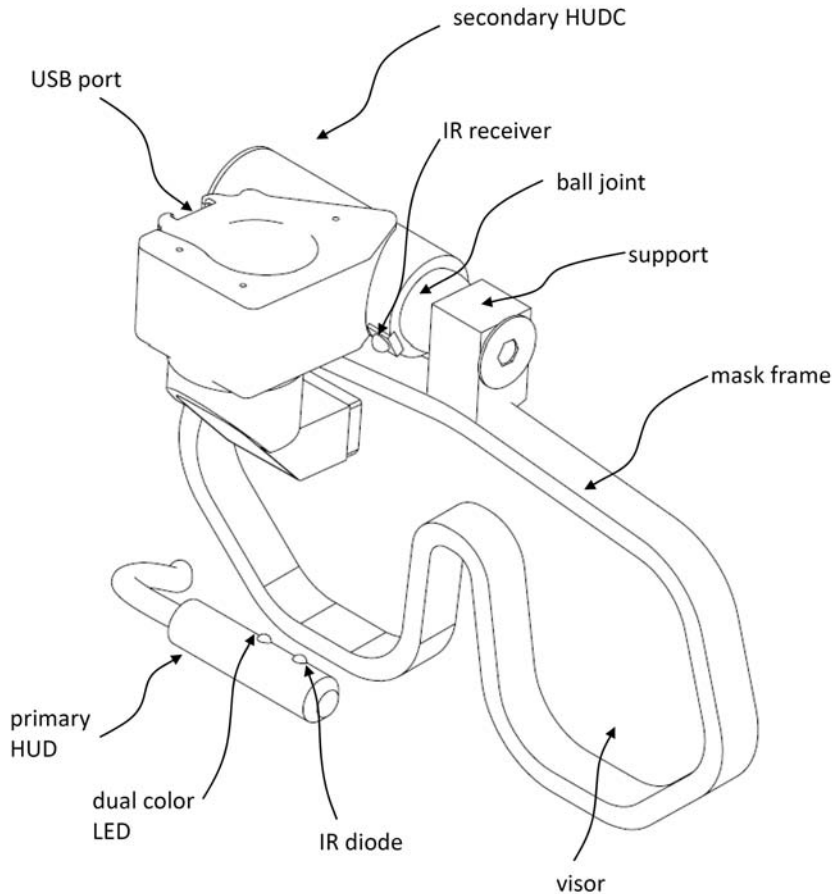
Wireless Data Transmission to the HUDC

Wireless systems used in SCUBA diving are based on electromagnetic data transmission with a low-frequency carrier (5–32 KHz). For instance, the DMR01 (Dynatron, Switzerland) (Mock & Voellm, 1992) is a low-cost, low-power digital receiver for underwater wireless data transmission used in popular DCs from Uwatec, Switzerland. Electromagnetic carrier frequencies from 5 to 32 kHz allow only low data transmission rates of a few bytes per second. This is sufficient to transmit simple data, such as tank pressure, but not adequate for all of the essential data from a rebreather with an update rate of 1–2 Hz. Another disadvantage of such systems is their magnetic signature, which does not allow their use during EOD missions.

An alternative underwater wireless data transmission could be Bluetooth or ZigBee-based devices, but with a 2.5-GHz carrier; the maximum transmission distance in sea water is limited to a few centimeters (Lloret et al., 2012). Acoustic modems based on ultrasound are suitable for underwater data transmission; however, as stealth and silence is of utmost importance for EOD and Special Forces divers, in general, such data transmission is also not acceptable. Optical data transmission fulfills antimagnetic requirements and is silent, but it requires a free line of sight between the transmitter and the receiver. In the case of an HUD, this line of sight can be achieved by placing the transmitter on the mouthpiece and the receiver directly above the secondary HUDC. The required transmitting distance

FIGURE 1

The primary HUD is located on the mouthpiece, and the secondary HUD is located on the frame of the diving mask. The primary HUD transmits data via an IR link.



(a few centimeters) is relatively short, which permits the use of infrared (IR) optical data transmission. Although the absorbance of IR light in water is of magnitudes higher than that of light with a shorter wavelength, such as blue (Pope & Fry, 1997), this remains a viable method of transmission.

Transmission Protocols

A variety of IR data transmission protocols exist. Before Bluetooth became available, the Infrared Data Association (IrDA) protocol (Knutsen & Brown, 2004) was popular for point-to-point wireless data transmission between handheld devices like cell phones or PDAs and a personal com-

puter. IrDA hardware is still available, but the complete implementation of IrDA requires a substantial software effort; in particular, the IrDA stack (required for pairing, handshaking, and controlling the data transmission) consisting of multiple layers has to be implemented. Other disadvantages of IrDA are the relatively short transmission range and its high sensitivity to external disturbances. While IrDA allows data rates of up to 1 GBit/s, the required data bandwidth for the rebreather is, at maximum, only a few hundred bits per second.

IR systems commonly found in the remote controls of home entertainment systems present an additional

and simpler option. These systems use a variety of methods for coding, for example, phase coding, pulse distance coding, or pulse length coding (Vishay, 2013). Although these codes are simple to implement, when it comes to transmitting several tens of bytes, it would be more favorable to use a preexisting hardware interface for the microcontroller. Instead of using software coding, it is possible to use the Universal Asynchronous Receiver/Transmitter (USART) interface at a suitable baud rate, in particular, the USART TX signal, to switch on and off a 36-kHz signal, which is then driving the IR diode. An ATxmega32A4 processor (Atmel) was chosen for the primary HUD. One of the internal timers is configured to generate a 36-kHz pulse width modulator (PWM) signal with a duty cycle of 10%. The output of the USART interface is configured as logic “and” with the PWM output signal and then further used to directly drive the IR diode.

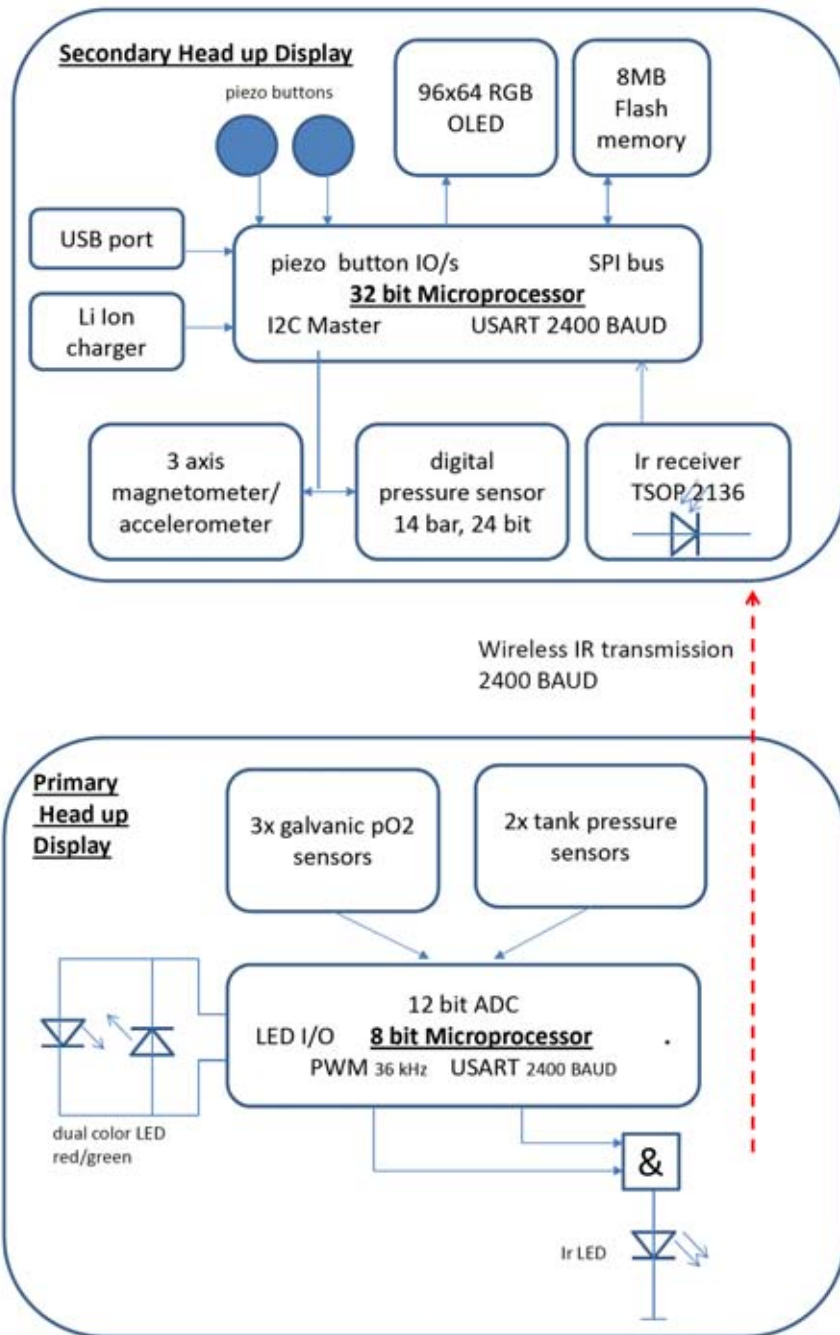
Demodulation of the signal is simple; the output of a suitable integrated demodulation circuit (TSOP 2136, Vishay) can be connected directly to the USART Rx pin of the AVR32 (Atmel) microcontroller of the secondary HUDC. The baud rate of the transmitter has to be carefully selected in order to match the specification of the receiver for minimum and maximum pulse length. When using a 36-kHz receiver, 2,400 bits/s is a suitable data transmission rate. If higher data rates are required, one may use a 450-kHz receiver and transmit with 19,200 bit/s; however, these receivers are difficult to find on the market.

Primary HUD Design

Figure 2 displays the overall electronic system layout. The core element

FIGURE 2

Electronic layout of the HUD system.



of the primary HUD is an 8-bit, low-power, ATxmega32 processor. This processor was chosen for four reasons:

- The 10-channel internal 12-bit analog-to-digital converter (ADC) with programmable amplification

allows the readout of galvanic O₂ sensors, as well as analog low-cost tank pressure sensors, without any additional analog circuitry.

- The internal clock of the processor is calibrated; thus, no external crystal is required.

- Atmel’s pico power technology allows an ultralow standby current of 0.7 μA, allowing a substantial reduction of the overall power consumption.

- The I/O (input/output) can be configured in many ways, including the hardware logic, “and” especially useful for the IR transmission.

One 4.2-V rechargeable Li Ion battery is used to power the circuit. Up to three O₂ sensor cells can be connected to the internal ADC through an 8-pin waterproof connector. This connector also allows access to the circuit programming interface and serves as a port to recharge the Li Ion battery. One I/O pin and a ground are used as water contact to switch on the primary HUD. Short-circuiting the contacts directly after startup enables the calibration mode.

Using IR remote control hardware, data transmitted are unidirectional. The primary HUD is programmed to transmit data via USART two times per second. The data are organized in a struct and include the pO₂ of three galvanic O₂ sensors, mV reading of the sensors, and tank pressures with a resolution of 0.1 bar (range: 0–300 bar). After the primary HUD is switched on, it sends an additional struct containing the serial number of the microcontroller, the software version, and all calibration data (mV readings of the O₂ sensors in O₂, ADC offset of the tank pressure sensors at 0 bar, and ADC readings at 200 bar tank pressure). An 8-bit checksum is included as the last 8-bit entry in each struct in order to detect transmission errors. Each struct consists of 24 bytes in total, and one transmission takes approximately 100 ms. In order not to block the processor during the transmission, the direct memory access is used to send the data for the USART

interface, so the microcontroller is free to process other tasks during the transmission of data.

Secondary HUDC Design

Rather than using an 8-bit microprocessor, as found in the primary HUD, an advanced 32-bit processor was selected. The main reason for this is that this processor also permits the calculation of modern and mathematically advanced decompression models in real time; otherwise, simplifications are required to calculate similar decompression schedules on an 8-bit processor (Kuch et al., 2011). The main specifications of the selected 32-bit AT32UC3B0256 processor include

- 256-kByte flash ram
- 32-kByte ram
- 10-bit ADC
- 1.8-V core voltage
- USB connector, including USB host
- direct memory access for serial peripheral interface (SPI), USART, and I2C
- event control system
- 12- to 66-MHz clock

One drawback of using microcontrollers with different architectures as in this case is the different endian signedness, which has to be taken into account when transmitting data from the 8-bit to the 32-bit microprocessor of more than 1 byte in size (e.g., float, double, etc.). A 96×64 pixel OLED display is connected to the microprocessor via the SPI and operates at 12 MHz. A step-up converter generates the required OLED drive voltage of 14 V. A 64-Mbit flash memory is incorporated to store dive relevant data, which are organized in a file allocation table (FAT) 16-file format. Once the microcontroller is connected to a USB bus, the internal memory is

recognized as mass storage memory, similar to a memory stick, and dive data can be read with file browsers like Windows Explorer. Depth is measured with a 24-bit digital pressure sensor (MS5803-14, Measurement Specialties, Switzerland). Data are read out via I2C interface two times per second. The conversion time of the sensor at its highest resolution is 10 ms. A digital three-axis magnetometer/accelerometer is connected to the microprocessor via I2C bus as well. It is used to calculate tilt and roll angles as well as the compass heading (ST Microelectronics, 2010). As in the primary HUD, a rechargeable Li Ion battery (type 16340) is included. An integrated charger circuit (MAX1555, Maxim IC) allows charging of the battery via USB in approximately 8 h. Two piezo discs are used as input buttons and are bonded to the inside of the polycarbonate housing with cyanacrylate glue. Pressing on the polycarbonate housing slightly deflects the piezo discs, generating a small voltage, which is sufficient to trigger an external interrupt on an I/O pin of the microprocessor. Except for one parallel load resistor of 1 M Ω , no additional analog signal conditioning circuits are necessary to interface the piezo discs. All of the electronic components are placed on a four-layer board with overall dimensions of 26×26 mm².

Optical Design

A typical HUD for diving is mounted in close vicinity (5–10 cm) from the diver's eye. A person with normal eyesight cannot focus on such short distances; thus, an optical system has to be introduced. In its simplest form, it consists of a single convex lens placed between the screen and the eye.

The smallest passive OLED screens available in small quantities have a diagonal of 0.6–1 inch. A single convex lens is magnifying the screen, which causes distortions of the image. In a previous paper, we described a two-lens system consisting of a concave lens and a convex lens. In this arrangement, an optical magnification of approximately 1 was achieved, which delivered good results in terms of readability. However, the lenses had a diameter, which was small compared to the OLED screen resulting in a small optical aperture. This caused a high loss of brightness, which made it difficult to read the display on the surface in bright sun.

The optical design of the secondary HUDC is detailed in Figure 3. It uses two lenses as well, but in contrast to our earlier system (Sieber et al., 2012), the concave lens, which is placed in 10-mm distance of the OLED, has a much larger diameter resulting in a brighter HUDC. The eyepiece is formed from a computer numerical control (CNC) machined planoconvex lens with a focal length of 45 mm. The plane side is in contact with water. Between the two lenses, a single-surface stainless steel mirror is placed to fold the optical path and reduce the overall dimensions. To be able to estimate the pressure resistance, a finite element analysis was done. The first prototypes of the housing, designed in SolidWorks 2011 (Dassault Systèmes), were CNC milled from black PVC (Figure 4).

Assembly

The optical parts were bonded to the PVC housing with ultraviolet curable glue. Before the lenses were inserted, the cavity inside the HUD was flushed with dry and clean air from a SCUBA tank to avoid water

FIGURE 3

The optical path of the secondary HUD consists of two lenses and a single surface mirror.

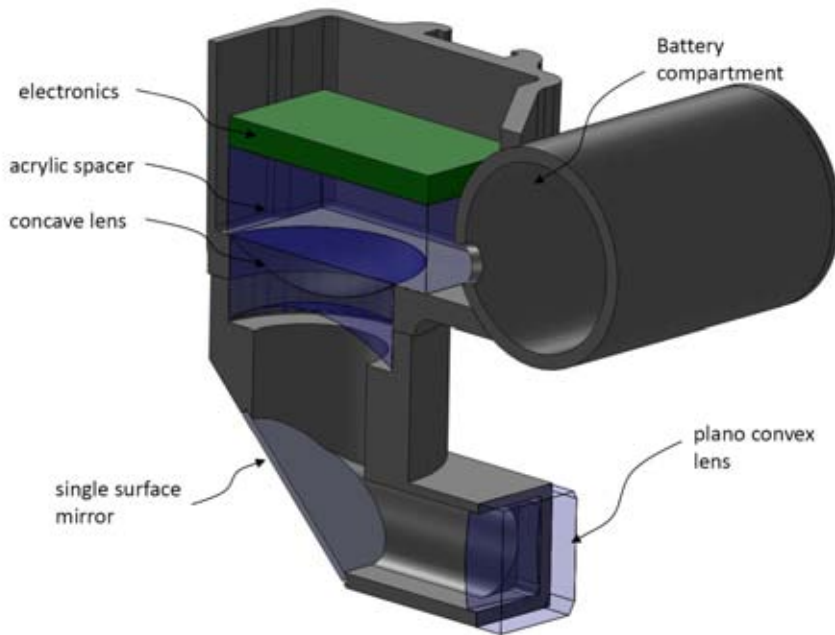


FIGURE 4

The primary HUD features two tank pressure sensors and can be connected to three galvanic pO_2 sensors.



condensation on the front lens during cold water diving. The electronic compartment was encapsulated in black polyurethane.

Software Development for the Primary HUD

The primary HUD reads up to three pO_2 sensors and two tank pressure sensors with a sampling rate of 1 Hz. Data are transmitted via an IR

link at 2,400 bit/s. To reduce the overall power consumption of the primary HUD, the ATXmeage remains in sleep mode as long as the device is out of the water. In order to detect an immersion, there are two water contacts at the side of the housing. One is connected to the ground, while the other one is connected to an I/O pin of the microcontroller. As soon as they are electrically connected (e.g., by water), an external interrupt is triggered, and the microprocessor wakes up. After a short initialization routine, which among other things initializes all the sensors, the program enters its normal operation mode. Ten seconds after leaving the water, detected again by the water contacts, the program sets the microprocessor back into sleep mode.

During normal operation, a bicolored LED informs the diver about the current status of the rebreather. To keep it simple, we limited the number of different blinking codes to four.

1. Green blinking, 500 ms on, 0.5 Hz: Everything is ok—the program runs, and all sensor values are within predefined limits.
2. Red blinking, 500 ms on, 0.5 Hz: Tells the diver to check the pO_2 —at least one of the oxygen sensors reads a pO_2 below 0.3 bar or above 1.5 bar.
3. Red blinking, 500 ms on, 1 Hz: Tells the diver that the pO_2 has reached a critical value—at least one of the oxygen sensors reads a pO_2 below 0.15 bar or above 1.6 bar.
4. No blinking: System is either off (which cannot happen under water, as long as the battery is not empty) or there is some sort of system failure. Additionally, the LED is used to communicate with the diver during calibration.

Since the included tank pressure sensors do not age, we hard-coded the calibration values for these sensors. Unfortunately, this is not possible for the oxygen sensors for two reasons. First, the divers can attach whatever galvanic oxygen sensor they want. Second, the output characteristic of galvanic oxygen sensors changes over their lifetime, which means recalibration will be inevitable.

To make the primary HUD as robust as possible, no buttons were included into the design. However, an input capability is required to initiate a sensor calibration. To solve this issue, a circuit was integrated that measures the resistance between the two wet contacts. Therefore, it is possible to differentiate between conductivity of water and, for instance, a metal. Based on this, a simple switching function was implemented: Within a short timeframe of a few seconds after primary HUD activation, the water contacts can be short circuited with a metal piece to initiate a pO_2 sensor calibration.

Calibration can be carried out either in air or in pure O₂.

Software Development for the Secondary HUDC

Depth Measurement and Decompression Modeling

The ambient pressure and surface pressure are acquired with a 24-bit digital pressure sensor. Pressure to depth conversion is performed according to the European Standard EN13319 where an increase of 1 bar of pressure results in a depth reading of 10 m.

In the first prototype, a Buehlmann ZH-L16C algorithm is implemented (Buehlmann et al., 2002) for decompression calculations. Nitrox (oxygen-enriched gas) and Trimix for open circuit and closed circuit diving are supported. Gradient factors (Baker, 1998) allow a personalized adaptation of the decompression schedule. A desktop software was developed under National Instruments Lab Windows to validate the decompression model against the original implementation from Baker.

Heading Calculation

An electronic compass can be designed from two orthogonally mounted magnetometers (two-axis magnetometer). These magnetometers are used to measure a 2D magnetic vector, which is then used for the heading calculation. It is necessary to hold the magnetometers horizontally, just like a traditional mechanical compass. When diving, where one is moving in a 3D space, typically no horizontal reference is available. Consequently, the compass is usually at least slightly tilted, and a single two-axis magnetometer would produce incorrect heading calculation. In cases of small tilt angles (usually referred to as pitch

and roll), compensation can be achieved with a two-axis accelerometer. Since the accelerometer output is subject to gravity, pitch and roll can be calculated directly from the acceleration vector. The angles are then used to calculate a tilt-compensated heading.

This compensation works reasonably well for small tilt angles. The HUDC, however, is mounted in a way that, when the diver adjusts the device by rotating it, a rather large pitch angle results. In such cases, simple compass designs based on two-axis magnetometer and two-axis accelerometer typically fail. Therefore, a three-axial magnetometer and a three-axial compass were integrated into the HUDC. This allows assessment of a true 3D magnetic and acceleration vector, which is then the basis for a tilt-compensated heading calculation (ST Microelectronics, 2010).

Such electronic compasses are subject to interferences and distortions requiring calibration to compensate. Two types of distortions influence the reading of the magnetometer. Hard iron distortions result only in an offset of the magnetic vectors. A calibration routine was implemented, which collects magnetometer readings while the device is randomly rotated in three dimensions by the user. Maximal and minimal readings are collected for each vector and used to calculate offset and gain for each magnetometer axis (Sieber et al., 2012). Soft iron distortions are difficult to compensate; therefore, a careful layout of the electronic circuit was required, where components containing nickel and others were placed in a safe distance of a few millimeters of the magnetometer.

File System and USB Mode

In predefined time intervals, all dive-relevant data including depth,

dive time, tissue tensions, pO₂, tank pressures, and decompression obligations are stored in files in a FAT 16-file system on the internal 64-MBit flash memory. All system-relevant events like startup time and date, user calibrations, or eventual hardware failures are stored in a separate file to achieve a continuous record of operation.

The secondary HUDC can be connected to the USB port of a personal computer or Android mobile phone. The HUDC is recognized as a mass storage device, and the files can be accessed. Additionally, it is also possible to upload a new firmware file, which is automatically updated after switching off the HUDC.

Results

One prototype each of the primary HUD and the secondary HUDC were assembled. These electronics were encapsulated in black polyurethane resin. A ball joint support was machined out of a PVC body and bonded to the frame of a diving mask.

The primary HUD is simple to install. As the input impedance of the three pO₂ channels is 50 kΩ and all three channels are independent from each other, it is possible to connect the HUD sensor interface to preexisting sensor readout hardware. For O₂ and diluent tank pressure readout, the HUD tank pressure sensors are connected to the first stages with off-the-shelf high-pressure hoses.

Initially, the assembled system was tested in an experimental pressure chamber to a maximum depth of 130 msw. After this test was successfully completed, the devices were mounted to an experimental, electronically controlled rebreather. Several in-water tests were carried out to a maximum depth of 10 mfw in an

indoor pool and at 30 msw in the Mediterranean Sea (Figure 5). During all the tests, the system worked flawlessly. An inbuilt test program, which checks the cyclic redundancy check of the transmitted data packages, showed that, in the pool, all received data packages were correct. In low visibility (<0.5 m) in a lake, less than 0.1% of the transmitted packages were corrupt.

A group of Special Forces test divers tried the mask during the Experience Week at Grundlsee, Austria (organized by Outer Limits, Austria). All divers reported that the image of the HUDC is clearly readable even when the silt is stirred up. The divers appreciated this true hands-free DC solution, especially when operating scooters or other underwater equipment.

The main specifications of the two devices are summarized below.

Primary HUD:

- Battery: rechargeable Li Ion
- Battery, 4.2 V, Trustfire 16340
- Power consumption: 10 mA > 2 years in standby mode
- Estimated autonomy: 60 h
- Dual-color LED (red and green)
- IR diode, 950 nm
- Resolution of the pO₂ sensor ADC: 0.1 mV
- Resolution of the tank pressure reading: 0.1 bar

FIGURE 5

Diver with a prototype of the HUD system.



Secondary HUDC:

- Processor: 32 bit, AVR32UC3B256, 12 MHz
- 14-bar ambient pressure sensor, 24 bit
- 64-MBit internal flash memory
- Battery: rechargeable Li Ion
- Battery, 4.2 V, Trustfire 16340
- Power consumption: 25 mA, 32 μ A, standby
- Autonomy: 25 h in diving, 2 years in standby mode
- Compass accuracy: $\pm 2^\circ$ for tilt angles up to $\pm 45^\circ$, $\pm 4^\circ$ for tilt angles between 45° and 70°
- Size: $52 \times 52 \times 56 \text{ mm}^3$
- Weight: 91 g including the battery
- Size and distance of the virtual image: approximately $30 \times 20 \text{ cm}^2$ in 1-m virtual distance
- Size of the visor: $20 \times 16 \text{ mm}^2$

The HUD system was tested according to EN250 and EN13319. Tests were carried out at DEKRA (notified body for personal protective equipment) in Essen, Germany. One concern was if the water absorption of the potting resin (Wevo 552 FL) could affect the function of the device. According to the specifications of the supplier, the water absorption of the potting material is less than 0.16%. In an experiment, an AtXmega processor was encapsulated with the resin and stored in artificial sea water for a period of 2 weeks at room temperature. No changes in functionality or electrical properties of the processor could be observed. The electrical sleep current of the processor before and after the experiment was 0.7 μ A; therefore, we concluded that the storage of the potted processor in sea water had no negative effects.

Conclusion

A novel HUD system was developed, which consists of a simple LED primary HUD located on the re-

breather mouthpiece and an advanced OLED-based secondary HUDC, which is mounted on the frame of a diving mask. The primary HUD reads three pO₂ sensors and two tank pressure sensors. A dual-color LED serves as a primary diver warning device. All data are transmitted via an IR link to the secondary HUDC, which also serves as a dive computer. Unlike other wireless underwater data transmission methods, the IR link can pass antimagnetic requirements, eliminating the need for cable connections, and is therefore useful for EOD divers. At the same time, it was shown that it is possible to miniaturize the HUDC to such an extent that it can easily be worn on the diver's mask without making the mask bulky.

The primary HUD as a first warning device is very simple to understand. The secondary HUDC presents all dive relevant information, including decompression obligations directionally heading to the diver. These design elements provide a unique advantage, especially in low visibility or "silt out" conditions, where the reading of a wrist-worn DC handset is difficult or even impossible.

Acknowledgments

The project was supported by the Center for Applied Technology in Leoben, Austria; the Austria Wirtschaftsservice AWS, Vienna, Austria; and the EU-FP7-Marie Curie Initial Training Network Phypode.

Corresponding Author:

Arne Sieber
SEABEAR Diving Technology,
Leoben, Austria, and
Chalmers University of Technology,
Gothenburg, Sweden
Email: Arne.Sieber@seabear-diving.com

References

- Ackerman**, E. 2013. Google gets in your face. *Spectrum*, IEEE, 50(1):26-29. Available at: <http://m.spectrum.ieee.org/consumer-electronics/gadgets/google-gets-in-your-face> (accessed 12 November 2013).
- Baker**, E.C. 1998. Understanding M values. Available at: <http://liquivision.com/docs/mvalues.pdf> (accessed 06 June 2013).
- Belcher**, E.O., Gallagher, D.G., Barone, J.R., & Honaker, R.E. 2003. Acoustic lens camera and underwater display combine to provide efficient and effective hull and berth inspections. In: *Proceedings of Oceans 2003*, pp. 1361-67. San Diego, CA: MTS/IEEE.
- Buehlmann**, A., Voellm, E.B., & Nussberger, P. 2002. *Tauchmedizin*. Auflage 5, ISBN-10: 3540429794, ISBN-13: 978-3540429791
- Gallagher**, D.G. 1999. Development of miniature, head-mounted, virtual image displays for navy divers. In: *OCEANS '99 MTS/IEEE*, pp. 1098-1104. Riding the Crest into the 21st Century. Vol. 3.
- Knutsen**, C.D., & Brown, J.M. 2004. *IrDA principles and protocols: The IrDA library Vol 1*. MCL Press, ISBN-13:978-0975389201. Available at: <http://irdajp.info/book.html> (accessed 08 May 2013).
- Koss**, B., & Sieber, A. 2011a. Development of a graphical head-up display (HUD) for rebreather diving. *Int J Soc Underwater Technol*. 29(4):203-8. <http://dx.doi.org/10.3723/ut.29.203>
- Koss**, B., & Sieber, A. 2011b. Head-mounted display for diving computer platform. *J Disp Technol*. 7(4):193-9. <http://dx.doi.org/10.1109/JDT.2010.2103299>
- Kuch**, B., Buttazzo, G., & Sieber, A. 2011. Bubble model based decompression algorithm optimized for implementation on a low power microcontroller. *Soc Underwater Technol*. 29(4):195-202. <http://dx.doi.org/10.3723/ut.29.195>
- Lloret**, J., Sendra, S., Ardid, M., & Rodrigues, J.J.P.C. 2012. Underwater wireless sensor communications in the 2.4 GHz ISM frequency band. *Sensors*. 12(4):4237-64. <http://dx.doi.org/10.3390/s120404237>
- Mock**, M., & Voellm, E.B. 1992. Patent US5392771. Underwater monitoring and communication system. Application date 17.8.1992.
- Pope**, R.M., & Fry, E.S. 1997. Absorption spectrum (380-700 nm) of pure water: II. Integrating cavity measurements. *Appl Opt*. 36(33):8710-23. <http://dx.doi.org/10.1364/AO.36.008710>
- Sieber**, A., Kuch, B., Enoksson, P., & Stoianova-Sieber, M. 2012. Development of a head-up displayed diving computer capability for full face masks. *Int J Soc Underwater Technol*. 30(4):195-9. <http://dx.doi.org/10.3723/ut.30.195>
- ST Microelectronics**. 2010. Application note AN3192. Using LSM303DLH for a tilt compensated electronic compass. Available at: http://www.st.com/web/en/resource/technical/document/application_note/CD00269797.pdf (accessed 22 May 2013).
- Vann**, R.D., Pollock, N.W., & Denoble, P.J. 2007. Rebreather fatality investigation. In: *Diving for science 2007*. Proceedings of the American Academy of Underwater Sciences 26th Symposium, pp. 101. Dauphin Island, AL: AAUS.
- Vishay**. 2013. Data formats for IR remote control, Rev. 2.0., 11 March 2013, document number 80071. Available at: <http://www.vishay.com/docs/80071/dataform.pdf> (accessed 08 May 2013).

An Experimental Deployment of a Portable Inflatable Habitat in Open Water to Augment Lengthy In-Water Decompression by Scientific Divers

AUTHORS

Michael Lombardi

Lombardi Undersea Resource Center,
Middletown, Rhode Island

Winslow Burleson

Arizona State University

Jeff Godfrey

University of Connecticut

Richard Fryburg

Subsalve USA, North Kingstown,
Rhode Island

Introduction

Historical Overview

The promise of undersea living or improving the experience of scientists and explorers along continental shelf margins has largely eluded modern ocean exploration efforts for more than half a century. The grander vision of realizing permanent undersea residence and colonies suffered setbacks that can be traced to the fall of the Sealab program in 1969 (Hellwarth, 2012). Although efforts in undersea living and habitation for science continue with government support in the United States, meaningful advancements and ambitions in terms of depth and duration have been considerably scaled back and remain precarious, with all missions taking place in relatively shallow waters. Most significantly, despite a record of successful missions, NOAA's Aquarius Reef

ABSTRACT

Undersea living in the science community has effectively risen and fallen within the last half century. The paradigm of residing on the seafloor within a fixed, permanent structure, while body tissues are saturated with inert breathing gasses, provides for extended-duration excursions from such a structure, although limits geographical productivity to within reasonable proximity of the habitat structure itself. Saturation diving exploration with science motives provided an exciting opportunity during the 1960s and 1970s, with timing lending itself well to providing a sea-to-space analog for human residence in a remote and confined space, as the space race was underway. With limited saturation diving for science occurring presently, today's marine science paradigm is trending toward advanced autonomous diving technologies and techniques, including mixed-gas use, rebreathers, and staged decompression. These emerging technologies afford an enhanced "commodity-style" approach to exploration, in which diving scientists can travel to any remote locale and spend longer durations underwater than they can with the previous and more common paradigm of lightweight, travel-friendly, conventional open-circuit scuba (using air as the breathing medium). Amiss in the new paradigm is the practical extension of depth. This is well within reach with the use of emerging technologies; however, end-users are often dissuaded from the incurrence of lengthy decompression (exposure to the marine environment during what is effectively an extended idle time) that is required when scientists return from relatively short working periods at extended depths. In an effort to address these issues, we describe here the development and experimental deployment of a new class of portable inflatable underwater habitats that provide for rapid deployments, free from surface support augmentation requirements typical of the existing alternatives for lengthy decompression dives. In the context of vastly expanding the commodity-style diving requirements of today's marine scientist and engineers, particularly in terms of increased depth and duration, we also discuss the further research and development applications that these habitats make possible.

Keywords: underwater habitat, rebreather, mixed-gas, scientific diving, decompression

Base Habitat in Key Largo, Florida, recently faced imminent shutdown due to loss of federal support in the wake of the United States' financial crises. Fortunately, the Aquarius Pro-

gram was rekindled with support from Florida International University in 2013 (Mesophotic.org, 2013) and currently remains the last permanent undersea habitat dedicated to

supporting scientific missions in the United States.

Living underwater has found some justifiable merit in the commercial sector, where industry-driven profits from resource exploitation provide sufficient capital to underwrite the substantial costs of the required technology and infrastructure to operate safely. Although it is commonly understood that risk aversion supports a trend toward replacing humans working underwater with new applications of advanced robotics and automated systems, such technologies are often viewed as permanent replacements. This misperception dates back to the early 1960s; the same time frame of the undersea habitation and resource exploitation boom—a time when the Shell Corporation claimed to have a robot that would “replace” divers (The Times News, 1962). Today, the fact remains that, more than a half century later, this replacement has not occurred. Placing humans on the seafloor to conduct meaningful work, across a multitude of industry and scientific communities, is still occurring with great frequency and is in high demand. In the scientific diving community, a small subset of occupationally classed diving operations, more than 100,000 dives are conducted annually within the United States (Dardeau et al., 2012). However, many of the same struggles exposed in the Sealab program (and similar habitat programs) remain: predominantly the aversion to accepting risk associated with the fundamental driver of placing humans on the seafloor, at unexplored or unstudied depths, and for periods of time to allow for productive work. At the core of these struggles is the challenge of effectively coupling human physiological limits with emerging tech-

nological approaches in ways that fundamentally improve the capacity for human intervention and innovation within the marine environment and on the seafloor, across the spectrum of both depth and time.

The Need for Novel Technologies That Support Improved Human Intervention Techniques

Marine scientists represent a population whose work requires scientific diving as a tool to afford observation and data gathering of diverse environmental parameters and personal interaction with seafloor flora and fauna. Given massive costs for operations, permanent undersea habitats offer very limited and largely ineffective opportunities for a growing scientific diving population that generally operates on lean field program budgets and thus increasingly can only afford to conduct fieldwork opportunistically.

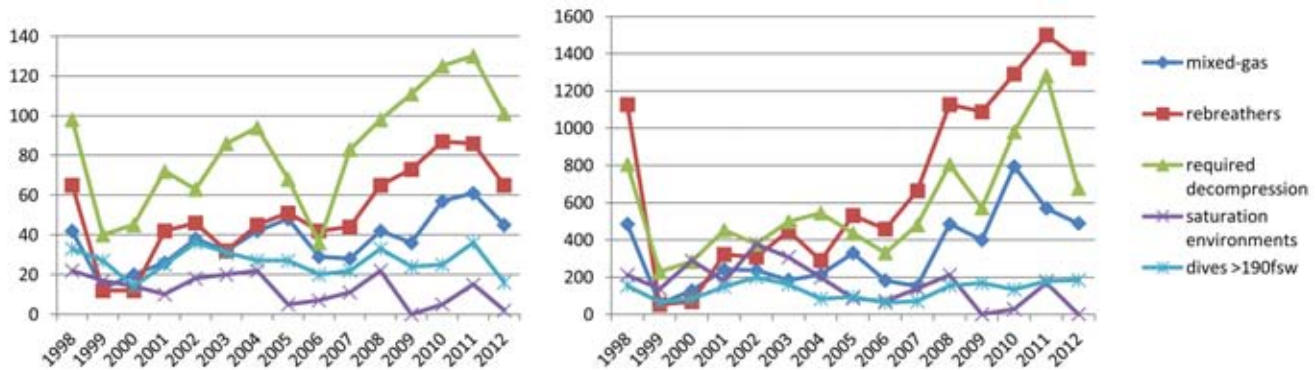
According to the American Academy of Underwater Sciences (AAUS) statistics reviewed from 1998 to 2012, there is a declining trend in both number of diver end-users and cumulative dives conducted from saturation (Figure 1). This is likely the result of realizing the limitations with shallow saturation diving as a tool for scientific diving, where geographical range is restricted to the habitat’s home base and depth is restricted to the immediate bathymetry. As the science community considers extending time underwater, increasing mobility, investigating a variety of sites, and extending operations to remote locales, the adoption of more advanced diving technologies and techniques are being explored, and their use is on the rise (Figure 1) with the desired intent of using these as “commodity tools.” This commodity-style approach to

diving has already occurred in the convention afforded by open-circuit scuba, where this mode of diving has become a standard tool in every diving scientists’ toolbox (in contrast to the inaccessibility of saturation or habitation models of fixed, controlled, costly, and permanent assets). This trend toward the broader adoption (or the commoditization) of increasingly advanced diving modalities is evident in Figure 1. These advanced modes offer opportunities for deeper depths and longer durations—effectively improvements on the prior commodity convention—and are evidence that scientific divers and exploration communities are both interested in and beginning to exert significant efforts to spend more time underwater in a cost-effective manner and with the opportunity to employ such capabilities across broader geographical locales than afforded with saturation diving.

Commodity technologies (open-circuit scuba) enabling end-user divers to effectively “pick up and go diving” have become effective for surface-to-surface scientific excursions in numerous types of environments, especially in remote environments, and to a broad spectrum of depths for decades. While trends in wet diving techniques indicate increasing use of frequency for decompression, rebreather, and mixed-gas diving, scientific diving activities below 60 msw (190 fsw threshold for AAUS depth reporting) have remained relatively constant (Figure 1). This may be due to several factors, including difficulty in attaining and maintaining deep diving proficiency within short field seasons, regulatory complexities such as insurance and liability concerns, and somewhat complex operational standards enforced at the home or host institution. Furthermore, limitations of working time at these

FIGURE 1

Trends in scientific divers' use of mixed-gas and rebreathers as modes of diving and in required decompression and saturation environments since 1998. Left graph indicates number of divers over time. Right graph indicates number of dives conducted over time. Data extracted from AAUS statistics database, accessed May 9, 2013.



depths, due to both the equipment required to be carried and the practicalities of carrying out lengthy decompression while exposed to the marine environment, can be psychological deterrents from carrying out decompression dives.

With the increasing availability of new commodity tools that improve human intervention within the marine environment and the resulting evident trend (Figure 1) in an increase of mixed-gas, decompression, and rebreather dives over time (but notably, not with increased depth), scientific divers are seeking to spend much greater time durations in the water. Looking ahead, as the existing advanced modes reach their limits in terms of these parameters, it is logical to consider the next steps in improving technologies or developing new technologies that support human intervention and how to make these increasingly accessible to the community that desires to use and benefit from them.

Our Realized Justification to Address the Need for Novel Technologies

Scientific field programs conducted in the Tongue of the Ocean (TOTO),

Andros, Bahamas (2010) and Exuma Sound, the Exumas, Bahamas (2011) provided novel access to mesophotic coral ecosystems (generally 60–130 msw; Puglise et al., 2009) using mixed-gas closed-circuit rebreathers (CCRs) (Lombardi & Godfrey, 2011). Dives were conducted to greater than 120 msw at each respective location by an autonomous team of two individual self-contained scientific divers without incident. While the dives were productive, with >35 min spent working at depths deeper than 80 msw on each dive, shallow decompression requirements accounted for the vast majority of the in-water dive time, that is, over 85 min or about 66% of total in-water time (Figure 2). Generally, these lengthy decompression exposures were cause for keeping planned total run times to less than 3 h for subsequent dives. This afforded contingency dive profiles of up to 4 h, which remains within the functional limitations of the divers' autonomous life support package. This package included a rebreather device and open-circuit bailout supplies that can be reasonably carried by each independent diver (not more than three AL80 cylinders each) while working from a small

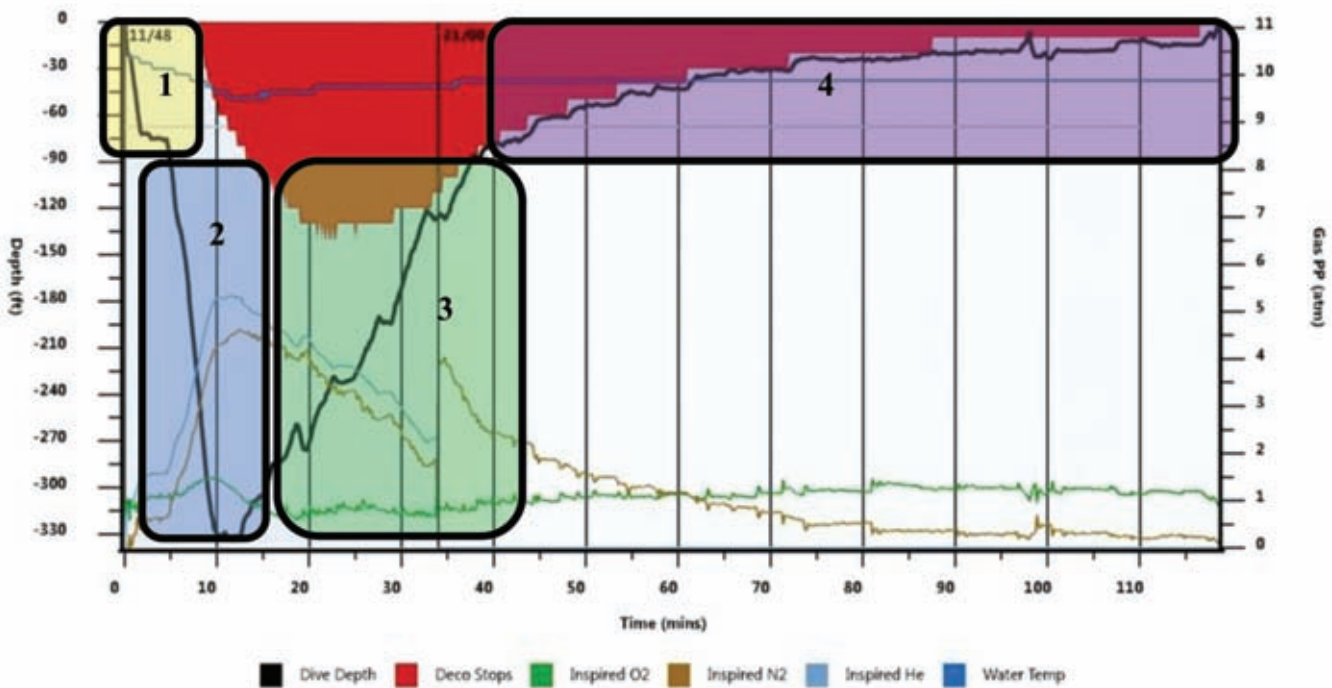
vessel. Pre-dive plans indicated that longer dives would push the limits of the full primary life support capacity reasonably carried by a single diver while working independently, free of surface or in-water support. Working bottom times were consequently restricted.

The scientific success and incident-free nature of the dives are encouraging with respect to extending both depth and duration of future dive profiles in ways that aim to improve intervention capacity and discovery potential. Lombardi and Godfrey (2011) describe approaching these working dives within the vertical Mesophotic Coral Ecosystem (vMCE) using a phased approach. While each identified dive phase (Figure 2) warrants further evaluation, the foremost resulting interest is to address the decompression phase of these deep dives. Decompression was carried out according to onboard rebreather computers using the Buhlman algorithm with gradient factors. Varied gradient factors, GF 5/95, 10/95, and 30/85, were anecdotally experimented with in an effort to maximize time spent on the vertical wall habitat. While ascending across the vertical plain, the ascent and early decompression can be coupled with

FIGURE 2

Sample scientific diving profile while working within the vMCE (in Lombardi & Godfrey, 2011). Profile breaks dive into phases based on specific operating procedures within that portion of the dive. Phase 4 indicates the lengthy decompression phase of the dive.

phase of dive	depth range (msw)	cumulative time in phase	avg dive time mean/stddev	% of dive
1	0 - 25	49 min	4 +/- 2	3
2	25 - 150	72 min	7 +/- 2	5
3	150 - 25	355 min	35 +/- 6	26
4	25 to surface	930 min	85 +/- 22	66



more productive work and thus reduce idle time spent in midwater while solely decompressing. Generally, the divers noted minimal work productivity benefits while forcing deeper decompression stops (GF 5/95) and therefore used GF 30/85 for all subsequently planned dives.

While mission objectives are typically completed before reaching the final stages of decompression, the longest portion of the in-water exposure remains. In this phase of the dive, ascending to the surface, without em-

ploying cumbersome surface technical support such as a pressurized bell, is not a viable option in the event of any in-water incidents, given the imminent threat of decompression sickness. Utilizing GF 30/85 encourages longer and shallower decompression stops. These stops account for the longest phase of in-water time, greater than 66% of the full surface to surface in-water immersion (Figure 2). The dive team described the final decompression phases for lengthy Mesophotic zone scientific exploration dives as

“wet, cold, and cumbersome.” During working dives conducted to 120 msw and greater, it was not uncommon to incur greater than 90 min of decompression at the 6 msw stop alone. These decompression phases are generally regarded as unproductive blocks of dive time.

Prior to engaging in a 2012 field season, the dive team sought to address the activity hazards associated with this lengthy decompression in this open-water environment (Figure 3). While hazards associated with equipment

FIGURE 3

Activity hazard analysis for the Phase 4 portion of decompression dives. Categorical hazards include those associated with environmental exposure, equipment used, and diver operations. Benefits and controls afforded by habitat use are identified for each categorical hazard.

Activity Hazards for Lengthy Decompression (Phase 4)

Hazard	Risk	In-Water Controls	Habitat Benefit/Controls
<i>environmental hazards</i>			
cold exposure	hypothermia	1. diver wears appropriate 'wet' exposure protection	1. removed entirely from heat conductive/water environment, no exposure
lengthy wet immersion	dehydration, pruned/soft skin	1. diver accesses hydration pack with fluids 2. diver wears drysuit 3. limit bottom time to reduce decompression exposure	1. diver accesses hydration pack with fluids, and/or food 2. exposure suit layers can be added/removed as required 3. bottom time can be lengthened
hazardous marine life	during decompression - stalking, bites, stings previously incurred during dive - prior bites, stings	1. reduce skin exposure with gloves, hood, full face mask 1. none - complete decompression (or abort) and administer first aid immediately upon surfacing	1. removed from natural environment, no exposure 2. remove injured diver from wet environment and provide preliminary treatment
currents	diver blown off site	1. physical lines used for diver transit 2. diver uses line reel/lift bag for drifting decompression 3. all redundant decompression gas supplies carried by diver for duration of dive to avoid lost cylinders	1. habitat provides destination point for final dive phase 2. diver can rest rather than 'hang on' for during lengthy stop
<i>equipment hazards</i>			
primary decompression gas source compromised	out of gas, reduction of required gas forced to utilize alternate decompression gas	1. carry redundant decompression gas in personal or team configuration 2. incorporate redundant surface supplied decompression gas via trapeze 3. stage redundant decompression gas 1. carry back-up computer or table 2. prepare for lengthened decompression time	1. alternate/redundant gas delivered in dry/controlled environment 2. redundant gas can be hard or soft plumbed into structure 3. habitat serves as depot/staging area for redundant gas supplies 1. alternate decompression schedules can be fixed as habitat contingency 2. longer decompression carried out in dry/controlled environment
CO2 scrubber failure	hypercapnea	1. diver has breathable OC gas source ready and immediately available	1. habitat provides fully redundant decompression gas supply
sensor/electronics failure	hypoxia/hyperoxia	1. diver utilizes redundant pO2 monitoring 2. dive aborted when primary monitoring fails	1. habitat provides fully redundant decompression gas supply
boom' scenario	rapid pO2 change, rapid buoyancy change	1. diver has breathable OC gas source ready and immediately available	1. habitat provides fully redundant decompression gas supply
<i>operational hazards</i>			
in-water injury - physical	cuts, scrapes, punctures, bites, stings	1. complete decompression, surface and carry out primary first aid response if warranted 2. abort dive, treat injury at surface, complete omitted decompression procedure	1. administer basic first aid upon reaching habitat, reduces primary response time 2. primary response in controlled environment without omitting decompression
in-water injury - physiological	DCS/DCI hypercapnea hyperoxia (due to pO2 creep or surge) hypoxia	1. identify IWR or omitted decompression procedures 1. diver has breathable OC gas source ready and immediately available 1. diver has breathable OC gas source ready and immediately available 2. verify proper diluent is feeding breathing circuit 3. verify solenoid/leaky valve, and/or O2 MAV are not stuck 'open' 4. verify ADV is working 5. verify diluent MAV is working 7. take action to decrease inspired pO2 1. diver has breathable OC gas source ready and immediately available 2. verify solenoid or leaky valve is working 3. verify oxygen MAV is working 4. verify ADV is not leaking hypoxic gas 5. take action to increase inspired O2	3. rebreather can be ditched, habitat provides fully redundant decompression gas supply 4. diver can be monitored for sign/symptom resolution 5. surface support/safety diver can intervene in dry/controlled environment
in-water injury - psychological	diver stress	1. encourage calm with dive partner 2. abort dive if stress distracts mission 3. enlist support diver to manage stress	

and operational procedures are factors, it became evident that many of these lengthy decompression activity hazards could be remedied by mitigating the risks associated with environmental exposure/immersion by the diver—removing the diver from the wet environment.

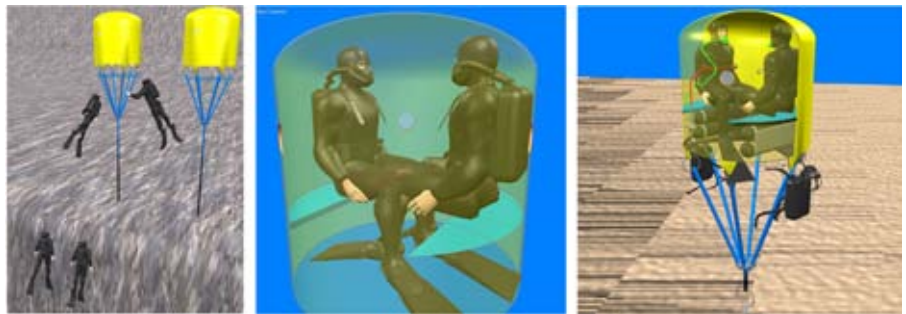
With the intent of extending working bottom times for future work and consequently incurring longer decompression obligations, the dive team moved forward with the design, construction, experimental deployment, and subsequent mission integration of a portable inflatable habitat as a possible solution to mitigate the activity hazards of lengthy decompression conducted by an autonomous team in an open-water environment.

Materials and Methods

Mission logistics for operating in a remote location with an autonomous two-person team, as well as study of prior art including Edwin's Link Submersible Portable Inflatable Dwelling (MacInnis, 1966), led to the choice of a flexible form-factor over a rigid structure for the purpose of ease of transport. Concept sketches (Figure 4) were generated to describe the basic envelope sought for the development project. The envelope pursued for development was a collapsible underwater tent, supported by a bridle attached to an anchorage, to be deployed to a fixed depth corresponding to the lengthy decompression that extended depth and duration dive excursions require. The tent structure would be equipped with bench seats and provide valve assemblies for inflation and deflation as necessary for both deployment and atmospheric management. This structure allows for variable life support systems to be integrated de-

FIGURE 4

Concept sketches of portable inflatable habitat structure in use. Habitat deployed at the reef crest serving as hub for dive staging (left). Two divers rest in habitat while each breathing independent primary life support used during the dive excursion (middle). Two divers rest in habitat while each breathing independent habitat-staged primary life support (right).



pending on mission requirements. The basic design envelope was developed over a period of 1 year and reflected the product of industry, academic, and private sector collaboration.

Design and Construction

System components include the following:

Tent/Shell

The primary structure is a 60-inch diameter by 60-inch tall fabric reinforced open-bottom vinyl shell supported by six 2-inch nylon safety straps and six stainless steel triangular fixation points. A tubular aluminum frame is affixed to 16 perimeter grommets RF welded to the inside perimeter of the shell, which support two bench seats. The shell includes three windows at eye level to permit outside observation. The tent is plumbed with two 3/4-inch NPT ports allowing fixation of quarter turn ball valves, one on the interior and one on the exterior, to allow for venting gas from the system. At 100% inflation, the tent/shell exerts 5,500 lb of buoyant force across the bridle.

Bridle

Six 20-foot-long straps (rated at 2,500 lb working strength each in choke configuration) are fixed one to each of the six stainless steel triangular fixation points. These join to two 20-foot long straps (rated at 8,800 lb working strength each in vertical configuration) connected by a 1-inch galvanized shackle (17,000 lb rated working strength). Each of the two downward straps is fixed to the anchorage, one via a three-quarter-inch shackle (9,500 lb rated working strength) and the other choked directly to the anchor pin.

Anchorage

The anchorage consists of a prior installed stainless eye pin drilled and epoxied into coral reef under an environmentally friendly mooring program installation coordinated by Environmental Moorings International while under contract with NOAA's Caribbean Marine Research Center. Previous tests in similar substrate indicate that the stainless pin will deform under a 20,000-lb pull test, with no pullout (Halas, personal communication, 2010).

Life Systems

For the initial experimental deployment, divers shed their open-circuit bailout cylinders and donned only their CCRs inside the habitat during lengthy decompression. No life support is provided by the surface.

Experimental Deployment

An experimental deployment was carried out at the Bock Wall dive site, Exumas, Bahamas (N 23.832, W -76.1529). This is one of the prior sites included in a regional environmental mooring program implemented by NOAA's Caribbean Marine Research Center. This site was chosen given the opportunistic stainless eye pin anchorage (Figure 5) that sits at the reef crest at approxi-

mately 20 msw and is immediately adjacent to the vertical MCE. Such permanent mooring hardware is now commonly used in tropical and subtropical environments with moderate to heavy vessel and dive traffic to avoid damage to coral reefs by dropping an anchor from the vessel.

The tent/shell and bridle were assembled at the surface prior to the dive, with careful inspections made of each fixation point. The system was folded and tied into a reasonably managed package to be carried by a single diver (Figure 5). The system was deployed in less than 30 min by the two-person dive team. Diver 1 entered the water, and the habitat system was handed to them from the vessel. Diver 2 entered the water and was handed the bench seat array. The

divers descended together, with the system, to the anchorage point and secured the two bottom straps making up the lower portion of the bridle. Lines used to pack the habitat for transport were removed and stowed. A small quantity of air was expelled from an independent aluminum 80 cubic foot scuba cylinder (AL80) into the bottom of the habitat, causing it to rise and extend the bridle.

The divers ascended, following the outstretched bridle, again inspecting its condition. The habitat was then reached, which rested at a depth of approximately 7 msw. The balance of the scuba cylinder was expelled into the habitat, causing it to displace all but the lower 1 foot of water in the habitat and to exert its maximum force on the bridle. Diver 2 placed the bench seat array into the habitat and held in place while both divers fixed the seats to the perimeter grommets using cable ties. The divers made a final visual inspection of all critical components and then entered the habitat one at a time. Each sat on a bench seat. Mouthpieces were removed briefly to communicate about the deployment process and to exchange initial thoughts on the overall comfort of the system.

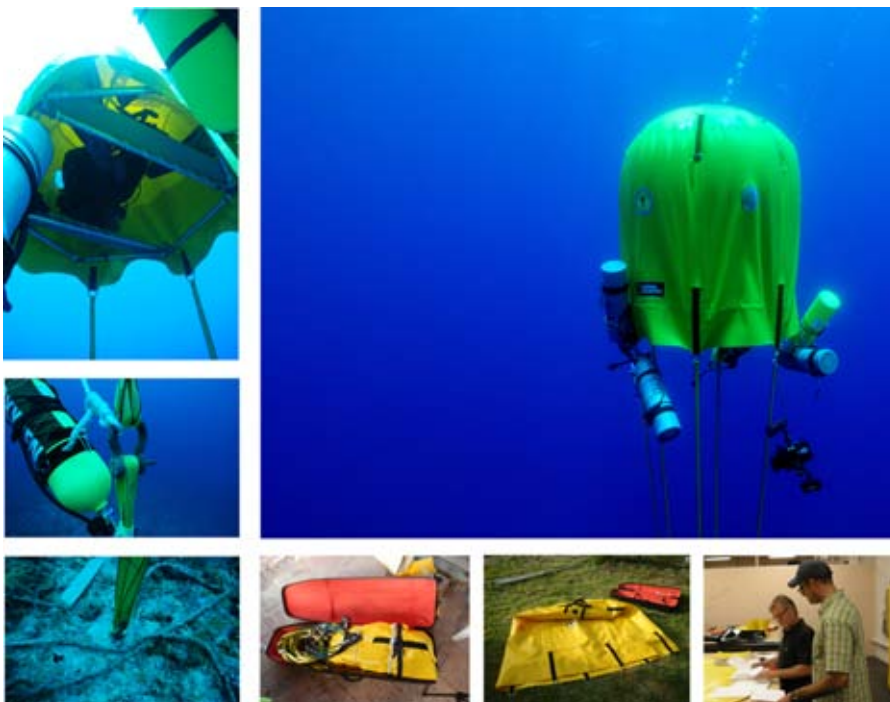
The divers exited the habitat one at a time, then surfaced, with a total dive time of less than 45 min.

Results Mission Integration

As proposed, the 2012 field program was to include the initial habitat deployment, followed by a series of five working dives within the vMCE, each progressing in depth and duration while making use of the habitat for the Phase 4 portion of the dive. Inclement weather delayed habitat deployment for 3 days, which resulted

FIGURE 5

Image plate revealing system components. Bench seat array from below (top left). Shackle mating bottom and top portions of bridle assembly (middle left). Stainless eye pin anchorage (bottom left). System packed for transport (bottom second from left). Habitat tent outstretched for inspection (bottom third from left). Authors Lombardi and Fryburg discuss design (bottom right). System successfully deployed and in use during lengthy decompression (main frame).



in a shorter mission; the habitat was used for only two working dives. Once deployed, the habitat remained in-water for the duration of the project, totaling an inflated and deployed duration of approximately 96 h on site.

The two working dives conducted were to 91 and 125 msw, respectively. Dives were planned to limit surface to surface time within the functional limitations of their primary life support, while providing for some contingency (approximately 4 h total immersion time). For this experimental deployment, the habitat was not relied on as decompression life support, but rather as augmentation of the planned dive for experimental purposes. It served to address the fit of portable habitats in mitigating the activity hazards (Figure 3) associated with lengthy decompression or Phase 4 of these deep scientific dives within the vMCE.

The two working dives were carried out successfully and without incident. Upon reaching the habitat, nearing the final decompression stop at 6 msw, the divers removed open-circuit bailout supplies and affixed these cylinders to the exterior of the habitat. Divers entered the habitat one at a time, while continuing to utilize their closed-circuit rebreather as primary life support. Once seated on the benches, an AL80 scuba cylinder of air was used to add gas to the habitat, displacing water to a satisfactory level near the bench seats. The divers found that, when sitting with the CCRs on their backs, it was more comfortable to allow water levels to increase to just above the diver's waist to displace a portion of the weight carried on the divers' backs. This arrangement satisfied the objective of removing the divers from the ambient environment, though it illustrates the need to improve system configuration for

comfort. Remaining decompression was carried out while at rest in the habitat.

Divers would occasionally remove their mouthpieces for a brief time period to communicate, though it should be noted that best efforts were made to reduce breathing the habitat's atmosphere via mouth or nose as this experimental deployment did not include habitat atmospheric management systems. The divers could also observe the outside environment via the three peripheral windows. Observations included small fishes peering through the windows and, generally, an attraction of larger reef fishes to the habitat structure.

Upon completing decompression, one diver exited the habitat at a time, picked up stowed open-circuit bailout cylinders, and then made a controlled ascent to the surface, completing the dive.

Discussion Benefits

Habitat benefits include providing a "dry" environment for diver rest, affording more direct diver-to-diver interaction and communication and providing an environment potentially suitable for conducting ancillary tasks such as preliminary sample processing. Diver function within this type of short to mid-duration space warrants continued evaluation to assess psychological benefits of dry versus wet immersion for these stays.

The most significant benefit stems from mitigating the activity hazards associated with Phase 4 lengthy decompression. These have been identified for previous vMCE scientific missions and categorized into environmental, equipment, and operational hazards (Figure 3). The convention for surface-

to-surface vMCE excursions has been to provide for in-water controls in response to the activity hazards. Throughout the experimental deployment, the divers made note of the benefits afforded from habitat integration (Figure 3). Benefits were apparent in each category of environmental, equipment, and operational hazards. Benefits stemmed from simplifying the divers' task load and removing them from the wet or ambient environment.

A future benefit that is immediately evident is being able to shed the primary life support system, which is often a closed-circuit rebreather. The complications of atmospheric management using a CCR can be limited, allowing for diver-operators to focus on atmospheric management of the habitat's atmosphere, independent of complex personal life support. While this will likely include a similar fundamental operating principle of carbon dioxide absorption and oxygen addition, management tasks can be shared by the dive team in a more relaxed manner.

Probable Complications

Complications were discussed prior to pursuing development. Obvious complications include added expense and increased logistical complexity when compared to an in-water only surface to surface mixed-gas CCR dive operation. The habitat assembly itself adds costs to the equipment required for these types of dives, though it is too early to assess the full cost-benefit and true financial benefit to a project as this portable habitat has not yet been applied in circumstances where its benefits are fully exploited. To do this, future work of increased depth and time at depth will force the habitat to be used as an essential and *dependent* piece of equipment, as dives will exceed the capacity of

personally carried life support (approximately 4 h immersion time). This dependence is also cause for considering further developments of habitat-specific life support systems, further redundant life support systems (Figure 6), and additional features to provide for comfortable lengthy stays. Using these types of habitats for extended stays will require dedicated atmospheric management and operator discipline for atmospheric control risks, including but not limited to elevated carbon dioxide levels and hypoxia.

While the system described is a portable unit for transport, there remains geographical restrictions in deployment, for example, an anchorage or other suitable means for securing the system to the seafloor is required. An advance mission, deploying an array of anchor points or moorings across a geographical region of interest, would provide for semipermanent study sites where one or more portable habitats can be deployed for mission-specific purposes. Using the bridle system also poses geographic restrictions

as the bridle is prefabricated at a specific length to place the habitat within the appropriate depth zone for the longest decompression obligations. While a variable depth system using a hoist mechanism with infinite adjustment, such as incorporated by Stone in Wakulla Springs, would allow for greater applicability across varying depth study sites, such a system would then pose the complication of ballasting the system such that the net buoyant force remains within the operating limits of a hoist mechanism. With required space within the habitat being fixed, ballast would come in the form of add-on weight, which may prove complex when working in a remote area. Alternatives to variable depth via a hoist mechanism may include a series of habitats at variable depths or transfer of the single habitat across a series of fixed loops or rigging. These evolutions are being considered carefully for future work, as variable depth capabilities will also allow divers to enter the habitat earlier in their decompression schedules. They will thus effectively be removed from the wet

environment for a greater portion of the idle time spent decompressing, again, mitigating risks associated with wet exposure (Figure 3).

Design Considerations

While numerous in-water hazards (Figure 3) are controlled by using the portable habitat, the habitat structure itself must also be assessed for various failure modes (Figure 6). While each component was constructed to meet a minimum 2:1 safety ratio, the unlikely event of a component failure needed to be addressed. Generally, a major component failure would leave the occupants immediately exposed to the ambient environment. As such, should the habitat be further developed for diver dependence as a primary life support system, efforts must be placed on redundant systems, and fly away systems where wet escape and further decompression could be safely carried out.

The consideration for mobility and cost-effectiveness of a wet dive team using CCRs needed to be maintained throughout the development process. Key design considerations included

FIGURE 6

Portable inflatable habitat failure mode analysis and recommended controls.

Failure Mode Analysis for Portable Habitat Use

Failure Mode	Risk	Controls
<i>system level</i>		
anchor failure	blow up, rapid ascent	1. use minimum 4:1 safety factor in design 2. adopt omitted decompression protocol
bridle failure	blow up, rapid ascent	1. use minimum 4:1 safety factor in design 2. adopt omitted decompression protocol
structure failure	dry environment floods diver re-exposed to wet environment	1. ensure immediate access to sufficient gas to commence decompression in open water 2. ensure exposure protection is donned or readily accessible
life system failure	loss of optimal breathing gas for decompression	1. ensure redundant life system in place
<i>operational level</i>		
inability to locate habitat	dependant on diver carried decompression gas	1. incorporate physical lines and rope highways to guide back to habitat 2. habitat becomes fixed in-water staging point on both descent and ascent

ability to meet rapid deployment requirements of a mission, a design to reduce activity hazards specific to the mission (Figure 3), a design to meet an accommodating form factor for the dive team, and should be inclusive of life systems integration and environmental control systems which match team equipment configuration and compatibility.

Generally, the design used for this experimental deployment matched all identified requirements. Four areas will continue to be the focus of ongoing development of this portable system. These include (1) basic life support systems for atmospheric management and redundant atmospheric management such that the habitat itself may be used for primary life support; (2) a variable depth capability comparable to the aforementioned Stone habitat used at Wakulla Springs; (3) improvements to permit making effective use of idle decompression time such as sleeping quarters, digital entertainment, work stations to begin sample processing, or improved observation capabilities; and (4) redundancy in the anchorage and bridle assembly.

With respect to the improvement of observation capabilities, a previous design by Clark (1972) sought to address this using a transparent film material for shell construction. The system offered vastly enhanced peripheral viewing of the environment. While transparent, the film required a net or mesh to provide shape and strength to the inflatable tent structure. Advances in available materials may provide for a more integrated and truly transparent system in the near future. This prospective added benefit of marine life observation with a transparent shell adds another dimension in making use of idle decompression time. The working divers

are still effectively immersed, with immediate and ready access to the shallow environments where decompression is being carried out. Limited wet excursions to carry out a task or the deployment of a remote observation tool or collection apparatus, in response to an opportunistic observation in the environment, will likely increase work productivity, thus reducing or eliminating truly idle time.

Newly Exposed Frontiers and Associated Risk

Previous efforts in habitation have largely focused on the idea of undersea permanence or living and working in the water column and on the seafloor. Efforts to pursue this have come at varying scales, though, until now, all have come with the commonality of requiring massive “top-down” infrastructure and support, which have restricted operations to fixed study sites. The expense associated with this is cost-prohibitive and lends little value to today’s human undersea science paradigms, in which the marine science community is eager to explore and study vast new geographic areas and multiple study sites.

The current diving paradigm is conducted through surface-to-surface approaches using commodity diving styles—predominantly scuba. Modes of scuba including mixed-gas, rebreathers, and decompression diving certainly fill an important niche, though they still come with limitations. Portable inflatable habitat technologies as a possible commodity tool, as opposed to permanent fixed habitats, offer a vehicle to (1) increase safety, by limiting diver’s wet exposure during decompression; (2) buffer idle time spent during decompressing; and (3) when used on shallow no-decompression dives, improve and vastly extend obser-

vation time. When coupling deep vMCE dives with this type of shallow outpost, day-to-day commodity-style diving can be meaningfully enhanced, opening up an increasingly significant new region of ocean space. This is a new “bottom-up” approach, providing full system autonomy that is at the same time highly portable.

This new found accessibility comes with newly exposed risks, though an incremental approach to continued innovation in this area will provide for mitigating these risks in a controlled manner.

Potential Role of Underwater Tents in the Not-Too-Distant Future

The integration of portable inflatable underwater habitats as a new commodity diving technology has the potential to open up a broad range of new diving experiences and profiles. Here we present a few of the possibilities that we anticipate emerging and maturing in the coming decade.

Extended Visitation Capacity Using Diving Outposts

As witnessed by the benefits of our initial deployments and the dramatic increase in demand for utilizing advanced diving modes by the scientific diving community, there is great potential for the type of flexible underwater habitats described in this paper to be widely employed by early adopters. We expect that this course of events will subsequently lead to a range of interesting features, configurations, and novel deployments. For example, the immediate next steps for our own development are to design and integrate multiple rebreather systems for use in the habitat itself. This will make the habitat capable of providing integrated life support that will, in turn, extend

the duration of the deepest portion of deep scientific dives.

In subsequent developments, extending the duration of integrated life support will lead to the mid-term realization of flexible habitats that will support divers' overnight stays. This could enable vastly extended decompression or prepare the crew for multi-day activities. As discussed, a variable depth capability would allow for decompression to occur while the habitat slowly rises through the water column, for example, during an overnight stay. This would enable the divers to realize significantly greater extensions of diving profiles—longer and deeper dives, with safe and relaxed decompression, while at rest overnight which is accepted as normal downtime during every human's diurnal cycle. While critics argue that similar technologies exist for modern era saturation and bell diving, the development effort to be placed is on increased portability, dramatically reduced costs, and eliminating required surface infrastructure and dependence. For consideration, the experimental system described and successfully deployed was transported in a suitcase and deployed rapidly from a small vessel with only minimal advance investment of the epoxied stainless pin used as an anchorage. Such investment includes just 1 day of advance labor per pin installation by a small team. This is a stark contrast to previous evolutions emphasizing human permanence with massive top-down requirements.

An ability to reside in a habitat overnight, coupled with the deployment of multiple tents within reasonable proximity, would enable a new class of multiday dives that could dramatically enrich the human experience underwater, ranging from more efficient scientific and engineering endeavors

within a greater range of depths and environments, to the opening up of a new class of saturation sport diving or tourism that has largely eluded the community for the past half-century. These could include a combination of deep and shallow outposts equipped with hookah type excursion capability, conventional scuba tanks, and/or rebreathers. Divers could traverse diverse saturation profiles, allowing them to, for instance, saturate at 20 msw and work laterally for as long as they like, followed by deeper downward excursions to carry out ancillary exploratory objectives. The dive might then culminate with variable depth decompression on a final overnight ascent to the surface.

Semipermanent Living Quarters

In the course of developing this flexible habitat, we have asked ourselves, "What would it take to make a habitat reasonably livable?" Flexible underwater tents might open the way for commoditizing semipermanent underwater living quarters in a wide range of environments across the planet. For instance, marine reserves or protected areas may include a series of staging areas to support deployment of these structures and facilitate a vastly enhanced human presence to carry out amplified science operations during precious field time.

A reference model, in terms of the use of space, is the Apollo Command/Service Module (CSM), which is capable of supporting a 14-day space mission. The CSM used for lunar missions had a cabin volume of 218 cubic feet (6.2 m³) living space. This space would yield 14,824 lb of buoyancy if submerged; adding a safety factor of 4 indicates a ballast requirement of 59,296 lb. While this is considerable, there are multiple ballast/anchorage

approaches that could be considered given today's mooring technology. First, having multiple smaller habitats with separate anchor points would greatly reduce the ballast requirement for any single anchor point. Anchoring/mooring technologies such as epoxied pins and drilled helical installations provide for relatively easy and inexpensive one-time setup across a variety of geographical locales and within varying substrates. The authors attest to this simplicity with firsthand experience installing such hardware across the spectrum of depths (to 100 fsw) and in varying substrates. Other approaches might include making opportunistic use of the local environment or target of interest—placing an inflatable habitat within a wreck, within a cave, under a ledge or mouth of a cave, within an iceberg (with suitable expandable insulation), or within manmade industrial spaces requiring exploration such as pipelines, tunnels, sumps, or aqueduct shafts.

While atmospheric management is the foremost consideration for near term evolutions of this innovation, other features required to support extended missions would certainly need to be addressed such as sustenance and waste products. While these have once been considered "rocket science" they are no longer; with multiple solutions having proven reliable by previous missions in space, on earth, at sea, and, most directly relevant, at depth. Many of these subsystems are off the shelf technologies at this point, requiring systems integration level engineering rather than complete novel system design.

Human-Robot Teams

Beyond the explicit features of the habitat and its capabilities, another exciting opportunity that a habitat

technology affords is a human platform for *in situ* mission planning and operation. While there are many exciting possibilities, we expect to see flexible habitats serving as command and control centers for hybrid human robot teams in the near term. Forthcoming collaborations will enable the integration of robotics in the form of both autonomous underwater vehicles and remotely operated vehicles (ROVs) to form hybrid human-robot exploration teams. A collocated underwater habitat in such a deployment would enable a “local” command center for multiple robotic activities, for example, scouting, routine monitoring or repair, or related standard activities, coupled with the ability to have close to real-time human intervention. This would enable, for example, a robot to prescout a vertical deep reef habitat and send imagery back to the divers in the habitat, until multiple targets of interest (and their corresponding precise depth and location coordinates) along the wall had been acquired and mapped. With these data, the divers could plan their dive for multiple contingencies that could serve to optimize scientific return and safety, planning which targets to visit first, for how long, and how to proceed in a considered manner. Conversely, a human exploration excursion may identify scientific targets of interest, which may be followed by immediate deployment of an ROV, from a command outpost or even controlled by the diver, allowing for the ROVs’ specialized instrumentation to be more accurately deployed via human intervention and guidance. This interaction will substantially reduce idle decompression time in between dive events or subsequent robotics deployments. Such *in situ* deployments involving robot and human teams operating at

close range will allow for a new diving paradigm enabling mutual support and ready follow-up with human and/or robotic intervention, as appropriate, when opportunities arise.

Acknowledgments

The authors would like to thank the National Geographic Society/Waitt Grants Program (Award W196-11 to ML) and Ocean Opportunity, Inc., for funding this field program. We also extend our thanks to the Bahamas Marine EcoCentre on Little Darby Cay, Exumas, Bahamas, and Mr. Wendell McKenzie for providing field support. Habitat illustrations provided by Anthony Appleyard. The authors also acknowledge their home institutions of Lombardi Undersea Resource Center, Arizona State University, the University of Connecticut at Avery Point, and Subsolve, Inc., for providing various in-kind assistance.

Corresponding Author:

Michael Lombardi
Lombardi Undersea Resource Center
307 Oliphant Lane #25, Middletown,
RI 02916
Email: michael@lombardiundersea.com

References

- Clark, J.F.** 1972. Lightweight Readily Portable Underwater Habitation and Method for Assembly and Emplacement. US Patent 3,706,206. Issued December 19, 1972.
- Dardeau, M.R., Pollock, N.W., McDonald, C.M., & Lang, M.A.** 2012. The incidence of decompression illness in 10 years of scientific diving. *Diving Hyperb Med.* 42(4):195-200. December 2012.
- Halas, J.** personal communication. 2010. Environmental Mooring International, Key Largo.

Hellwarth, B. 2012. Sealab: America’s Forgotten Quest to Live and Work on the Ocean Floor. New York: Simon & Schuster. ISBN 978-0-7432-4745-0. LCCN 2011015725.

Lombardi, M.R., & Godfrey, J. 2011. In-Water Strategies for Scientific Diver-Based Examinations of the Vertical Mesophotic Coral Ecosystem (vMCE) from 50 to 150 meters, ed. Pollock, N.W., pp. 13-21. In: *Diving for Science 2011. Proceedings of the American Academy of Underwater Sciences 30th Symposium.* Dauphin Island, AL: AAUS.

MacInnis, J.B. 1966. Living under the sea. *Sci Am.* 214(3):24-33.

Mesophotic.org. Available from: <http://www.mesophotic.org/2013/02/florida-university-to-take-over-operations-of-aquarius-underwater-habitat/> (accessed May 17, 2013).

Puglise, K.A., Hinderstein, L.M., Marr, J.C.A., Dowgiallo, M.J., & Martinez, F.A. 2009. Mesophotic Coral Ecosystems Research Strategy. NOAA Technical Memorandum NOS NCCOS 98 and OAR OER 2. 24 pp.

The Times News. October 31, 1962. Oil Firm Says Its Robot Will Replace Divers. Florida university to take over operations of Aquarius underwater habitat. 87(261).

Manufacturing Imperfection Sensitivity Analysis of Spherical Pressure Hull for Manned Submersible

AUTHORS

Bhaskaran Pranesh
 Dharmaraj Sathianarayanan
 Sethuraman Ramesh
 Gidugu Ananda Ramadass
 National Institute of Ocean
 Technology, Chennai, India

Introduction

Manned submersibles are designed and developed for applications like deep sea exploration, inspection, engineering intervention, etc. These operations are carried out by one, two, or three scientists sitting inside a pressure hull along with a pilot and at times have work capabilities by using robotic arms or other custom tooling. A pressure hull may be considered as a thin sphere, and it is a curved shell where thickness is small as compared to diameter of the body. A pressure hull is the main component in a manned submersible because it is a safe living space for pilots and scientists in deep water. The pressure hull must have enough strength to withstand high hydrostatic pressure, yet should be as light as possible for easy handling.

Analytical calculations are available in the literature for perfect geometry but rarely for imperfect geometry. The comparison of collapse pressure of a cylindrical shell may be obtained from numerical and experimental methods (Boote, 1997). The numerical results are in agreement with experimental results for actual imperfections

ABSTRACT

Any pressure hull invariably has imperfections as a result of the manufacturing procedure. Imperfections in a spherical pressure hull are the basis for localized buckling and deformation behavior. Numerical analysis and analytical calculations are carried out to predict the buckling behavior and strength of a pressure hull made of titanium alloy (Ti-6Al-4V) for both perfect and imperfect pressure hulls. Finite element analysis is carried out for different imperfection angles to see the effect on strength and buckling. Results of numerical analysis show that there is considerable reduction in both buckling pressure and strength as a result of imperfections. Hence, allowable deviation due to imperfection for a spherical pressure hull has to be considered for thickness calculations.

Abbreviations:

- P external pressure (Design pressure)
- D_m mean diameter of the pressure hull
- R_m mean radius of the pressure hull
- R_i imperfect radius of the pressure hull
- t thickness of the pressure hull
- ΔR imperfect deviation
- δ imperfection angle
- σ hoop stress
- P_y pressure at yield strength of the material
- P_b buckling pressure
- E Young's modulus of the material
- μ Poisson's ratio
- MSW meters of sea water
- APDL ANSYS Parametric Design Language

Keywords: manned submersible, pressure hull, buckling, imperfection, finite element analysis

measured. The authors carried out numerical analyses for different imperfect deviations at a central angle of 20° and derived the ultimate pressure formulae from finite element analysis. The results are verified through the experimental method (Pan & Cui, 2010; Pan, Cui, Shen, & Liu, 2010; Pan, Cui, & Shen, 2012).

Once the material crosses the yield limit and undergoes plastic deformation, it will not regain its original dimensions, so it adversely affects the functionality of the system. It is better to have yield strength as the limiting factor in pressure hull design. It is necessary to understand the reduction of strength and decrease in the buckling

pressure for different imperfection angles having yield strength as the limit. This paper describes the design and analysis of a pressure hull for a maximum operating depth of 6,000 MSW. The design of a pressure hull for deep water applications is an engineering challenge because of extreme pressure conditions and imperfections during manufacturing. In the present paper, a pressure hull has been designed using Det Norske Veritas (DNV, 1988) rules and finite element analysis. Analysis is done for the design depth of 9,000 MSW (1.5 times the operating depth) (Pan et al., 2010). Basic thickness (minimum thickness) calculated from finite element analysis is used further for imperfection analysis. Imperfection analysis is done for different imperfect deviations to understand how manufacturing imperfections affect the buckling pressure and strength of the pressure hull.

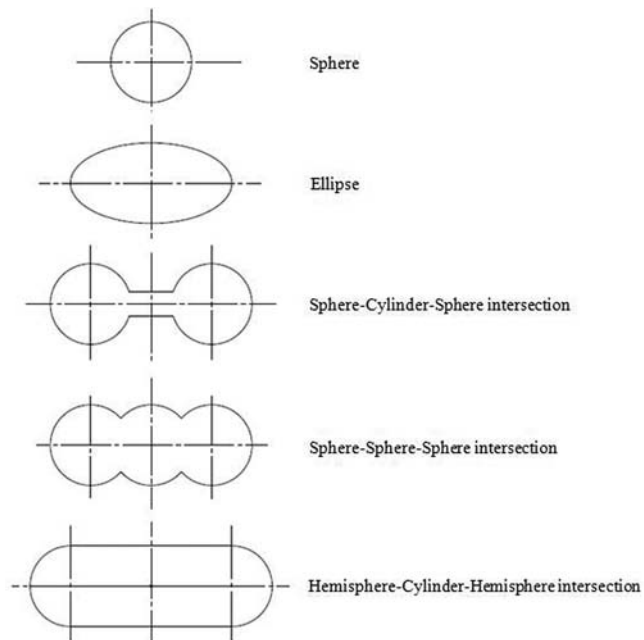
Shape of the Pressure Hull

The different possible shapes for the pressure hull—sphere, ellipse, sphere-cylinder-sphere combination, sphere-sphere-sphere combination, and other shapes—are shown in Figure 1 (Busby, 1976). Sphere shape is better than cylinder because required thickness of a sphere is one half of the thickness of cylinder of the same diameter. So, sphere is the most efficient and simple shape for a pressure hull to resist external hydrostatic pressure.

Structurally, it has the lowest weight per unit volume, but a spherical shape offers less internal space for housing personnel and equipment than a long circular cylinder with the same internal diameter. A spherical pressure hull gives better strength-to-weight ratio as compared to a cylinder. The stresses in a sphere are equal in all directions,

FIGURE 1

Different possible shapes of pressure hulls (Busby, 1976).



ignoring the effects of penetrations, supports, and imperfection.

The sphere gives the minimum weight-to-displacement ratio. Hence, the sphere is a more suitable shape for deep water applications.

Selection of Material

The selection of material depends on the strength it offers and the density. The design requirement is that the selected material should be suitable for a collapse depth of 9,000 m (1.5 times the operating depth). Figure 2 gives the collapse depth for different materials (Busby, 1976).

Figure 2 shows that steel and aluminum can be used for greater water depth with higher wall thickness, which in turn increases the weight of the pressure hull because the strength is less as compared to titanium alloy (Ti-6Al-4V), glass, or GRP. Commonly used materials in engineering design are steel, aluminum, and titanium,

and their material behavior is known. Having strength, less weight, designability, and fabricability in mind, titanium alloy (Ti-6Al-4V) is chosen as the pressure hull material. The advantages of choosing titanium alloy are high strength, low weight, and high corrosion resistance.

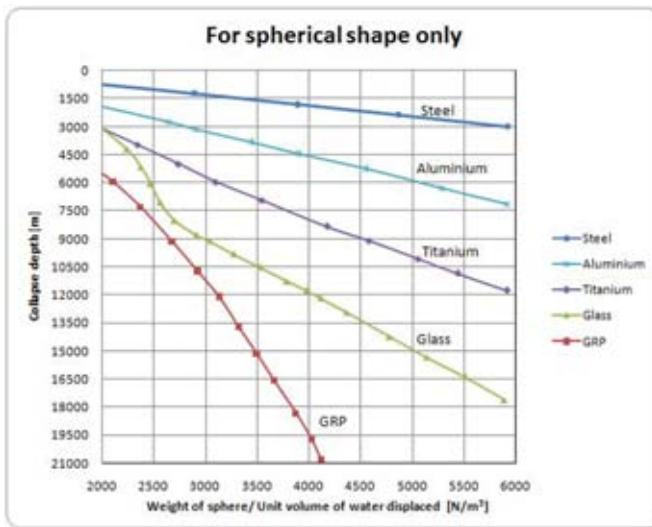
Geometric Parameters and Material Properties

Pan et al. (2010) have compared the existing designs of pressure hulls rated for 6,000 m of water depth. Their minimum internal diameter is 2,100 mm. The parameters assumed for a pressure hull made of titanium alloy analyzed in the present study are given below (Table 1).

Internal diameter	
of sphere hull	= 2,100 mm
Density of sea water	= 1,025 kg/m ³
Operating depth	= 6,000 m
	(Hydrostatic pressure
	~600 bar)

FIGURE 2

Collapse depth versus weight/unit volume of water displaced (Busby, 1976).



Design depth = 9,000 m
(Hydrostatic pressure ~ 900 bar)

Static Stress and Buckling Analysis (Analytical)

A spherical shell subjected to external hydrostatic pressure, assumed to be free of geometrical imperfections and free of initial stresses, develops a membrane state of stress (Nash, 1995). Hoop stress of sphere sub-

jected to external pressure is given by Young (2002) as

$$\sigma = \frac{PD_m}{4t} \quad (1)$$

Buckling pressure (when the sphere does not have any manufacturing defect) can be calculated by Nash (1995) and Young (2002):

$$P_b = \frac{2Et^2}{R_m^2 \sqrt{3(1-\mu^2)}} \quad (2)$$

Using equation (1), $t = 52$ mm, and substituting value of t in (2), $P_b = 339$ MPa.

DNV Approach to Find Thickness and Buckling Pressure

DNV is one of the common rules followed in manned submersibles design (DNV, 1988). Other standards, like ASME, ABS, BV, etc., can also

be used for designing the pressure hull, but each will have a different factor of safety and a different resulting thickness. DNV is chosen for the pressure hull design in this paper because it is commonly used in marine industries. It can be used to verify the analytical calculations. Thickness arrived from DNV can be used as a basic thickness for the pressure hull.

1. Thickness of the Shell

The thickness of the shell is calculated by

$$t = \frac{pD_1}{40\sigma_t - p} \text{ in mm.} \quad (3)$$

σ_t = Design stress in MPa = 620 MPa

p = Design pressure in bar (Design pressure is defined as the maximum pressure for which the submersible is designed to operate.)

D_1 = Internal diameter in mm

Using equation (3), $t = 52$ mm.

2. Elastic/Plastic Instability

When the pressure hull is subjected to external pressure then, the following condition must be satisfied.

$$p < \frac{p_{cr} \cdot \Psi}{\gamma \cdot \gamma_m \cdot K} \quad (4)$$

p_{cr} = Characteristic buckling resistance

γ = Load coefficient = 1.1 (applicable only for $p > 50$ bar)

γ_m = Material coefficient = 1

Ψ = Coefficient to reflect the post buckling behavior = 0.75 (for sphere)

K = Coefficient depends on type of structural member (this value depends on slenderness ratio λ)

$$= 0.7 + 0.6 \lambda \text{ (applicable only for } \lambda \text{ between 0.5 to 1)} \quad (5)$$

$$\lambda = \text{Slenderness ratio} = \sqrt{\frac{\sigma_f}{\sigma_e}} \quad (6)$$

$$\sigma_e = \text{Elastic buckling stress of imperfect sphere} = 0.605 \rho \frac{t}{R} E \quad (7)$$

$$\rho = \text{Reduction factor due to shape imperfection} = \frac{0.5}{\sqrt{1 + \frac{R}{100}}} \quad (8)$$

$$\text{Characteristic buckling resistance is } p_{cr} = 20 \varphi \frac{t}{R} \sigma_f \quad (9)$$

$$\varphi = \text{Plasticity modification factor} = \frac{1}{\sqrt{1 + \lambda^4}} \quad (10)$$

Using equations (5), (6), (7), (8), (9), and (10),

$\rho = 0.456$; $\sigma_e = 1639.7$ MPa; $\lambda = 0.753$; $\varphi = 0.869$; $p_{cr} = 801$ MPa, and $K = 1.15$. From equation (4), 90 MPa $<$ 475 MPa. Hence, the design is safe.

Finite Element Analysis Approach

Finite element analysis is carried out using a commonly used software, ANSYS. To arrive at the basic thickness of the pressure hull, 1/8 of the model is taken for the analysis by assuming loading and geometry conditions are symmetric, but for the actual pressure hull, it is not so. For computation, the following are used:

- Element type: SOLID95 (3D solid element has 20 nodes and 3 degree of freedom at each node)
- Linear material model
- Four elements across the thickness
- Symmetric boundary conditions

Initial thickness used for the analysis is 52 mm (from DNV approach). Results of the finite element analysis show that the maximum displacement and maximum von-Mises stress are 3.9 mm and 668 MPa, respectively. The minimum required factor of safety is 1.5, but from the above results is 1.39. Hence, the thickness is increased to 58 mm. The stress plot is shown in Figure 3, and results are satisfactory after increasing the thickness.

Stability Analysis of a Perfect Sphere

In stability analysis, both strength and buckling calculations are carried out. When $\frac{t}{D}$ is very small, that is, thickness is small as compared to diameter, the pressure hull fails by buckling rather than by yield, and when thickness increases the pressure hull fails at yield rather than buckling, though at a higher pressure. Yield pressures (P_y) and buckling pressure (P_b) are calculated for different thicknesses

using equations (1) and (2), respectively. The equations (1) and (2) are valid only for ratio $\frac{D}{t} > 20$ (Nash, 1995).

Figure 4 shows that there is an intersection of curves at ratio $\frac{t}{D} = 0.006$ and corresponding $\frac{t}{D}$ ratio is called critical $\frac{t}{D}$ ratio. If $\frac{t}{D}$ ratio $<$ 0.006 , it is called the buckling stage of failure, and if $\frac{t}{D} > 0.006$, it is called the yield stage of failure. The yield stage of failure will have higher buckling pressure because of a sharp increase in the curve.

For a perfect titanium pressure hull of diameter of 2,100 mm and thickness of 58 mm (i.e., ratio $\frac{t}{D} = 0.0276$) (i.e., without any imperfections), the possibility of failure is a result of yielding because material will reach yield pressure first then buckling pressure. Yield pressure and buckling pressure will vary for the real manufactured pressure hull because of manufacturing imperfections on the pressure hull.

Stability Analysis of an Imperfect Sphere

Manufacturing processes like deep drawing and welding introduce imperfection as a local deviation in geometry, as shown in Figure 5. Manufacturing errors result in deviation from the perfect sphere and cause an imperfect sphere. Imperfection leads to reduction in strength of the pressure hull through bending strength of the pressure hull. Strength decreases when the geometry changes from “flat spot” to “flatter.” A flat spot is a deviation from actual geometry having a higher radius with a finite center, whereas flatter is a deviation from actual geometry with a higher radius having an infinite center.

Stress analysis is done for the full sphere with $R = 1,050$ mm, $t = 58$ mm, $R_i = 1,300$ mm, $\delta = 20^\circ$,

FIGURE 3

von-Mises stress plot in MPa for 58 mm thickness.

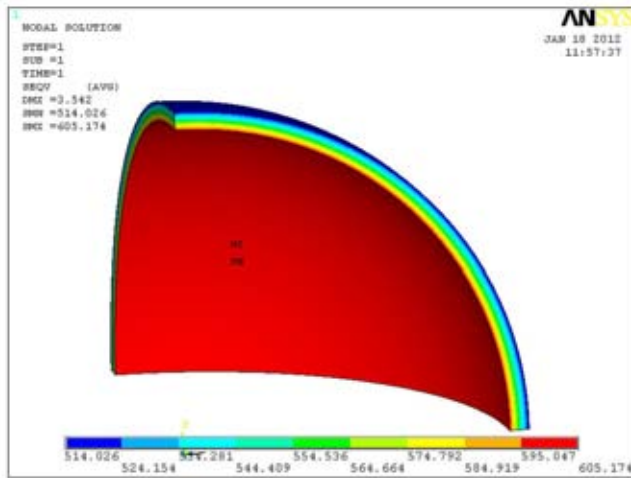
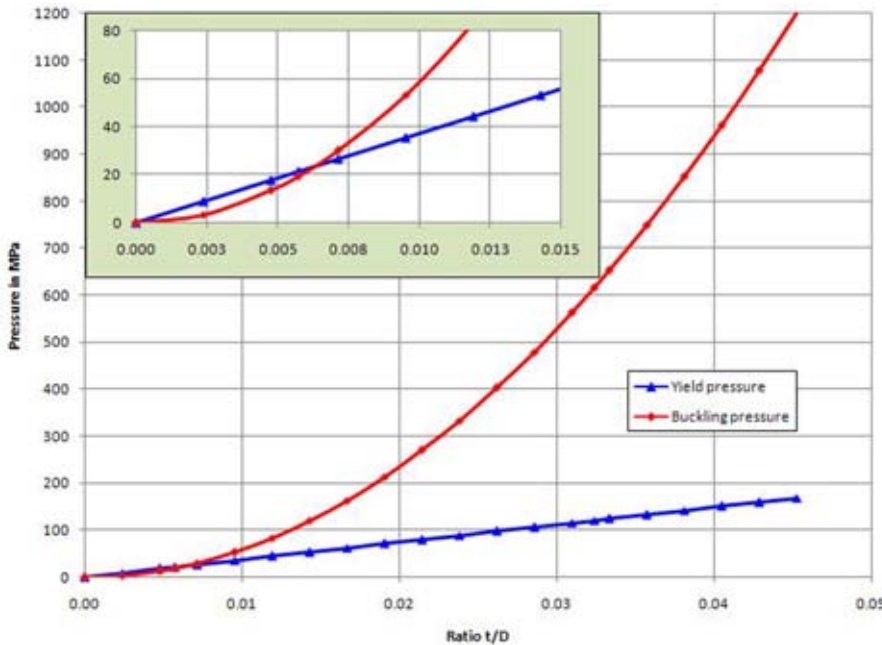


FIGURE 4

Pressure versus t/D ratio.



$\Delta R = 12.87$ mm, external pressure = 60 MPa. The displacement plot (Figure 6) shows that localized deformation of 5.22 mm and stress plot (Figure 7) give combined hoop and bending stress of 773.98 MPa as opposed to the stress value of 605.17 MPa obtained in the case of a perfect sphere (Figure 3).

There is an increase in stress by 27.8% on the sphere as compared to a perfect sphere. Buckling factor is reduced from 6.55 to 5.66, but still the buckling pressure is higher than the yield pressure. [Buckling factor is defined as the ratio between the buckling pressure and the applied pressure (60 MPa).]

Imperfection Sensitivity Analysis

A pressure hull is sensitive to imperfect deviation. ANSYS APDL (ANSYS Parametric Design Language) has been created for generating an imperfect sphere in the form of a “flat spot” to “flatter” by feeding known parameters radius of perfect sphere, thickness, and imperfection radius and chord length indirectly in the form of imperfection angle. APDL does the following activities: meshing, assigning material properties, static analysis, and buckling analysis. All degrees of freedom are fixed except radial direction on key points where the major axis of the sphere intersects. Outputs from the above analysis are deflection, stress, buckling factor, and mode shape.

When the imperfection angle (δ) decreases from 20° to 0° keeping the imperfect deviation constant, deviation shape changes from “flat spot” to “flatter.” Imperfect angle = 0° indicates perfect sphere. Figure 8 shows the results of stress analysis for the following parameters. $R = 1,050$ mm, $t = 58$ mm, $\delta = 5^\circ$, $\Delta R = 4.22$ mm, external pressure = 60 MPa. Maximum possible imperfect deviation for $\delta = 5^\circ$ is 4.22 mm. At $\Delta R = 4.22$ mm, geometry becomes “flatter” beyond which the only possible imperfection is “dimple” but for $\delta = 20^\circ$ and $\Delta R = 4.22$ mm imperfect geometry is not flatter; it forms an imperfection in the form of a convex shape. The comparison of numerical analysis results is given in Table 2.

Figure 9 shows the plot between buckling pressure versus deviation. When the imperfection angle is higher and deviation increases, there is a drop in the buckling pressure. Buckling pressure is almost constant for an imperfection angle of 5° .

FIGURE 5

Imperfect geometry.

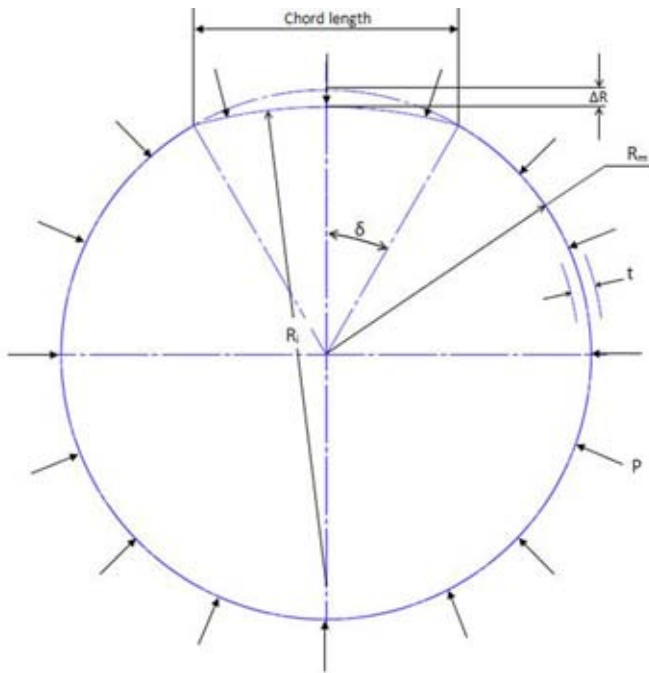
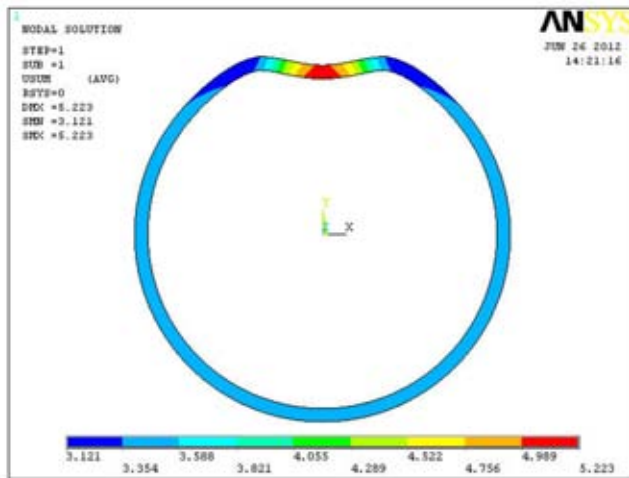


FIGURE 6

Displacement plot in mm ($t = 58$ mm, $\delta = 20^\circ$, $\Delta R = 12.87$ mm).



At deviation $\Delta R = 12$ mm and $\delta = 20^\circ$ buckling pressure is found to be 345 MPa, which is 3.8 times higher than the design pressure of 90 MPa. Although there is a drop in the buckling pressure, still it is higher than the yield pressure.

Figure 10 shows that when deviation increases there is a decrease in factor of safety (i.e., increase in stress). The numerical analysis results shows the stress pattern of the localized stress migrating from edge to center, which is the result of imperfect deviation

changes from “flat spot” to “flatter.” Stress on the edge behaves like a flat spot with fixed support, whereas the stress on the center behaves like a flatter with simple support.

The flat spot behaves like an intersecting sphere on the main sphere, but flatter behaves like a flat plate with external pressure. So the strength of the pressure hull depends on both shape and magnitude of imperfection. Geometric imperfection introduces bending stresses in addition to circumferential stresses. So, the imperfection leads to large displacement and higher stress on the pressure hull.

This imperfection is a result of a localized manufacturing defect. It is impossible for the manufacturer to have a zero rate of imperfection. Hence, the designer has to specify the imperfection tolerance. As per DNV rules for classification/certification, the local imperfection tolerance is not to exceed 0.5% of the nominal mean radius of the spherical shell (DNV, 1988). For the present case, the tolerance is 5.4 mm. Figure 10 shows that for imperfect tolerance of 5.4 mm the factor of safety are closer to 1.4 but the minimum required factor of safety is 1.5. Hence, the thickness of the pressure hull has to be increased to account for localized imperfection.

The revised thickness is the sum of basic thickness and thickness to take care of imperfection. By considering the imperfection, the required thickness for the pressure hull is 64 mm.

Results and Discussion

Analytical calculations are carried out to find the thickness and buckling pressure. The initial thickness of the pressure hull is found to be 52 mm. Analytical calculations have an assumption of a thin shell, and mean

FIGURE 7

von-Mises stress plot in MPa ($t = 58 \text{ mm}$, $\delta = 20^\circ$, $\Delta R = 12.87 \text{ mm}$).

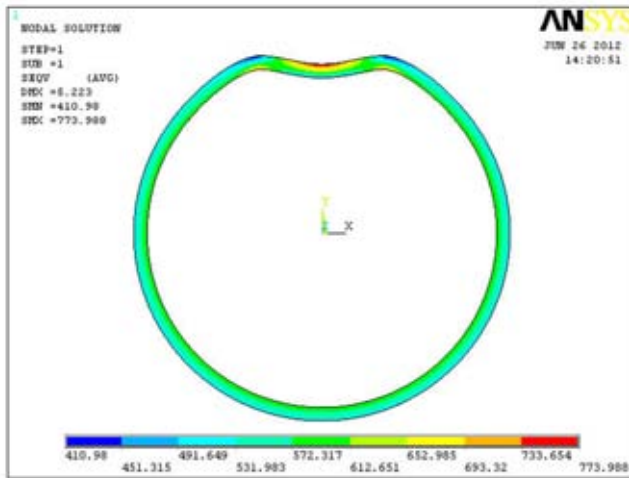


FIGURE 8

von-Mises stress plot in MPa ($t = 58 \text{ mm}$, $\delta = 5^\circ$, $\Delta R = 4.22 \text{ mm}$).

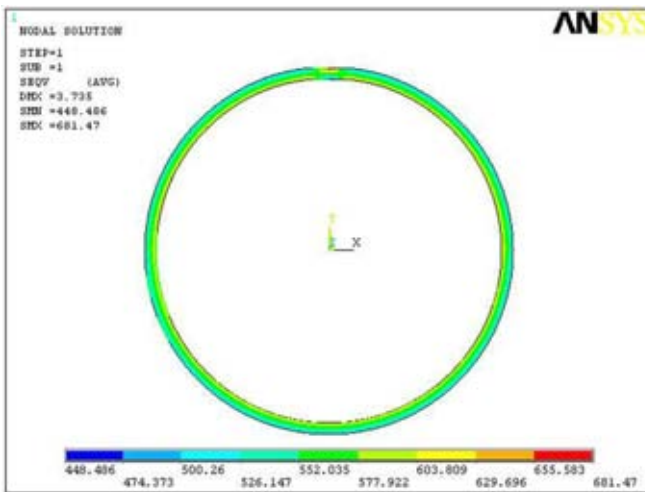


TABLE 2

Numerical results for different imperfection angles for the same deviation.

Imperfection Angle (δ)	Deviation (ΔR) in mm	Displacement in mm	Stress in MPa	Factor of Safety	Buckling Pressure in MPa	Shape of Imperfection	Location of Stress
5°	4.22	3.74	681	1.37	392	100% flat	Stress at center of imperfection
20°	4.22	4.02	644	1.44	380	Convex	Stress at edge of imperfection

diameter is taken for the calculations. But in the case of finite element analysis, thickness is modeled as a parameter. There is a variation of stress across the thickness, and maximum stress is on the inner surface of the pressure hull. The calculated factor of safety is 1.39. To have a minimum factor of safety of 1.5, the thickness is increased to 58 mm.

Imperfect sphere analysis is carried out by considering additional parameters imperfection angles and imperfect deviation along with basic thickness of 58 mm. Finite element analysis is carried out for an imperfect sphere by varying the imperfection angle and imperfect radius. Stress, deflection, and buckling pressure are the output from the analysis. Results show that there is a drop in the factor of safety and buckling pressure whenever there is an increase in imperfection on the sphere. There has to be minimum manufacturing tolerance without compromising on the minimum required strength. In order to have both tolerance and minimum strength, thickness of the pressure hull is increased to 64 mm.

Conclusions

The radial imperfection on the radius is considered for the analysis. It is impossible for the manufacturer to

FIGURE 9

Buckling pressure versus deviation.

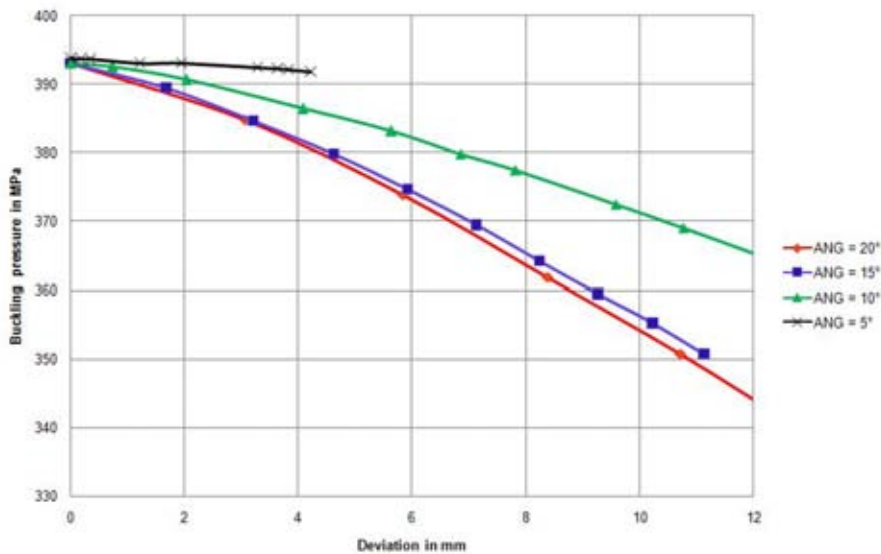
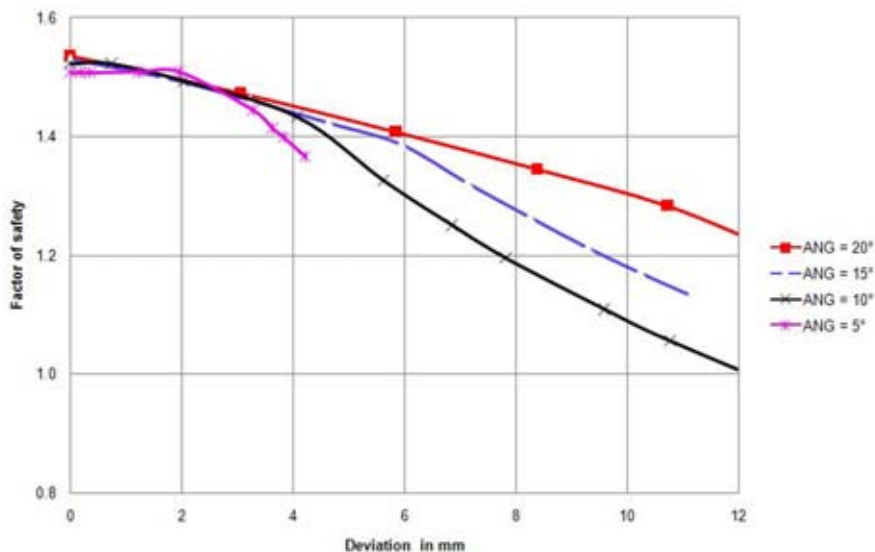


FIGURE 10

Factor of safety versus deviation.



manufacture the perfect sphere. In the above analysis, imperfection is considered at one place, but in reality it may be in a number of places at random intervals. Since the imperfection is a localized behavior, the effect is same in all imperfection places.

1. Basic thickness from the above analysis is 58 mm. This thickness is increased to 64 mm by considering the localized imperfection based on the allowable limit of imperfection tolerance obtained from DNV.

2. Localized imperfection leads to an increase in local deformation and reduction in strength (i.e., increase in stress). This localized stress can be reduced by increasing the thickness of the pressure hull. Pressure hull failure can be avoided by anticipating the percentage of deviation that might occur during manufacturing based on how much the thickness has to be increased from base thickness.
3. These results have to be further studied by conducting experiments for the scaled models.

Acknowledgments

The authors gratefully acknowledge the support extended by the Ministry of Earth Science, Government of India, in funding this research. The authors would like to express sincere thanks to the Director of the National Institute of Ocean Technology (NIOT) for his continuous support of research activities and also would like to thank the team members of the submersibles and gas hydrates group of NIOT.

Corresponding Author:

Bhaskaran Pranesh
National Institute of
Ocean Technology,
Velachery-Tamparam Road, Pallikaranai,
Chennai - 600 100, India
Email: pranesh@niot.res.in

References

- Boote, D.** 1997. Elastic instability of thin cylindrical shells: Numerical and experimental investigation. *J Ocean Eng.* 24(2):133-60. [http://dx.doi.org/10.1016/0029-8018\(96\)00004-2](http://dx.doi.org/10.1016/0029-8018(96)00004-2).
- Busby, F.** 1976. *Manned Submersibles*. Virginia: Office of the Oceanographer of the Navy. 776 pp.

- Det Norske Veritas.** 1988. Rules for Certification/Classification of Submersibles. Norway: DNV. 64 pp.
- Nash, W.A.** 1995. Hydro Statically Loaded Structures; The Structural Mechanics, Analysis and Design of Powered Submersibles. England: Elsevier. 195 pp.
- Pan, B.B., & Cui, W.C.** 2010. An overview of buckling and ultimate strength of spherical pressure hull under external pressure. *J Mar Struct.* 23(3):227-40. <http://dx.doi.org/10.1016/j.marstruc.2010.07.005>.
- Pan, B.B., Cui, W.C., & Shen, Y.S.** 2012. Experimental verification of the new ultimate strength equation of spherical pressure hulls. *J Mar Struct.* 29(1):169-76. <http://dx.doi.org/10.1016/j.marstruc.2012.05.007>.
- Pan, B.B., Cui, W.C., Shen, Y.S., & Liu, T.** 2010. Further study on the ultimate strength analysis of spherical pressure hulls. *J Mar Struct.* 23(4):444-61. <http://dx.doi.org/10.1016/j.marstruc.2010.11.001>.
- Young, W.C., & Budynas, R.G.** 2002. *Roark's Formulas for Stress and Strain.* New York: Mc-Graw Hill. 855 pp.

A New Generation of ADS Capabilities

AUTHOR

James F. Clark
J. F. White Contracting Company,
Framingham, Massachusetts

Background of CAT/DEL 210-G

In 2007, New York City Department of Environmental Protection (NYCDEP) awarded a \$1.1 billion contract to the SEW Joint Venture (Skanska/Ecco/White) for construction of the largest drinking water treatment facility ever built anywhere in the world. This massive project, CAT/DEL 210-G, was designed to provide ultraviolet light disinfection for the principal water supply to New York City at a site in Westchester County where the Catskill and Delaware Aqueducts pass in close proximity. The Delaware Aqueduct at this location is a deep rock tunnel, but during construction in the 1930s, the Board of Water Supply (predecessor of NYCDEP) designed a massive underground vault structure as an accessible connection to the aqueduct near ground level. It was originally anticipated that water treatment could be required someday in the future. After 75 years, the future had arrived, and ultraviolet treatment was the process designated for the main water supply to New York City (Figure 1).

Underwater Inspection and Repair

At the outset of our work in 2010, a 16-inch blow-off line connected the uptake shaft to the sidewall of the ad-

ABSTRACT

This paper presents a case study describing submerged work at Shaft 19 of the Delaware Aqueduct, which evolved to become the most complex atmospheric diving suit (ADS) project ever undertaken. The limitations imposed by existing atmospheric systems are considered along with very significant improvements in ADS capability now being developed for both commercial and scientific diving.

For more than a century, ADS has offered the enticing potential of allowing men to work effectively at great depths without suffering the effects of increased pressure. Unfortunately, early suits did not function well at depth, and pilots could be more accurately described as observers peering through the small viewports of “diving bells” outfitted with crippled appendages. The modern rotary joint was patented in 1985 offering great promise, but even during the past 25 years, atmospheric diving has remained specialized, underutilized, and largely left in the wake of remarkable advances in saturation diving and remotely operated vehicle (ROV) technology.

Underwater work performed at Shaft 19 contributed to development of Exosuit™, the next generation in atmospheric diving. Substantial improvements in mechanical suit design have been integrated with an optical fiber umbilical, computerized control systems, and modern electronics to dramatically improve ADS capabilities.

The Exosuit itself can power multiple tools, a variety of hand pod end-effectors are presently maturing, and atmospheric diving may now be poised to assume far greater significance in deep diving operations.

Keywords: Exosuit™, atmospheric diving suit, ADS

acent but deeper downtake shaft. This interconnection was originally intended to allow gravity drainage of the upstream aqueduct tunnel by discharge through the blow-off line, which could be controlled by a water hydraulic valve installed within a sump at the base of the uptake. NYCDEP recog-

FIGURE 1

UV plant construction in 2010.



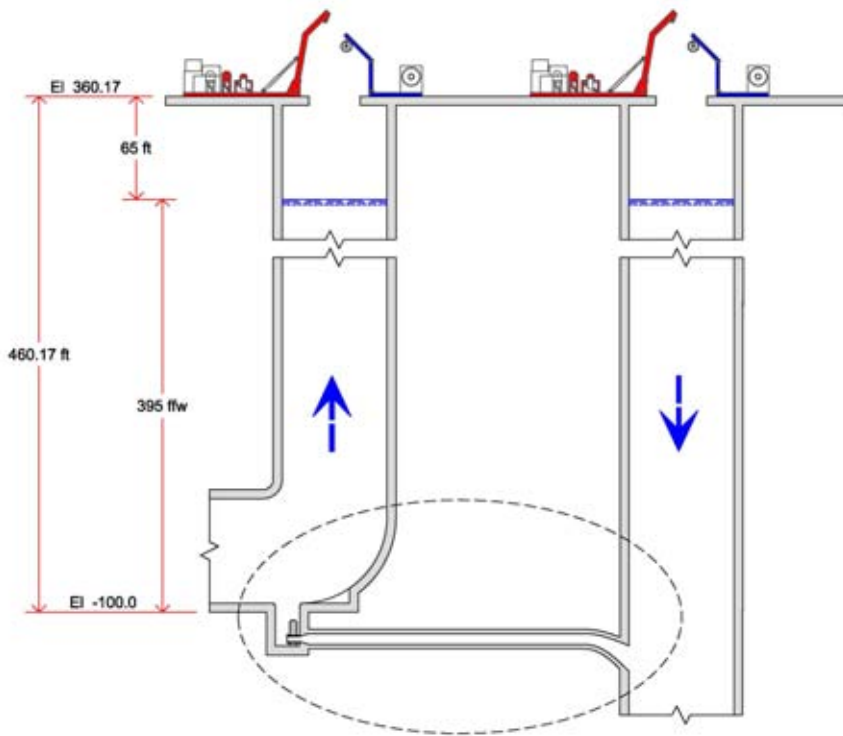
nized that this blow-off valve was no longer operational, and remotely operated vehicle (ROV) inspections performed during the project design phase also revealed that it was not fully closed. SEW was, therefore, directed to either repair or permanently seal the blow-off system to prevent water from being shunted directly from the uptake into the downtake shaft without passing through the requisite ultraviolet treatment process due to this unacceptable cross-connection (Figure 2).

Operational Difficulties and Constraints

The Diving Division of J. F. White Contracting Company was initially tasked by SEW with the responsibility

FIGURE 2

Depiction of shafts and interconnecting blow-off line.



of developing appropriate underwater procedures for remediation of the 16-inch bypass. All operations and equipment had to accommodate a variety of project-specific requirements and constraints imposed by NYCDEP. These challenges ultimately influenced developments of a new generation of atmospheric diving suit (ADS) with improved capacity for scientific as well as commercial operations.

When work commenced at Shaft 19, there appeared to be a possibility that the blow-off valve could be repaired or perhaps actuated once to be fully closed and sealed. The valve was situated in a small sump beneath sediment, debris, and cast iron gratings at the bottom of the uptake shaft elbow; therefore, it was difficult to gain access and perform an evaluation. Once this valve had been inspected, NYCDEP needed time to fully assess remediation alternatives with respect to cost, long-

term durability, and security of the water supply. Even after engineering decisions had been resolved for Shaft 19, underwater operations had to be integrated with other repairs within the aqueduct system and coordinated with changing environmental conditions affecting water quality.

Remediation of the blow-off system was undertaken in phases with the schedule restricted to intervals of reduced water demand between October and May.

Phase 1: Expose and inspect blow-off valve so that NYCDEP and consulting engineers could develop remediation criteria. Phase 1 was performed during the spring and fall of 2010 and resulted in a determination that the blow-off line would be permanently sealed at both ends and

then completely filled with grout.

Phase 2: Install a special 250-lb (pressure rating) “oil field blind flange” on the intake flange of the 16-inch blow-off valve in the sump at the base of the uptake shaft. Mount a permanent stainless steel bulkhead plate (5-foot square by 1-inch thick) on the curved wall of the downtake shaft to seal the discharge outlet from the blow-off line. Phase 2 sealed both ends of the blow-off line and was completed during the spring of 2011.

Phase 3: Completely fill the blow-off line with 5,000 psi grout between the oil field blind flange and the downtake bulkhead plate. Phase 3 was completed during the fall of 2011.

This interrupted work schedule dictated multiple mobilizations and demobilizations, but additional constraints imposed by NYCDEP also affected our underwater protocols.

- Work hours were generally restricted between 2200 and 0600, 6 days per week excluding Sundays. Operations also had to respond on a daily basis to DEP interruptions determined by ambient turbidity or work in progress at other locations.
- Available deck space at Shaft 19 was very limited, and numerous other topside construction activities had to be accommodated. The deck area was actually an “island” surrounded by a 60-foot-deep excavation and accessible only by footbridge or crane lift for significant loads.

- All underwater equipment had to be removed from the submerged shafts after each work shift. Ultimately, a support truss (Figure 3) was allowed to remain underwater between shifts, but it was jacked in place with a water hydraulic system and then additionally tethered by four synthetic fiber lines tensioned to strong-back beams at deck level.
- Work performed at Shaft 19 had to comply with NYCDEP water quality regulations:
All equipment entering shafts was disinfected in accordance with American Water Works Association standards.
No wire rope was permitted to contact the water surface due to contamination by lubricants.
Only water-powered hydraulics were allowed underwater due to a potential for contamination with even benign hydraulic oils. Only electrically powered launch and recovery systems or double encapsulated hydraulic units were allowed on deck.
- All diving operations had to incorporate provisions to prevent turbidity:
Underwater debris was loaded into closing containers lined with filter fabric.

FIGURE 3

Support truss being lowered into downtake shaft.



Decant water from all sediment extraction operations was pumped topside for off-site disposal.

Fines created by concrete drilling had to be filtered, contained, and removed from the shafts.

All grout, slurry, and decant water was contained and removed from the water supply.

Our initial project responsibility was to determine the underwater procedures and equipment that could best accomplish the blow-off remediation safely, economically, and on schedule.

Designation of Manned Diving System

Our initial surveys at Shaft 19 were undertaken by an inspection class Falcon ROV outfitted with a five-function manipulator. This effort identified the difficult tasks that would subsequently be required to gain access at the blow-off valve and then implement a repair. ROVs provided regular inspection capabilities and very significant diving support throughout the course of this project, but we determined at the outset that remote vehicles alone could not perform all the operations that would be needed. Manned diving was required, and it could have been accomplished either by saturation diving or ADS. Atmospheric diving was clearly the preferred economic choice.

The restricted deck area of the Shaft 19 “island” could not accommodate most saturation systems, and significant engineering costs would have also been incurred for the design and refit of bell handling systems with synthetic line (wire not allowed by NYCDEP). Ultimately, a second bell and launch and recovery systems would also have had to be deployed

to support simultaneous diving operations in both the uptake and downtake shafts during grout injection. Recurring phases of mob/demob for a saturation system would have been expensive, and work postponements imposed by NYCDEP water supply requirements would also have been extremely costly. These considerations made ADS the logical choice of diving system, but many unique challenges still had to be overcome.

Management of ADS Operations

The selection of ADS for manned diving intervention was an easy decision principally driven by economics, but the appropriate integration of suit, support systems, and tooling proved to be immensely more complex. The evolution of this process exposed many practical limitations of atmospheric diving for unique, complex, and nonrepetitive applications.

On behalf of SEW, the CAT/DEL 210-G joint venture general contractor, we initially attempted to engage an ADS provider as a full-service subcontractor to perform all the atmospheric diving work. After our initial ROV inspections, it became apparent that the ADS systems would have to be equipped with special tooling, unique installation fixtures would have to be designed and fabricated within a very restrictive time frame, and the ADS team would also have to be prepared to develop engineering adaptations on site in response to unforeseen problems.

One major ADS provider offered suits and pilots on a day-rate basis but determined that they could not perform the specialized engineering required for this project. Another

provider offered sophisticated design engineering, but they could not offer a convincing fabrication program for specialized underwater tooling or deployment of the construction oriented ADS diving teams required.

R. T. (Phil) Nuytten, the principal of Nuytco Research, Ltd., patented the modern rotary joint (Nuytten, 1985), and he is widely recognized as the innovator most responsible for developing effective atmospheric diving systems. We naturally contacted Nuytco for ADS services; however, they already had submersible operations scheduled within the same time frame. They could not deliver their regular subsea products while additionally fulfilling SEW demands for field operations combined with the design, development, and fabrication of multiple ADS tooling systems.

It soon became apparent that there was no sole source provider offering the comprehensive ADS capabilities within the time frame required by SEW and NYCDEP. We, therefore, developed an operational partnership by which the J. F. White Dive Division teamed with Nuytco Research to provide ADS capabilities and SeaView Systems to provide ROV support services to complete the underwater operations at Shaft 19. This cooperative effort resulted in successful project performance for SEW and also directly contributed to development of the Exosuit™.

Performing ADS Operations

Although the underwater work at Shaft 19 was only a minute component of the overall SEW construction effort, it was critical in nature, and the schedule was very demanding. There was absolutely no flexibility available to the

contractor when the water supply to New York City was designated for night shift shutdowns (2200–0600 h) months in advance to facilitate the work. We were given, for example, an interval of 6 months to design, fabricate, and proof test a system for mounting a 5-foot square stainless steel bulkhead plate on the curved wall of the downtake shaft. This bulkhead was intended to seal the 16-inch blow-off line at the downtake shaft during grout injection. This might not have been difficult even at 400 ffw except for unusual constraints:

- The blanking plate had to be removed and reinserted on a daily basis until eight preliminary mechanical anchor studs could be properly torqued to secure the bulkhead during normal aqueduct flow. We were unable to install and torque eight studs during a single work shift (8 hours between opening and closing concrete shaft covers); therefore, a triangular support truss was allowed to remain underwater between shifts after being jacked in place with a water hydraulic system and additionally tethered by four synthetic fiber lines tensioned to strong-back beams at deck level.
- The 1,200-lb blanking plate had to be positioned during each shift within a tolerance of 0.025 inch, and all studs had to be drilled parallel, with axial run-out along the stud less than 0.010 inch despite the curvature of the concrete shaft wall.
- The shaft wall was core drilled to accept 1 × 16-inch stainless steel mechanical anchor studs utilizing a custom-built electrical drill system, which also collected and extracted drill fines.

In the 6-month interval following the Phase 1 inspections, our underwater

team had to develop a variety of ADS-compatible tooling and fixtures to seal the blow-off piping (Phase 2) in preparation for the subsequent grouting phase.

J. F. White was responsible for the downtake support truss, downtake blanking plate, and alignment frame. These fixtures were adjustable to accommodate discontinuities in the shaft, actuated by water hydraulic jacks or rams, and designed to position the blanking plate within a 0.025-inch tolerance each time it was brought into position on the wall of the downtake shaft. The blanking plate and its alignment frame were removed at the conclusion of each work shift until 8 of the total 30 stainless anchor studs (1 × 16 inch) had been installed and torqued to secure it permanently in position. As the support frame was being lowered during the beginning of each work shift, the ROV could set it on the support truss and the ADS would make hose connections for the water hydraulic lines (Figures 3 and 4).

Concurrently, Nuytco Research developed the oil field blind flange and practiced installing it by ADS on a full-scale valve mock-up in their test tank. This mechanism was simple in concept but required considerable practice and coordination with very skilled ADS pilots to seal the blow-off flange during a single work shift (Figure 5).

SeaView Systems developed and fabricated electrically powered tooling for core drilling, stud installation, and torquing the bulkhead nuts. This machinery was designed around their proprietary “backbone system” for integrated topside electronic control, and each tool was configured to be handled and engaged by ADS. The topside electronics could adjust rotation speed, torque, quill feed pressure,

FIGURE 4

Blanking plate with alignment frame being lowered into downtake shaft.



FIGURE 5

ADS practicing in mock-up replicating sump and blow-off valve.



quill travel distance, and position by use of a touch-screen computer interface. The SeaView rotary torque tool was also deployed to actuate mechanisms on the sump blanking plate and the oil field blind flange.

Work-class ROVs can perform very complex tasks, but the support tooling and control systems must be developed in advance. We believed

from the outset of this project that ADS operations could be more quickly adapted to unforeseen conditions than an ROV. This proved true when NYCDEP determined that a bronze grate and debris within the blow-off discharge line had to be removed rather than grouted in place. We were directed with only 24 hours of notice to remove the grate at 405 ffw within the downtake shaft. This became a relatively simple construction site mechanical problem because we had only to develop tooling that could be manipulated by the ADS. Our blanking plate alignment frame was quickly modified so that the ADS could control an abrasive blade saw (Figure 6).

The deep diving work at Shaft 19 was successfully completed, and ADS was undoubtedly the best choice for this underwater intervention. Our ADS costs are estimated between 25% and 35% of saturation diving when considering only the multiple mobilizations and time delays imposed by NYCDEP. Special engineering costs associated with bell deployment into the active water supply would further favor ADS. Even multiple work-class ROVs could not have operated effectively in the limited visibility of Shaft 19 as the combination of ADS with ROV support.

FIGURE 6

Abrasive saw tested topside by ADS pilot, Doug Bishop.



Lessons Learned

Lessons learned during the underwater construction at Shaft 19 may well be applicable to similar projects as well as deep water (1,000 fsw) science. If a project cannot be completed solely by ROVs and the working duration or depths encountered are too great for bounce diving, a choice will probably be made between saturation diving and ADS. The decision will be determined by considering all the interrelated operational factors.

Mobilization for ADS diving is perhaps an order of magnitude less expensive than a saturation spread, but that disparity must be balanced against project duration and underwater work requirements.

Atmospheric diving suits can offer manned performance with respect to range of motion, manipulation, and dexterity that is perhaps 50–85% the capacity of a working gas or saturation diver. ADS capabilities improve toward the higher end of that range when special tooling can be developed and tested in advance.

ADS can successfully perform many basic diver functions, but an atmospheric diving operation has to be supported with tooling developed for the anticipated tasks and adapted to function with the suit. Tooling for atmospheric diving must be carefully planned as it is for ROV operations. The tool must be integrated with the atmospheric suit; it is not as simple as handing a new underwater tool to a gas diver and expecting effective performance. Tools can be standardized for repetitive work, but unusual tasks undertaken for construction or science will likely require special tooling and pilot training to handle each specific application.

Next-Generation ADS

All diving at Shaft 19 was performed with the Newtsuit designed by Phil Nuytten in 1985 but now utilizing technology nearly 25 years old and perhaps past its prime. Nuytco Research had been gradually developing a new generation ADS, designated as the Exosuit, for a number of years prior to our work for SEW in 2010 and 2011. ADS performance at Shaft 19 was so successful that J. F. White placed an order for the first Exosuit. At the time of this writing, this first Exosuit has passed pressure testing certification to 1,400 fsw and has been delivered to J. F. White. It incorporates modern developments in electronic control and optical fiber data transmission with multiple mechanical improvements gained during operational experience at Nuytco.

- **Thrusters:** Exosuit thrusters have approximately twice the bollard pull of thrusters on the older Newtsuit. This added power can be a significant advantage working in a current or applying force to tooling. The maneuverability and positioning capability of the Exosuit is further improved because forward and reverse thruster power is controlled by the speed and direction of rotation, not by a variable pitch propeller as in older suits. This new ADS can be more easily flown by less experienced pilots and more accurately controlled by skilled divers.
- **Power Ports:** The Exosuit includes four additional power supply ports, each capable of delivering approximately 1 hp. Additional thrusters could be added to the suit to accommodate special circumstances, but these ports also provide the capacity to run additional electric tooling directly by a suit whip, not a separate power umbilical from the surface.

- During our work at Shaft 19, we often had six synthetic tether lines deployed in addition to the ADS umbilical, ROV umbilical, water hydraulic supply line, and then an electrical power supply to each tool. The ability to power tools directly from the Exosuit will be a significant advantage for construction as well as scientific applications where suction motors for biological collection, drills for coral coring, or special tooling for archaeological specimen preparation could be directly powered from the Exosuit.
- **Topside Control:** Most modern thruster-powered ADS have been controlled with foot pedals leaving the hand pods available for other tasks. The Exosuit can be flown in this manner, but it can also be independently piloted by topside control. It could be utilized as an ROV equipped with its standard high-definition cameras if that deployment proved advantageous, but perhaps, more importantly, an incapacitated pilot could be flown around obstructions to safely clear the umbilical for retrieval to the surface. An inexperienced ADS pilot with appropriate safety training but little suit time could also be flown by topside control to a particular work site. A skilled archaeologist, for example, could be flown to a site where he would only have to manipulate the ADS hand pods or specialized tooling to evaluate a critical specimen.
- **Suit Flexibility:** Atmospheric diving capabilities were very limited until invention of the rotary joint (Nuytten, 1985). Modern ADS then became practical for underwater work, but friction in a joint exposed to pressure can limit suit dexterity and tire the working

pilot. The Exosuit utilizes a newly designed rotary joint, which reduces friction under pressure by approximately 50% as compared to previous ADS. Every pilot movement of the suit legs, arms, or hand pods is more precise and less tiring. This flexibility will clearly assist positioning of the suit when working on bottom or in restricted areas.

- **Fiber Optics:** The Exosuit umbilical includes optical fiber in addition to power conductors and strength members. This fiber provides data transmission for high-definition video, sonar, and other digital sensor systems. Voice transmission over fiber is superior to copper, and unlike older suits, cabin life support data can be monitored directly by the topside supervisor without interrupting pilot attention to the task at hand.

The Exosuit also incorporates many small modifications that would go unnoticed by a general observer, but they will be immensely appreciated by pilots and will become obvious during an assessment of work performance. The pilot's range of vision through the new face dome is exceptional, slight modification of the torso eases pilot entry into the arms, and hand pods have been improved and include threaded mounting lugs to accommodate special tooling. In combination, these and other advances qualify the Exosuit as a new generation of ADS, but they also set the stage for development of additional capabilities (Figures 7 and 8).

New ADS Capabilities

Nuytco Research is presently developing a free-swimming untethered version of the Exosuit. This capability would be derived from the reduced

FIGURE 7

Newtsuit in operation.

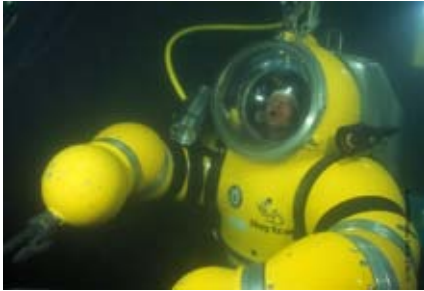


FIGURE 8

Exosuit performing acceptance tests.



friction offered by Phil Nuytten's new joint design and could benefit specific scientific or military applications.

J. F. White and Nuytco Research are both presently evaluating the advantages of mating an Exosuit with a tether management system mounted aboard a small submersible. This combination would be free of any umbilical to the surface; incorporate the capacity for self-rescue; and offer a very capable platform for underwater construction, science, or salvage.

Atmospheric suits are usually equipped with manipulators resembling pliers that can open, close, and lock a grip. This limited dexterity often slows a pilot's work as compared to a gas diver and creates the need for special adaptive tooling. The development of a manipulator more closely

FIGURE 9

Prototype prehensor developed by Nuytco Research.



FIGURE 10

Anthropomorphic ADS prehensor invented by Vishwa Robotics.



replicating a human hand would provide immense advantage underwater. Nuytco Research has been developing their prehensor hand as depicted below, and concurrently, several other designs are emerging from robotic and biomedical laboratories. It is probably a safe prediction that improved hand mechanisms will be working underwater within the next few years (Figures 9 and 10).

Acknowledgments

The author wishes to express his appreciation to Nuytco Research, Ltd., of Vancouver, BC, and SeaView Systems, Inc., of Dexter, MI, for their effort and cooperation during the Shaft 19 project and other underwater endeavors. The anthropomorphic pre-

hensor mechanism depicted above has been invented by Bhargav Gajjar of Vishwa Robotics in Cambridge, MA.

Author:

James F. Clark

J. F. White Contracting Company
10 Burr Street, Framingham, MA 01701

Email: jclark@jfwhite.com

Reference

Nuytten, R.T. 1985. U.S. Patent No. 4,549,753 entitled "Rotary Joint"; 29OCT85.

Take Me Back Down: The Best “Over the Counter” Remedy for DCIs

AUTHOR

Joseph Dituri
 CDR U.S. Navy (ret.)
 Gallant Aquatic Ventures
 International, Tampa, Florida

The following is a first-hand example of how a series of unfortunate events were made better by going back into the water for in-water recompression. The article does not offer medical advice. It serves as a personal account from which people may consider learning about an alternate means of immediate response to decompression illness (DCI).

Immediately upon ascending the ladder onto the boat, I knew something was wrong. I felt “funny.” We just completed a 400-fsw (feet of seawater) dive for 25 min of bottom time using all the appropriate gasses, making all required gas changes, and completing all decompression stops. I did a quick check of my dive buddy and saw that he was fine. After removing my wetsuit, one of the support divers noticed the blotchy red patch that had started to form over my left shoulder and around the left side of my abdomen transcending around to my left lower back. It had been less than 15 min on the surface, and I was sitting while the boat was making its way back to port. Next, I had a flash of nondescript internal pain to my left knee. I began to rub it and wondered how long it would be until we were near the second dive site where we would afford the support divers an opportunity to dive (we found it important to re-

ward those who were helping us with a fun dive). My entire thought process was driven toward getting myself back into the water. This thought, I believe, came from the adaptive unconscious (described in the later part of the commentary), which bears considerable importance to the ability to decide the correct course of action. About 15 min later, I began to feel that all-too-familiar pain, only now it was in my right knee. Bilateral and progressively worsening symptoms began to cause me great concern. This was the point at which I knew I was in significant trouble.

Not wanting to be a bother to the four divers who had endured my 4-h dive while they sat on the boat taking turns being in the water to support us, I concealed my pain and stomached a brief offload period at the dock, which was about 45 min after surfacing. I could not, however, conceal the coughing fit that ensued with a small clearing of my throat while they were loading some drinks from the bait and tackle shop. This uncontrollable coughing progressed, and the friend driving the boat got everyone back in the boat and sped out of the channel toward deeper water. At this time, my rash was puffy and red, and pressing on it left an indent. I had pain in both knees, which was a 5 on a scale of 1 to 10. I was hacking so badly; I could not carry on conversation. At the speed with which the symptoms were progressing, I believe I would not have survived the lengthy transit to a hyperbaric facility, which would have included a 10-min ambulance response

time, followed by a 30-min ambulance ride to the chamber, or the almost assured 45-min wait at the Emergency Room (ER) while doctors poured over me trying to find out what was wrong. At the local medical facilities, the chamber is not located at the same place as the hospital ER. I needed a cure NOW and *hair of the dog that bit me* was the only immediate remedy available.

After the 3–5 min it took to get the boat to ~45 feet of water, I grabbed an open circuit steel 72 cubic foot cylinder filled with 100% oxygen that had a green regulator on it (to ensure someone did not inadvertently breathe from it at an improper depth). I put it under my arm while someone tossed the anchor. Knowing full well I might be in the water for a while, I had begun to step into a wetsuit at the dock. I could not manage to pull it any higher than up to around my hips. Face mask donned, but unable to put fins or other equipment on, I fell forward off the boat into the water.

I do not recall clearing my ears, the journey downward, or hitting the bottom. I became aware again when Jennifer, who apparently followed my descent, grabbed my arm and pulled me from 40–45 fsw up to hang on the anchor line at 30 fsw. Jennifer had little more than an old style Hawaiian backpack for diving and was known for being able to dress for diving very quickly. She undoubtedly saved my life. (Thank you for that, Jennifer!) By the time my dive buddy from the deep dive got dressed and reentered the

water, I had been able to pull my wetsuit up over my shoulders, was lucid, and had a plan for my in-water recompression cobbled on Jennifer's slate. I had complete resolution of symptoms within minutes. I was a different person from the uncontrollable cough-laden, bilateral pain-filled, shell of a man who thought it was a good idea to reenter the water 5 min earlier. One of the divers brought me my rebreather, and I followed out my decompression plan, uneventfully watching the support divers enjoy their "fun dive" from my perch at the anchor line while slowly ascending from 30 to 20 and finally 10 fsw and then surfaced.

I had a fleeting thought to go to the Diving Medical Physician at Mobile Diving Salvage Unit, where I was stationed, but I was too embarrassed and did not want to face the ridicule or have to explain to the Navy what I was doing at 400 fsw on the weekend while I was on liberty. I thought I was fine until later that night when my abdomen and shoulder area that displayed the initial rash had become very painful to the touch. I was unable to sleep because when those areas touched the bed, it produced an intense amount of pain and endorphin release. After making my way to the chamber and a short ride in a "round room," I was without pain or residual marks and very fortunately alive today to tell the tale.

This true story is one that could happen without warning or expectation, as it did to me. With this truth, I intend to invite you into an alternate view of in-water recompression and afford you an opportunity to discover a possible tool that could save your life if performed properly. I recognized the many mistakes I made in this scenario. First was ignoring the most common

symptom of DCI: denial. I initially knew I had DCI but denied the severity. The second mistake was delaying recompression. My final mistake was not being checked by a physician knowledgeable in diving medicine following my life-saving in-water recompression.

If you are walking down a street and you see a truck coming toward you, do you have time to weigh all the options prior to jumping out of the way? The answer, of course, is no. Why would I have immediately thought that the "necessary" thing to do was get back in the water? Divers are an intelligent unique breed. In my opinion, one of the most important traits allowing divers to evolve into technical diving and rebreather diving is to have a decision-making process that is capable of making rapid judgments based on little information. This notion parallels survival skill sets.

As the psychologist Timothy D. Wilson writes in his book *Strangers to Ourselves*, the mind relegates a great deal of its high-level sophisticated thinking to its unconscious. Our adaptive unconscious does an excellent job of sizing up the world, warning people of danger, and setting goals and initiating action in a sophisticated and efficient manner. Wilson says that we toggle back and forth between conscious and unconscious parts of the brain. Whenever we are faced with an emergent situation, we invoke the unconscious part of our brains to assist in making the decisions. I believe that my adaptive unconscious was working to help me recognize I was in trouble. In Malcolm Gladwell's book *Blink*, he suggests that the rapid answer is most often correct. The quality of a decision is not directly proportional to the time, effort, and energy to make

that decision. Knowledge is power, but a delay in taking action may cause irreparable damage. Prior to making the decision to go back in the water, an astute technical diver would seek proper training to prepare themselves for making the correct decision once the inevitable happens.

If we knew exactly what caused Decompression Sickness (DCS), the divers at large may feel differently, but since scientists have been unable to find an exact cause, we are merely trying to treat the symptoms. DCS is so multifaceted that some researchers have spent their whole lives trying to find the cure/cause to no end. If you ask a diver who is newly certified, "What causes DCS?" their answer would be, "I don't know...I think it has something to do with bubbles." If you ask a dive master what causes DCS, you will likely get a description of a soda bottle being opened too quickly and the soda fizzing out. If you ask an experienced technical diving instructor or a person trained in hyperbaric medicine what causes DCS, you will likely get discussions of the phagocyte and leukocyte reaction to a foreign body in your blood stream coupled with the need for adequate hydration. If you ask the top five scientists who work in decompression physiology, "What causes DCS?" their answer would be, "I don't know...I think it has something to do with bubbles."

This is just one case where the contentious practice of in-water recompression was the best *over-the-counter remedy*. This could have gone very wrong, and I may not have survived the descent. Other technical divers/authors including Richard Pyle, Don Shirley, and Tom Mount have scribed their accounts of the utility of this "trade secret" in a variety of online articles, and the "science" of IWR

is just now emerging. There are two major points to take away from this commentary:

1. in-water recompression is the best source for immediacy of care when a diver has a DCS and
2. in-water recompression is not the only thing a diver needs to do if they have DCS.

In-water recompression is by no means a medical treatment, and one should seek medical attention after any attempt at IWR. IWR is merely a method of lessening the severity of issues that a diver will encounter because of DCS and affording immediacy of care.

Author:

Joseph Dituri
Gallant Aquatic Ventures
International
Email: joe@gallantaquatic.com

My Daddy Wears a Different Kind of Suit to Work

By Josephine A. Dituri and Joseph Dituri
Gallant Aquatic Ventures International, 2011
54 pp., \$19.99

Reviewed by Brian Bordieri

A selection that weaves work and play together for children with ocean loving parents, *My Daddy Wears a Different Kind of Suit to Work* offers divers and nondivers alike a glimpse of how our children view diving parents, our gear, our stories, and the connection between modern life and the sea. Written for young children to be read to or for emerging readers to connect text and illustrations, the pages hold the attention of the intended audience after many repeated readings. There is evidence of genuine family exploration of the underwater world through conversations recalled by a curious child, and there is balance between the technical and human sides of diving for a living. Informal expression allows children to participate in the story of dad's adventures and learn about the obstacles as well as on-the-job vocabulary without being pushed away with technical jargon.

Perhaps the best attribute of this work is the conversation it allows between divers and their children. My own little ones have had questions about diving, poked around my equipment, and happily pointed out divers on TV when they appear—but I had never encountered a book that collects so many of these ques-

tions and the right answers for children into one sitting. It is also a great way to introduce young readers to the notion that there is such a wide range of possible careers out there to be explored. We enjoyed the illustrations that accompanied each page. Each contained enough detail to support the story yet remained whimsical.

The book is a must-own for any active diver with growing children. Having read countless books on a nearly unlimited range of topics, this book has become a quick favorite because of the relevance of the story within. Good books help readers to connect, and this work allows children to connect with diving parents on an activity that they are just not ready for themselves. My daughter asks me to take her diving regularly, and the day she turns 10 she will be signed up for classes; but for now, we will continue to explore the sea's shallows directly in summer and in the armchair in winter using this book as that connection.

- Ahmed, S. (3) 99-117
 Alemany, F. (1) 101-117
 Alsenas, G.M. (2) 59-69
 Álvarez, D. (1) 101-117
 Álvarez, E. (1) 101-117
 Álvarez-Ellacuria, A. (1) 101-117
 Amon, E. (1) 47-54, (4) 164-176
 Ananthapadmanabhan, A. (3) 55-71
 Annamalai, S. (3) 55-71
 Ansorena, L. (1) 101-117
 Arslan, H. (3) 99-117
 Atmanand, M.A. (3) 55-71
 Auster, P.J. (1) 33-46
 Balaguer, P. (1) 101-117
 Baldwin, K. (4) 7-8, 45-56
 Ballou, P.J. (1) 83-95
 Bang-Andreasen, H. (4) 80-93
 Baowei, S. (4) 94-100
 Barceló, B. (1) 101-117
 Barnes, J. (4) 67-79
 Barrett, S.B. (4) 9-17
 Belloni, C.S.K. (4) 23-35
 Beltrán, J.P. (1) 101-117
 Brekken, T. (1) 47-54
 Brooks, B. (6) 7-15
 Buckley, E. (5) 104-116
 Burleson, W. (6) 52-63
 Buzzacott, P. (6) 27-41
 Cañellas, T. (1) 101-117
 Carlson, T.J. (4) 113-121
 Carrasco, M.A. (1) 101-117
 Casas, B. (1) 101-117
 Castilla, C. (1) 101-117
 Chatterjee, P. (4) 36-44
 Chen, S. (1) 96-100
 Chitwood, J.E. (3) 5-12
 Choi, E.Y. (4) 113-121
 Churchill, J.H. (4) 122-136
 Clark, A.M. (5) 7-18
 Clark, J.F. (6) 73-79
 Cohen, P. (3) 13-18
 Cole, R. (1) 7-18
 Conti, D. (1) 101-117
 Cooper, C. (3) 19-26
 Copping, A.E. (4) 113-121
 Cowles, G.W. (4) 122-136
 Cruz, N.A. (2) 43-58
 Cui, W. (1) 67-82, (3) 37-54
 Cusí, S. (1) 101-117
 Dalglish, F.R. (5) 128-147
 DeCew, J. (4) 45-56
 deCharon, A. (5) 26-30
 Delaney, J.R. (5) 31-36
 Deng, Z.D. (4) 113-121
 Dewhurst, T. (4) 45-56
 Diedrich, A. (1) 101-117
 Dituri, J. (6) 80-82
 Dufresne, N.P. (4) 193-205
 Durairaj, M. (3) 55-71
 Enoksson, P. (6) 27-41, 42-51
 Escudier, R. (1) 101-117
 Esser, D. (3) 27-36
 Fan, S. (3) 81-98
 Ferreira, B.M. (2) 43-58
 Fish, F.E. (5) 37-44
 Forristall, G. (3) 19-26
 Freitag, L. (5) 45-50
 Fritz, H.M. (4) 101-112
 Fryburg, R. (6) 52-63
 Fu, T. (4) 113-121
 Garau, B. (1) 101-117
 Gardiner, A. (4) 164-176
 Gilbert, S.A. (5) 104-116
 Godfrey, J. (6) 52-63
 Golob, M. (6) 16-26
 Gómara, S. (1) 101-117
 Gómez, M. (1) 101-117
 Gómez-Pujol, L. (1) 101-117
 Green, B.E. (4) 151-163
 Griesbauer, L. (5) 19-25
 Grilli, S. (4) 7-8
 Güney, C.B. (1) 134-145
 Guo, W. (1) 67-82
 Haas, K.A. (4) 101-112
 Hakim, A.R. (4) 122-136
 Hansen, R.E. (5) 117-127
 Hanson, H.P. (2) 59-69, (4) 18-22
 Hao, D. (4) 94-100
 Harmer, A. (4) 137-141
 Heslop, E. (1) 101-117
 Hogan, T.W. (4) 137-141
 Hou, B. (1) 96-100
 Houlsby, G.T. (4) 23-35
 Howes, B.L. (4) 7-8, 142-150
 Hu, Z. (1) 67-82
 Irish, J.D. (1) 19-32
 Jacobson, J. (3) 13-18
 Jenssen, N.A. (2) 14-30
 Jochens, A.E. (1) 5-6, 118-133, (2) 6-7
 Juzà, M. (1) 101-117
 Kamenkovich, V.M. (1) 55-66
 Karalekas, P. (4) 57-66
 Kebkal, O. (2) 43-58
 Kerkeni, S. (2) 14-30
 Kessler, M. (6) 27-41
 Kinder, J. (1) 7-18
 King, J.P. (4) 67-79
 Kirincich, A. (4) 206-217
 Kocak, D.M. (5) 5-6, 7-18
 Kohnen, W. (5) 56-68
 Kowalski, G.J. (4) 57-66
 Kracker, L. (1) 33-46
 Kusinski, G. (3) 5-12, 13-18
 Lagerloef, G. (5) 26-30
 Lan, Z. (1) 96-100
 Lana, A. (1) 101-117
 Laoulache, R.N. (4) 36-44
 Lettenmaier, T. (1) 47-54, (4) 164-176
 Lim, S.D. (2) 70-81
 Lindstrom, E. (5) 26-30
 Linebaugh, C. (4) 137-141
 Linke, P. (3) 27-36
 Liu, C. (1) 67-82
 Liu, F. (1) 67-82
 Lizarán, I. (1) 101-117
 Lombardi, M. (6) 5-6, 52-63
 Lora, S. (1) 101-117
 Løset, S. (2) 14-30
 Lovelace, E. (4) 57-66
 Lucyshyn, T. (6) 27-41
 Luther, M.E. (5) 104-116
 MacDonald, D.G. (4) 7-8, 151-163

- MacNicoll, M.T. (4) 177-186
Madden, D. (6) 42-51
Mahfuz, H. (2) 59-69
Manriquez, M. (1) 101-117
March, D. (1) 101-117
Martínez-Ledesma, M. (1) 101-117
Martinez, J.J. (4) 113-121
Martin, A.Y. (5) 72-83
Matzner, S.A. (4) 113-121
Mason, E. (1) 101-117
Massuti, E. (1) 101-117
Matos, A.C. (2) 43-58
Mazzoleni, A.P. (2) 70-81
McCormick, M.E. (4) 187-192
Meadows, G. (5) 104-116
Melo, A.B. (5) 97-103
Merrill, M.L. (4) 7-8
Merz, C.R. (4) 218-225
Metrikin, I. (2) 14-30
Mezgec, Z. (6) 16-26
Mierzwa, C.E. (5) 84-96
Mitchell, T. (3) 19-26
Miyazaki, M.R. (2) 31-42
Moran, S. (4) 164-176
Murtha, R.C. (4) 187-192
Myers, J.R. (4) 113-121
Na, W-B. (3) 72-80
Narayanaswamy, V. (3) 55-71, (4) 80-93
Nasr, A. (3) 13-18
Ochoa, E. (6) 7-15
Oguz, T. (1) 101-117
Oney, S.K. (4) 137-141
Orfila, A. (1) 101-117
Ouyang, B. (5) 128-147
Park, J-k. (2) 70-81
Pascual, A. (1) 101-117
Pec, M. (6) 16-26
Peirano, A. (3) 118-127
Penland, L. (6) 7-15
Petrioli, C. (2) 43-58
Petroccia, R. (2) 43-58
Phillips, R. (1) 47-54
Pitarch, S. (1) 101-117
Porak, D.N. (4) 226-239
Pranesh, B. (6) 64-72
Price, V.E. (1) 33-46
Purcell, H. (5) 104-116
Quinlan, B. (2) 70-81
Raju, R. (3) 55-71
Ramadass, G.A. (3) 55-71, (6) 64-72
Ramesh, S. (6) 64-72
Rayburn, J.T. (1) 55-66
Reglero, P. (1) 101-117
Reif, S. (6) 27-41, 42-51
Ren, H. (4) 113-121
Renault, L. (1) 101-117
Ro, P.I. (2) 70-81
Rohrer, J. (4) 177-186
Roque, D. (1) 101-117
Rowell, M. (4) 45-56, 67-79
Ruiz, J. (1) 101-117
Ruiz, S. (1) 101-117
Ryan, M.S. (2) 8-13
Salisbury, J.E. (1) 19-32
Sathianarayanan, D. (6) 64-72
Sayol, J.M. (1) 101-117
Schechner, Y.Y. (5) 148-150
Schilling, T. (5) 69-71
Schlezingner, D.R. (4) 142-150
Schmidt, M. (3) 27-36
Schroeder Jr., A.J. (3) 5-12, 13-18
Schuster, A. (6) 27-41, 42-51
Sebastian, K. (1) 101-117
Shellito, S. (1) 19-32
Sieber, A. (6) 27-41, 42-51
Song, J. (1) 96-100
Spaccini, D. (2) 43-58
Stear, J. (3) 19-26
Steinbeck, J. (4) 137-141
Steinmetz, J. (4) 187-192
Stojanovic, M. (5) 45-50
Sweeney, E. (5) 97-103
Swift, M.R. (4) 45-56
Tamburri, M.N. (5) 104-116
Tangora, M. (5) 51-55
Tannuri, E.A. (2) 31-42
Taylor, C.D. (4) 142-150
Thiagarajan, K.P. (4) 177-186
Tintoré, J. (1) 101-117
Torner, M. (1) 101-117
Valenko, D. (6) 16-26
Vandemark, D. (1) 19-32
VanZwieten Jr., J.H. (4) 226-239
Vélez-Belchí, P. (1) 101-117
Villate, J.L. (5) 97-103
Vizoso, G. (1) 101-117
von Jouanne, A. (1) 47-54, (4) 164-176
Vuorenkoski, A.K. (5) 128-147
Wang, X. (1) 96-100
Wang, Z. (1) 96-100
Watson, S.M. (1) 118-133
Wenlong, T. (4) 94-100
White, J.W. (2) 8-13
Wiles, B. (4) 226-239
Willden, R.H.J. (4) 23-35
Willis, Z. (5) 19-25
Withrow, J. (4) 137-141
Wood, S.L. (5) 84-96
Woolsey, C. (3) 81-98
Wosnik, M. (4) 45-56, 67-79, 193-205
Yang, X. (4) 101-112
Yonsel, F. (1) 134-145
Yoon, H-S. (3) 72-80
Yu, W. (1) 7-18
Zhaoyong, M. (4) 94-100
Zhou, F. (2) 59-69
Zhu, M. (1) 67-82

Subject Index

Industry and Technology

Buoy Technology

Ocean Climate: “*Off the Shelf*”, R. Cole, J. Kinder, W. Yu (1) 7-18

Experience With Moored Observations in the Western Gulf of Maine From 2006 to 2012, J.D. Irish, D. Vandemark, S. Shellito, J.E. Salisbury (1) 19-32

A Novel Ocean Sentinel Instrumentation Buoy for Wave Energy Testing, A. von Jouanne, T. Lettenmaier, E. Amon, T. Brekken, R. Phillips (1) 47-54

The Gulf of Mexico Coastal Ocean Observing System: An Integrated Approach to Building an Operational Regional Observing System, A.E. Jochens, S.M. Watson (1) 118-133

Subsurface Mooring Stability in the Presence of Vertical Shear, H.P. Hanson (4) 18-22

Testing the WET-NZ Wave Energy Converter Using the Ocean Sentinel Instrumentation Buoy, T. Lettenmaier, A. von Jouanne, E. Amon, S. Moran, A. Gardiner (4) 164-176

Wave Energy Conversion for Shoreline Protection, M. E. McCormick, R.C. Murtha, J. Steinmetz (4) 187-192

U.S. IOOS: An Integrating Force for Good, Z. Willis, L. Griesbauer (5) 19-25

Verification of Wave Measurement Systems, M.E. Luther, G. Meadows, E. Buckley, S.A. Gilbert, H. Purcell, M.N. Tamburri (5) 104-116

A Diver’s Automatic Buoyancy Control Device and Its Prototype Development, D. Valenko, Z. Mezgec, M. Pec, M. Golob (6) 16-26

Cables and Connectors

Ocean Climate: “*Off the Shelf*”, R. Cole, J. Kinder, W. Yu (1) 7-18

Anchor Drop Tests for a Submarine Power-Cable Protector, H-S. Yoon, W-B. Na (3) 72-80

Understanding the Planetary Life Support System: Next-Generation Science in the Ocean Basins, J.R. Delaney (5) 31-36

Deepwater Field

Development Technology

On 7,000 m Sea Trials of the Manned Submersible *Jiaolong*, W. Cui, F. Liu, Z. Hu, M. Zhu, W. Guo, C. Liu (1) 67-82

Numerical Simulation of Dynamic Positioning in Ice, I. Metrikin, S. Løset, N.A. Jenssen, S. Kerkeni (2) 14-30

DeepStar®: 22 Years of Success
DeepStar: A Global Deepwater Technology Development Program, G. Kusinski, A.J. Schroeder Jr., J.E. Chitwood (3) 5-12

DeepStar 11304: Laying the Groundwork for AUV Standards for Deepwater Fields, J. Jacobson, P. Cohen, A. Nasr, A.J. Schroeder Jr., G. Kusinski (3) 13-18

DeepStar Metocean Studies: 15 years of Discovery, C. Cooper, T. Mitchell, G. Forristall, J. Stear (3) 19-26

Development of the *Jiaolong* Deep Manned Submersible, W. Cui (3) 37-54

Anchor Drop Tests for a Submarine Power-Cable Protector, H-S. Yoon, W-B. Na (3) 72-80

Consideration of a Variable Frequency Energy Conversion System for Marine and Onshore Wind Energy Extraction, C.R. Merz (4) 218-225

Manufacturing Imperfection Sensitivity Analysis of Spherical Pressure Hull for Manned Submersible, B. Pranesh, D. Sathianarayanan, S. Ramesh, G.A. Ramadass (6) 64-72

Diving

Development of the *Jiaolong* Deep Manned Submersible, W. Cui (3) 37-54

Wrecks on the Bottom: Useful, Ecological Sentinels?, A. Peirano (3) 118-127

Long-Term Methods for High-Definition Image Maps of Benthic Surveys, L. Penland, B. Brooks, E. Ochoa (6) 7-15

A Diver’s Automatic Buoyancy Control Device and Its Prototype Development, D. Valenko, Z. Mezgec, M. Pec, M. Golob (6) 16-26

Compact Recreational Rebreather With Innovative Gas Sensing Concept and Low Work of Breathing Design, A. Sieber, A. Schuster, S. Reif, M. Kessler, T. Lucyshyn, P. Buzzacott, P. Enoksson (6) 27-41

Head-Up Display System for Closed Circuit Rebreathers With Antimagnetic Wireless Data Transmission, A. Sieber, A. Schuster, S. Reif, D. Madden, P. Enoksson (6) 42-51

An Experimental Deployment of a Portable Inflatable Habitat in Open Water to Augment Lengthy In-Water Decompression by Scientific Divers, M. Lombardi, W. Burlleson, J. Godfrey, R. Fryburg (6) 52-53

Manufacturing Imperfection Sensitivity Analysis of Spherical Pressure Hull for Manned Submersible, B. Pranesh, D. Sathianarayanan, S. Ramesh, G.A. Ramadass (6) 64-72

A New Generation of ADS Capabilities, J.F. Clark (6) 73-79

Take Me Back Down: The Best “Over the Counter” Remedy for DCIs, J. Dituri (6) 80-82

Dynamic Positioning

Numerical Simulation of Dynamic Positioning in Ice, I. Metrikin, S. Løset, N.A. Jenssen, S. Kerkeni (2) 14-30

A General Approach for Dynamic Positioning Weathervane Control, M.R. Miyazaki, E.A. Tannuri (2) 31-42

Investigation of Underwater Acoustic Networking Enabling the Cooperative Operation of Multiple Heterogeneous Vehicles, N.A. Cruz, B.M. Ferreira, O. Kebkal, A.C. Matos, C. Petrioli, R. Petroccia, D. Spaccini (2) 43-58

Analysis of Underwater Acoustic Communication Channels, S. Ahmed, H. Arslan (3) 99-117

Subsurface Mooring Stability in the Presence of Vertical Shear, H.P. Hanson (4) 18-22

A View through the Waves, Y.Y. Schechner (5) 148-150

A Diver’s Automatic Buoyancy Control Device and Its Prototype Development, D. Valenko, Z. Mezgec, M. Pec, M. Golob (6) 16-26

Manned Underwater Vehicles

On 7,000 m Sea Trials of the Manned Submersible *Jiaolong*, W. Cui, F. Liu, Z. Hu, M. Zhu, W. Guo, C. Liu (1) 67-82

Development of the *Jiaolong* Deep Manned Submersible, W. Cui (3) 37-54

Analysis of Underwater Acoustic Communication Channels, S. Ahmed, H. Arslan (3) 99-117

Advantages of Natural Propulsive Systems, F.E. Fish (5) 37-44

Review of Deep Ocean Manned Submersible Activity in 2013, W. Kohnen (5) 56-68

An Experimental Deployment of a Portable Inflatable Habitat in Open Water to Augment Lengthy In-Water Decompression by Scientific Divers, M. Lombardi, W. Burlleson, J. Godfrey, R. Fryburg (6) 52-63

Manufacturing Imperfection Sensitivity Analysis of Spherical Pressure Hull for Manned Submersible, B. Pranesh, D. Sathianarayanan, S. Ramesh, G.A. Ramadass (6) 64-72

A New Generation of ADS Capabilities, J.F. Clark (6) 73-79

Moorings

Ocean Climate: "Off the Shelf", R. Cole, J. Kinder, W. Yu (1) 7-18

The Gulf of Mexico Coastal Ocean Observing System: An Integrated Approach to Building an Operational Regional Observing System, A.E. Jochens, S.M. Watson (1) 118-133

DeepStar®: 22 Years of Success
DeepStar: A Global Deepwater Technology Development Program, G. Kusinski, A.J. Schroeder Jr., J.E. Chitwood (3) 5-12

Subsurface Mooring Stability in the Presence of Vertical Shear, H.P. Hanson (4) 18-22

Dynamics of a Floating Platform Mounting a Hydrokinetic Turbine, T. Dewhurst, M.R. Swift, M. Wosnik, K. Baldwin, J. DeCew, M. Rowell (4) 45-56

U.S. IOOS: An Integrating Force for Good, Z. Willis, L. Griesbauer (5) 19-25

Verification of Wave Measurement Systems, M.E. Luther, G. Meadows, E. Buckley, S.A. Gilbert, H. Purcell, M.N. Tamburri (5) 104-116

Oceanographic Instrumentation

Ocean Climate: "Off the Shelf", R. Cole, J. Kinder, W. Yu (1) 7-18

SOCIB: The Balearic Islands Coastal Ocean Observing and Forecasting System Responding to Science, Technology and Society Needs, J. Tintoré, G. Vizoso, B. Casas, E. Heslop, A. Pascual, A. Orfila, ... M. Manriquez (1) 101-117

The Gulf of Mexico Coastal Ocean Observing System: An Integrated Approach to Building an Operational Regional Observing System, A.E. Jochens, S.M. Watson (1) 118-133

Investigation of Underwater Acoustic Networking Enabling the Cooperative Operation of Multiple Heterogeneous Vehicles, N.A. Cruz, B.M. Ferreira, O. Kebkal, A.C. Matos, C. Petrioli, R. Petroccia, D. Spaccini (2) 43-58

Recent Development in IR Sensor Technology for Monitoring Subsea Methane Discharge, M. Schmidt, P. Linke, D. Esser (3) 27-36

Analysis of Underwater Acoustic Communication Channels, S. Ahmed, H. Arslan (3) 99-117

Assessment of Zooplankton Injury and Mortality Associated With Underwater Turbines for Tidal Energy Production, D.R. Schlezinger, C.D. Taylor, B.L. Howes (4) 142-150

Consideration of a Variable Frequency Energy Conversion System for Marine and Onshore Wind Energy Extraction, C.R. Merz (4) 218-225

Motivations and Methods for Modern Maritime Communications: A Survey of

Recent and Emerging Trends, D.M. Kocak, A.M. Clark (5) 7-18

U.S. IOOS: An Integrating Force for Good, Z. Willis, L. Griesbauer (5) 19-25

Recent Trends in Underwater Acoustic Communications, M. Stojanovic, L. Freitag (5) 45-50

Verification of Wave Measurement Systems, M.E. Luther, G. Meadows, E. Buckley, S.A. Gilbert, H. Purcell, M.N. Tamburri (5) 104-116

A View through the Waves, Y.Y. Schechner (5) 148-150

Offshore Structures

Multichannel Cathodic Protection Monitoring System for Offshore Structures, X. Wang, Z. Lan, J. Song, Z. Wang, S. Chen, B. Hou (1) 96-100

Numerical Simulation of Dynamic Positioning in Ice, I. Metrikin, S. Løset, N.A. Jenssen, S. Kerkeni (2) 14-30

Static and Fatigue Analysis of Composite Turbine Blades Under Random Ocean Current Loading, F. Zhou, H. Mahfuz, G.M. Alsenas, H.P. Hanson (2) 59-69

Conceptual Design of Ocean Compressed Air Energy Storage System, S.D. Lim, A.P. Mazzoleni, J.-k. Park, P.I. Ro, B. Quinlan (2) 70-81

DeepStar®: 22 Years of Success
DeepStar: A Global Deepwater Technology Development Program, G. Kusinski, A.J. Schroeder Jr., J.E. Chitwood (3) 5-12

DeepStar 11304: Laying the Groundwork for AUV Standards for Deepwater Fields, J. Jacobson, P. Cohen, A. Nasr, A.J. Schroeder Jr., G. Kusinski (3) 13-18

DeepStar Metocean Studies: 15 years of Discovery, C. Cooper, T. Mitchell, G. Forristall, J. Stear (3) 19-26

Anchor Drop Tests for a Submarine Power-Cable Protector, H.-S. Yoon, W.-B. Na (3) 72-80

The Muskeget Channel Tidal Energy Project: A Unique Case Study in the Licensing and Permitting of a Tidal Energy Project in Massachusetts, S.B. Barrett (4) 9-17

Dynamics of a Floating Platform Mounting a Hydrokinetic Turbine, T. Dewhurst, M.R. Swift, M. Wosnik, K. Baldwin, J. DeCew, M. Rowell (4) 45-56

Velocity Deficit and Swirl in the Turbulent Wake of a Wind Turbine, N.P. Dufresne, M. Wosnik (4) 193-205

Consideration of a Variable Frequency Energy Conversion System for Marine and Onshore Wind Energy Extraction, C.R. Merz (4) 218-225

Remotely Operated Vehicles

Investigation of Underwater Acoustic Networking Enabling the Cooperative Operation of Multiple Heterogeneous Vehicles, N.A. Cruz, B.M. Ferreira, O. Kebkal, A.C. Matos, C. Petrioli, R. Petroccia, D. Spaccini (2) 43-58

DeepStar®: 22 Years of Success
DeepStar: A Global Deepwater Technology Development Program, G. Kusinski, A.J. Schroeder Jr., J.E. Chitwood (3) 5-12

DeepStar 11304: Laying the Groundwork for AUV Standards for Deepwater Fields, J. Jacobson, P. Cohen, A. Nasr, A.J. Schroeder Jr., G. Kusinski (3) 13-18

Recent Development in IR Sensor Technology for Monitoring Subsea Methane Discharge, M. Schmidt, P. Linke, D. Esser (3) 27-36

Reliability-Centered Development of Deep Water ROV ROSUB 6000, V. Narayanaswamy, R. Raju, M. Durairaj, A. Ananthapadmanabhan, S. Annamalai, G.A. Ramadass, M.A. Atmanand (3) 55-71

Analysis of Underwater Acoustic Communication Channels, S. Ahmed, H. Arslan (3) 99-117

U.S. IOOS: An Integrating Force for Good, Z. Willis, L. Griesbauer (5) 19-25

Advantages of Natural Propulsive Systems, F.E. Fish (5) 37-44

2013 State of ROV Technologies, T. Schilling (5) 69-71

Unmanned Maritime Vehicles: Technology Evolution and Implications, A.Y. Martin (5) 72-83

A View through the Waves, Y.Y. Schechner (5) 148-150

Renewable Energy

Ocean Climate: "Off the Shelf", R. Cole, J. Kinder, W. Yu (1) 7-18

A Novel Ocean Sentinel Instrumentation Buoy for Wave Energy Testing, A. von Jouanne, T. Lettenmaier, E. Amon, T. Brekken, R. Phillips (1) 47-54

Static and Fatigue Analysis of Composite Turbine Blades Under Random Ocean Current Loading, F. Zhou, H. Mahfuz, G.M. Alsenas, H.P. Hanson (2) 59-69

Conceptual Design of Ocean Compressed Air Energy Storage System, S.D. Lim, A.P. Mazzoleni, J.-k. Park, P.I. Ro, B. Quinlan (2) 70-81

Anchor Drop Tests for a Submarine Power-Cable Protector, H.-S. Yoon, W.-B. Na (3) 72-80

The Muskeget Channel Tidal Energy Project: A Unique Case Study in the Licensing and Permitting of a Tidal Energy Project in Massachusetts, S.B. Barrett (4) 9-17

- Subsurface Mooring Stability in the Presence of Vertical Shear, H.P. Hanson (4) 18-22
- A Numerical Analysis of Bidirectional Ducted Tidal Turbines in Yawed Flow, C.S.K. Belloni, R.H.J. Willden, G.T. Houslyby (4) 23-35
- Performance Modeling of Ducted Vertical Axis Turbine Using Computational Fluid Dynamics, P. Chatterjee, R.N. Laoulache (4) 36-44
- Dynamics of a Floating Platform Mounting a Hydrokinetic Turbine, T. Dewhurst, M.R. Swift, M. Wosnik, K. Baldwin, J. DeCew, M. Rowell (4) 45-56
- Modeling Hydrokinetic Turbine Performance in the Mississippi River, P. Karalekas, G.J. Kowalski, E. Lovelace (4) 57-66
- Experimental Evaluation of a Mixer-Ejector Marine Hydrokinetic Turbine at Two Open-Water Tidal Energy Test Sites in NH and MA, M. Rowell, M. Wosnik, J. Barnes, J.P. King (4) 67-79
- Challenges in Realizing Reliable Subsea Electric Power Grid for Tidal Energy Farms, V. Narayanaswamy, H. Bang-Andreasen (4) 80-93
- Design of a Novel Vertical Axis Water Turbine With Retractable Arc-Type Blades, T. Wenlong, S. Baowei, M. Zhaoyong, D. Hao (4) 94-100
- Theoretical Assessment of Ocean Current Energy Potential for the Gulf Stream System, X. Yang, K.A. Haas, H.M. Fritz (4) 101-112
- Design and Implementation of a Marine Animal Alert System to Support Marine Renewable Energy, Z.D. Deng, T.J. Carlson, T. Fu, H. Ren, J.J. Martinez, J.R. Myers, ... A.E. Copping (4) 113-121
- The Impact of Tidal Stream Turbines on Circulation and Sediment Transport in Muskeget Channel, MA, A.R. Hakim, G.W. Cowles, J.H. Churchill (4) 122-136
- A Field Program for Developing a Baseline Characterization of Ichthyoplankton Near a Potential OTEC Facility, T.W. Hogan, J. Withrow, C. Linebaugh, A. Harmer, J. Steinbeck, S.K. Oney (4) 137-141
- Assessment of Zooplankton Injury and Mortality Associated With Underwater Turbines for Tidal Energy Production, D.R. Schlezinger, C.D. Taylor, B.L. Howes (4) 142-150
- The Use of Numerical Modeling to Optimize a New Wave Energy Converter Technology, B.E. Green, D.G. MacDonald (4) 151-163
- Testing the WET-NZ Wave Energy Converter Using the Ocean Sentinel Instrumentation Buoy, T. Lettenmaier, A. von Jouanne, E. Amon, S. Moran, A. Gardiner (4) 164-176
- Modeling of the Efficiency of a Semisubmerged Ocean Wave Energy Converter, M.T. MacNicoll, K.P. Thiagarajan, J. Rohrer (4) 177-186
- Wave Energy Conversion for Shoreline Protection, M.E. McCormick, R.C. Murtha, J. Steinmetz (4) 187-192
- Velocity Deficit and Swirl in the Turbulent Wake of a Wind Turbine, N.P. Dufresne, M. Wosnik (4) 193-205
- Toward Real-Time, Remote Observations of the Coastal Wind Resource Using High-Frequency Radar, A. Kirincich (4) 206-217
- Consideration of a Variable Frequency Energy Conversion System for Marine and Onshore Wind Energy Extraction, C.R. Merz (4) 218-225
- An Analysis of Florida's Sea Water Cooling Resource, D.N. Porak, J.H. VanZwieten Jr., B. Wiles (4) 226-239
- Global Review of Recent Ocean Energy Activities, A.B. Melo, E. Sweeney, J.L. Villate (5) 97-103
- Verification of Wave Measurement Systems, M.E. Luther, G. Meadows, E. Buckley, S.A. Gilbert, H. Purcell, M.N. Tamburri (5) 104-116
- Ropes and Tension Members**
- Ocean Climate: "Off the Shelf", R. Cole, J. Kinder, W. Yu (1) 7-18
- Subsurface Mooring Stability in the Presence of Vertical Shear, H.P. Hanson (4) 18-22
- Seafloor Engineering**
- Conceptual Design of Ocean Compressed Air Energy Storage System, S.D. Lim, A.P. Mazzoleni, J-k. Park, P.I. Ro, B. Quinlan (2) 70-81
- DeepStar[®]: 22 Years of Success
DeepStar: A Global Deepwater Technology Development Program, G. Kusinski, A.J. Schroeder Jr., J.E. Chitwood (3) 5-12
- Anchor Drop Tests for a Submarine Power-Cable Protector, H-S. Yoon, W-B. Na (3) 72-80
- Analysis of Underwater Acoustic Communication Channels, S. Ahmed, H. Arslan (3) 99-117
- 2013 State of ROV Technologies, T. Schilling (5) 69-71
- Underwater Imaging**
- Use of High-Resolution DIDSON Sonar to Quantify Attributes of Predation at Ecologically Relevant Space and Time Scales, V.E. Price, P.J. Auster, L. Kracker (1) 33-46
- Bonhomme Richard*: Connecting the Past With the Future, M.S. Ryan, J.W. White (2) 8-13
- DeepStar 11304: Laying the Groundwork for AUV Standards for Deepwater Fields, J. Jacobson, P. Cohen, A. Nasr, A.J. Schroeder Jr., G. Kusinski (3) 13-18
- Development of the *Jiaolong* Deep Manned Submersible, W. Cui (3) 37-54
- Analysis of Underwater Acoustic Communication Channels, S. Ahmed, H. Arslan (3) 99-117
- Wrecks on the Bottom: Useful, Ecological Sentinels?, A. Peirano (3) 118-127
- Assessment of Zooplankton Injury and Mortality Associated With Underwater Turbines for Tidal Energy Production, D.R. Schlezinger, C.D. Taylor, B.L. Howes (4) 142-150
- Synthetic Aperture Sonar Technology Review, R.E. Hansen (5) 117-127
- Extended-Range Undersea Laser Imaging: Current Research Status and a Glimpse at Future Technologies, F.R. Dalgleish, A.K. Vuorenkoski, B. Ouyang (5) 128-147
- A View through the Waves, Y.Y. Schechner (5) 148-150
- Long-Term Methods for High-Definition Image Maps of Benthic Surveys, L. Penland, B. Brooks, E. Ochoa (6) 7-15
- Unmanned Maritime Vehicles**
- SOCIB: The Balearic Islands Coastal Ocean Observing and Forecasting System Responding to Science, Technology and Society Needs, J. Tintoré, G. Vizoso, B. Casas, E. Heslop, A. Pascual, A. Orfila, ... M. Manriquez (1) 101-117
- Investigation of Underwater Acoustic Networking Enabling the Cooperative Operation of Multiple Heterogeneous Vehicles, N.A. Cruz, B.M. Ferreira, O. Kebkal, A.C. Matos, C. Petrioli, R. Petroccia, D. Spaccini (2) 43-58
- DeepStar[®]: 22 Years of Success
DeepStar: A Global Deepwater Technology Development Program, G. Kusinski, A.J. Schroeder Jr., J.E. Chitwood (3) 5-12
- DeepStar 11304: Laying the Groundwork for AUV Standards for Deepwater Fields, J. Jacobson, P. Cohen, A. Nasr, A.J. Schroeder Jr., G. Kusinski (3) 13-18
- Recent Development in IR Sensor Technology for Monitoring Subsea Methane Discharge, M. Schmidt, P. Linke, D. Esser (3) 27-36
- Elements of Underwater Glider Performance and Stability, S. Fan, C. Woolsey (3) 81-98
- Analysis of Underwater Acoustic Communication Channels, S. Ahmed, H. Arslan (3) 99-117
- Motivations and Methods for Modern Maritime Communications: A Survey of Recent and Emerging Trends, D.M. Kocak, A.M. Clark (5) 7-18

U.S. IOOS: An Integrating Force for Good,
Z. Willis, L. Griesbauer (5) 19-25

Advantages of Natural Propulsive Systems,
F.E. Fish (5) 37-44

Unmanned Maritime Vehicles: Technology
Evolution and Implications, A.Y. Martin
(5) 72-83

State of Technology in Autonomous
Underwater Gliders, S.L. Wood, C.E. Mierzwa
(5) 84-96

Synthetic Aperture Sonar Technology Review,
R.E. Hansen (5) 117-127

Education and Research

Biological/Chemical Oceanography

Experience With Moored Observations in the
Western Gulf of Maine From 2006 to 2012,
J.D. Irish, D. Vandemark, S. Shellito,
J.E. Salisbury (1) 19-32

Use of High-Resolution DIDSON Sonar
to Quantify Attributes of Predation at
Ecologically Relevant Space and Time Scales,
V.E. Price, P.J. Auster, L. Kracker (1) 33-46

The Gulf of Mexico Coastal Ocean Observing
System: An Integrated Approach to Building
an Operational Regional Observing System,
A.E. Jochens, S.M. Watson (1) 118-133

Electrochemical Cell Applications for Ballast
Water Treatment, C.B. Güney, F. Yonsel
(1) 134-145

Recent Development in IR Sensor Technology
for Monitoring Subsea Methane Discharge,
M. Schmidt, P. Linke, D. Esser (3) 27-36

Wrecks on the Bottom: Useful, Ecological
Sentinels?, A. Peirano (3) 118-127

A Field Program for Developing a Baseline
Characterization of Ichthyoplankton Near
a Potential OTEC Facility, T.W. Hogan,
J. Withrow, C. Linebaugh, A. Harmer,
J. Steinbeck, S.K. Oney (4) 137-141

Assessment of Zooplankton Injury and
Mortality Associated With Underwater
Turbines for Tidal Energy Production,
D.R. Schlezinger, C.D. Taylor, B.L. Howes
(4) 142-150

U.S. IOOS: An Integrating Force for Good,
Z. Willis, L. Griesbauer (5) 19-25

Advantages of Natural Propulsive Systems,
F.E. Fish (5) 37-44

An Experimental Deployment of a Portable
Inflatable Habitat in Open Water to Augment
Lengthy In-Water Decompression by Scientific
Divers, M. Lombardi, W. Bursleson, J. Godfrey,
R. Fryburg (6) 52-63

Marine Archaeology

Bonhomme Richard: Connecting the Past With
the Future, M.S. Ryan, J.W. White (2) 8-13

Wrecks on the Bottom: Useful, Ecological
Sentinels?, A. Peirano (3) 118-127

Synthetic Aperture Sonar Technology Review,
R.E. Hansen (5) 117-127

Long-Term Methods for High-Definition Image
Maps of Benthic Surveys, L. Penland, B. Brooks,
E. Ochoa (6) 7-15

A New Generation of ADS Capabilities,
J.F. Clark (6) 73-79

Marine Education

SOCIB: The Balearic Islands Coastal
Ocean Observing and Forecasting System
Responding to Science, Technology and Society
Needs, J. Tintoré, G. Vizoso, B. Casas,
E. Heslop, A. Pascual, A. Orfila, ...
M. Manriquez (1) 101-117

The Gulf of Mexico Coastal Ocean Observing
System: An Integrated Approach to Building
an Operational Regional Observing System,
A.E. Jochens, S.M. Watson (1) 118-133

Investigation of Underwater Acoustic
Networking Enabling the Cooperative
Operation of Multiple Heterogeneous Vehicles,
N.A. Cruz, B.M. Ferreira, O. Kebkal,
A.C. Matos, C. Petrioli, R. Petroccia,
D. Spaccini (2) 43-58

Development of the *Jiaolong* Deep Manned
Submersible, W. Cui (3) 37-54

Analysis of Underwater Acoustic
Communication Channels, S. Ahmed,
H. Arslan (3) 99-117

Experimental Evaluation of a Mixer-Ejector
Marine Hydrokinetic Turbine at Two
Open-Water Tidal Energy Test Sites in NH
and MA, M. Rowell, M. Wosnik, J. Barnes,
J.P. King (4) 67-79

U.S. IOOS: An Integrating Force for Good,
Z. Willis, L. Griesbauer (5) 19-25

A New Generation of ADS Capabilities,
J.F. Clark (6) 73-79

Marine Engineering

Ocean Climate: "Off the Shelf", R. Cole,
J. Kinder, W. Yu (1) 7-18

On 7,000 m Sea Trials of the Manned
Submersible *Jiaolong*, W. Cui, F. Liu, Z. Hu,
M. Zhu, W. Guo, C. Liu (1) 67-82

Ship Energy Efficiency Management Requires a
Total Solution Approach, P.J. Ballou (1) 83-95

SOCIB: The Balearic Islands Coastal Ocean
Observing and Forecasting System Responding to
Science, Technology and Society Needs, J. Tintoré,
G. Vizoso, B. Casas, E. Heslop, A. Pascual,
A. Orfila, ... M. Manriquez (1) 101-117

Electrochemical Cell Applications for Ballast
Water Treatment, C.B. Güney, F. Yonsel
(1) 134-145

Numerical Simulation of Dynamic Positioning
in Ice, I. Metrikin, S. Løset, N.A. Jenssen,
S. Kerkeni (2) 14-30

A General Approach for Dynamic Positioning
Weathervane Control, M.R. Miyazaki,
E.A. Tannuri (2) 31-42

Investigation of Underwater Acoustic
Networking Enabling the Cooperative
Operation of Multiple Heterogeneous Vehicles,
N.A. Cruz, B.M. Ferreira, O. Kebkal,
A.C. Matos, C. Petrioli, R. Petroccia,
D. Spaccini (2) 43-58

Static and Fatigue Analysis of Composite
Turbine Blades Under Random Ocean Current
Loading, F. Zhou, H. Mahfuz, G.M. Alsenas,
H.P. Hanson (2) 59-69

Conceptual Design of Ocean Compressed
Air Energy Storage System, S.D. Lim,
A.P. Mazzoleni, J.-k. Park, P.I. Ro,
B. Quinlan (2) 70-81

DeepStar[®]: 22 Years of Success
DeepStar: A Global Deepwater Technology
Development Program, G. Kusinski,
A.J. Schroeder Jr., J.E. Chitwood (3) 5-12

Development of the *Jiaolong* Deep Manned
Submersible, W. Cui (3) 37-54

Elements of Underwater Glider Performance and
Stability, S. Fan, C. Woolsey (3) 81-98

Analysis of Underwater Acoustic
Communication Channels, S. Ahmed,
H. Arslan (3) 99-117

Subsurface Mooring Stability in the Presence of
Vertical Shear, H.P. Hanson (4) 18-22

A Numerical Analysis of Bidirectional Ducted
Tidal Turbines in Yawed Flow, C.S.K. Belloni,
R.H.J. Willden, G.T. Housby (4) 23-35

Experimental Evaluation of a Mixer-Ejector
Marine Hydrokinetic Turbine at Two Open-
Water Tidal Energy Test Sites in NH and MA,
M. Rowell, M. Wosnik, J. Barnes, J.P. King
(4) 67-79

Challenges in Realizing Reliable Subsea Electric
Power Grid for Tidal Energy Farms,
V. Narayanaswamy, H. Bang-Andreasen
(4) 80-93

Design of a Novel Vertical Axis Water Turbine
With Retractable Arc-Type Blades, T. Wenlong,
S. Baowei, M. Zhaoyong, D. Hao (4) 94-100

Design and Implementation of a Marine
Animal Alert System to Support Marine
Renewable Energy, Z.D. Deng, T.J. Carlson,
T. Fu, H. Ren, J.J. Martinez, J.R. Myers, ...
A.E. Copping (4) 113-121

A Field Program for Developing a Baseline
Characterization of Ichthyoplankton Near
a Potential OTEC Facility, T.W. Hogan,
J. Withrow, C. Linebaugh, A. Harmer,
J. Steinbeck, S.K. Oney (4) 137-141

Assessment of Zooplankton Injury and Mortality Associated With Underwater Turbines for Tidal Energy Production, D.R. Schlezinger, C.D. Taylor, B.L. Howes (4) 142-150

The Use of Numerical Modeling to Optimize a New Wave Energy Converter Technology, B.E. Green, D.G. MacDonald (4) 151-163

Modeling of the Efficiency of a Semisubmerged Ocean Wave Energy Converter, M.T. MacNicoll, K.P. Thiagarajan, J. Rohrer (4) 177-186

Toward Real-Time, Remote Observations of the Coastal Wind Resource Using High-Frequency Radar, A. Kirinchich (4) 206-217

Consideration of a Variable Frequency Energy Conversion System for Marine and Onshore Wind Energy Extraction, C.R. Merz (4) 218-225

An Analysis of Florida's Sea Water Cooling Resource, D.N. Porak, J.H. VanZwieten Jr., B. Wiles (4) 226-239

Advantages of Natural Propulsive Systems, F.E. Fish (5) 37-44

The Future of Maritime Propulsion: "Reading the Propulsion Crystal Ball", M. Tangora (5) 51-55

Manufacturing Imperfection Sensitivity Analysis of Spherical Pressure Hull for Manned Submersible, B. Pranesh, D. Sathianarayanan, S. Ramesh, G.A. Ramadass (6) 64-72

A New Generation of ADS Capabilities, J.F. Clark (6) 73-79

Marine Geodetic Information Systems

Analysis of Underwater Acoustic Communication Channels, S. Ahmed, H. Arslan (3) 99-117

A View through the Waves, Y.Y. Schechner (5) 148-150

Marine Materials

Static and Fatigue Analysis of Composite Turbine Blades Under Random Ocean Current Loading, F. Zhou, H. Mahfuz, G.M. Alsenas, H.P. Hanson (2) 59-69

Anchor Drop Tests for a Submarine Power-Cable Protector, H-S. Yoon, W-B. Na (3) 72-80

Ocean Exploration

Ocean Climate: "Off the Shelf", R. Cole, J. Kinder, W. Yu (1) 7-18

On 7,000 m Sea Trials of the Manned Submersible *Jiaolong*, W. Cui, F. Liu, Z. Hu, M. Zhu, W. Guo, C. Liu (1) 67-82

SOCIB: The Balearic Islands Coastal Ocean Observing and Forecasting System Responding to Science, Technology and Society

Needs, J. Tintoré, G. Vizoso, B. Casas, E. Heslop, A. Pascual, A. Orfila, ... M. Manriquez (1) 101-117

Bonhomme Richard: Connecting the Past With the Future, M.S. Ryan, J.W. White (2) 8-13

Numerical Simulation of Dynamic Positioning in Ice, I. Metrikin, S. Løset, N.A. Jenssen, S. Kerkeni (2) 14-30

Investigation of Underwater Acoustic Networking Enabling the Cooperative Operation of Multiple Heterogeneous Vehicles, N.A. Cruz, B.M. Ferreira, O. Kebkal, A.C. Matos, C. Petrioli, R. Petroccia, D. Spaccini (2) 43-58

Recent Development in IR Sensor Technology for Monitoring Subsea Methane Discharge, M. Schmidt, P. Linke, D. Esser (3) 27-36

Development of the *Jiaolong* Deep Manned Submersible, W. Cui (3) 37-54

Analysis of Underwater Acoustic Communication Channels, S. Ahmed, H. Arslan (3) 99-117

Wrecks on the Bottom: Useful, Ecological Sentinels?, A. Peirano (3) 118-127

Advantages of Natural Propulsive Systems, F.E. Fish (5) 37-44

Recent Trends in Underwater Acoustic Communications, M. Stojanovic, L. Freitag (5) 45-50

2013 State of ROV Technologies, T. Schilling (5) 69-71

Long-Term Methods for High-Definition Image Maps of Benthic Surveys, L. Penland, B. Brooks, E. Ochoa (6) 7-15

An Experimental Deployment of a Portable Inflatable Habitat in Open Water to Augment Lengthy In-Water Decompression by Scientific Divers, M. Lombardi, W. Bursleson, J. Godfrey, R. Fryburg (6) 52-63

A New Generation of ADS Capabilities, J.F. Clark (6) 73-79

Physical Oceanography/Meteorology

Ocean Climate: "Off the Shelf", R. Cole, J. Kinder, W. Yu (1) 7-18

Experience With Moored Observations in the Western Gulf of Maine From 2006 to 2012, J.D. Irish, D. Vandemark, S. Shellito, J.E. Salisbury (1) 19-32

Comparison of the Observed Mixed Layer Depth in the Lee of the Hawaiian Island to the Modeled Mixed Layer Depth of the Regional Navy Coastal Ocean Model, J.T. Rayburn, V.M. Kamenkovich (1) 55-66

SOCIB: The Balearic Islands Coastal Ocean Observing and Forecasting System Responding to Science, Technology and Society Needs, J. Tintoré, G. Vizoso, B. Casas,

E. Heslop, A. Pascual, A. Orfila, ... M. Manriquez (1) 101-117

The Gulf of Mexico Coastal Ocean Observing System: An Integrated Approach to Building an Operational Regional Observing System, A.E. Jochens, S.M. Watson (1) 118-133

A General Approach for Dynamic Positioning Weathervane Control, M.R. Miyazaki, E.A. Tannuri (2) 31-42

DeepStar[®]: 22 Years of Success
DeepStar: A Global Deepwater Technology Development Program, G. Kusinski, A.J. Schroeder Jr., J.E. Chitwood (3) 5-12

DeepStar Metocean Studies: 15 years of Discovery, C. Cooper, T. Mitchell, G. Forristall, J. Stear (3) 19-26

Analysis of Underwater Acoustic Communication Channels, S. Ahmed, H. Arslan (3) 99-117

Subsurface Mooring Stability in the Presence of Vertical Shear, H.P. Hanson (4) 18-22

U.S. IOOS: An Integrating Force for Good, Z. Willis, L. Griesbauer (5) 19-25

Verification of Wave Measurement Systems, M.E. Luther, G. Meadows, E. Buckley, S.A. Gilbert, H. Purcell, M.N. Tamburri (5) 104-116

Remote Sensing

The Gulf of Mexico Coastal Ocean Observing System: An Integrated Approach to Building an Operational Regional Observing System, A.E. Jochens, S.M. Watson (1) 118-133

Bonhomme Richard: Connecting the Past With the Future, M.S. Ryan, J.W. White (2) 8-13

Investigation of Underwater Acoustic Networking Enabling the Cooperative Operation of Multiple Heterogeneous Vehicles, N.A. Cruz, B.M. Ferreira, O. Kebkal, A.C. Matos, C. Petrioli, R. Petroccia, D. Spaccini (2) 43-58

DeepStar[®]: 22 Years of Success
DeepStar: A Global Deepwater Technology Development Program, G. Kusinski, A.J. Schroeder Jr., J.E. Chitwood (3) 5-12

DeepStar 11304: Laying the Groundwork for AUV Standards for Deepwater Fields, J. Jacobson, P. Cohen, A. Nasr, A.J. Schroeder Jr., G. Kusinski (3) 13-18

Analysis of Underwater Acoustic Communication Channels, S. Ahmed, H. Arslan (3) 99-117

Motivations and Methods for Modern Maritime Communications: A Survey of Recent and Emerging Trends, D.M. Kocak, A.M. Clark (5) 7-18

Ocean Salinity and the Aquarius/SAC-D Mission: A New Frontier in Ocean Remote Sensing, G. Lagerloef, A. deCharon, E. Lindstrom (5) 26-30

Synthetic Aperture Sonar Technology Review, R.E. Hansen (5) 117-127

Extended-Range Undersea Laser Imaging: Current Research Status and a Glimpse at Future Technologies, F.R. Dalgleish, A.K. Vuorenkoski, B. Ouyang (5) 128-147

A View through the Waves, Y.Y. Schechner (5) 148-150

Underwater Communications

Motivations and Methods for Modern Maritime Communications: A Survey of Recent and Emerging Trends, D.M. Kocak, A.M. Clark (5) 7-18

Recent Trends in Underwater Acoustic Communications, M. Stojanovic, L. Freitag (5) 45-50

Government and Public Affairs

Marine Law and Policy

Use of High-Resolution DIDSON Sonar to Quantify Attributes of Predation at Ecologically Relevant Space and Time Scales, V.E. Price, P.J. Auster, L. Kracker (1) 33-46

SOCIB: The Balearic Islands Coastal Ocean Observing and Forecasting System Responding to Science, Technology and Society Needs, J. Tintoré, G. Vizoso, B. Casas, E. Heslop, A. Pascual, A. Orfila, ... M. Manriquez (1) 101-117

The Gulf of Mexico Coastal Ocean Observing System: An Integrated Approach to Building an Operational Regional Observing System, A.E. Jochens, S.M. Watson (1) 118-133

Electrochemical Cell Applications for Ballast Water Treatment, C.B. Güney, F. Yonsel (1) 134-145

Anchor Drop Tests for a Submarine Power-Cable Protector, H-S. Yoon, W-B. Na (3) 72-80

The Muskeget Channel Tidal Energy Project: A Unique Case Study in the Licensing and Permitting of a Tidal Energy Project in Massachusetts, S.B. Barrett (4) 9-17

Assessment of Zooplankton Injury and Mortality Associated With Underwater Turbines for Tidal Energy Production, D.R. Schlezinger, C.D. Taylor, B.L. Howes (4) 142-150

Marine Security

A General Approach for Dynamic Positioning Weathervane Control, M.R. Miyazaki, E.A. Tannuri (2) 31-42

Investigation of Underwater Acoustic Networking Enabling the Cooperative Operation of Multiple Heterogeneous Vehicles, N.A. Cruz, B.M. Ferreira, O. Kebkal, A.C. Matos, C. Petrioli, R. Petroccia, D. Spaccini (2) 43-58

Advantages of Natural Propulsive Systems, F.E. Fish (5) 37-44

Ocean Economic Potential

Ship Energy Efficiency Management Requires a *Total Solution* Approach, P.J. Ballou (1) 83-95

SOCIB: The Balearic Islands Coastal Ocean Observing and Forecasting System Responding to Science, Technology and Society Needs, J. Tintoré, G. Vizoso, B. Casas, E. Heslop, A. Pascual, A. Orfila, ... M. Manriquez (1) 101-117

Conceptual Design of Ocean Compressed Air Energy Storage System, S.D. Lim, A.P. Mazzoleni, J-k. Park, P.I. Ro, B. Quinlan (2) 70-81

Modeling Hydrokinetic Turbine Performance in the Mississippi River, P. Karalekas, G.J. Kowalski, E. Lovelace (4) 57-66

Experimental Evaluation of a Mixer-Ejector Marine Hydrokinetic Turbine at Two Open-Water Tidal Energy Test Sites in NH and MA, M. Rowell, M. Wosnik, J. Barnes, J.P. King (4) 67-79

Challenges in Realizing Reliable Subsea Electric Power Grid for Tidal Energy Farms, V. Narayanaswamy, H. Bang-Andreasen (4) 80-93

Design of a Novel Vertical Axis Water Turbine With Retractable Arc-Type Blades, T. Wenlong, S. Baowei, M. Zhaoyong, D. Hao (4) 94-100

Theoretical Assessment of Ocean Current Energy Potential for the Gulf Stream System, X. Yang, K.A. Haas, H.M. Fritz (4) 101-112

Design and Implementation of a Marine Animal Alert System to Support Marine Renewable Energy, Z.D. Deng, T.J. Carlson, T. Fu, H. Ren, J.J. Martinez, J.R. Myers, ... A.E. Copping (4) 113-121

Assessment of Zooplankton Injury and Mortality Associated With Underwater Turbines for Tidal Energy Production, D.R. Schlezinger, C.D. Taylor, B.L. Howes (4) 142-150

The Use of Numerical Modeling to Optimize a New Wave Energy Converter Technology, B.E. Green, D.G. MacDonald (4) 151-163

Modeling of the Efficiency of a Semisubmerged Ocean Wave Energy Converter, M.T. MacNicoll, K.P. Thiagarajan, J. Rohrer (4) 177-186

Velocity Deficit and Swirl in the Turbulent Wake of a Wind Turbine, N.P. Dufresne, M. Wosnik (4) 193-205

Toward Real-Time, Remote Observations of the Coastal Wind Resource Using High-Frequency Radar, A. Kirincich (4) 206-217

Consideration of a Variable Frequency Energy Conversion System for Marine and Onshore Wind Energy Extraction, C.R. Merz (4) 218-225

An Analysis of Florida's Sea Water Cooling Resource, D.N. Porak, J.H. VanZwieten Jr., B. Wiles (4) 226-239

U.S. IOOS: An Integrating Force for Good, Z. Willis, L. Griesbauer (5) 19-25

Ocean Observing Systems

Ocean Climate: "*Off the Shelf*", R. Cole, J. Kinder, W. Yu (1) 7-18

Use of High-Resolution DIDSON Sonar to Quantify Attributes of Predation at Ecologically Relevant Space and Time Scales, V.E. Price, P.J. Auster, L. Kracker (1) 33-46

SOCIB: The Balearic Islands Coastal Ocean Observing and Forecasting System Responding to Science, Technology and Society Needs, J. Tintoré, G. Vizoso, B. Casas, E. Heslop, A. Pascual, A. Orfila, ... M. Manriquez (1) 101-117

The Gulf of Mexico Coastal Ocean Observing System: An Integrated Approach to Building an Operational Regional Observing System, A.E. Jochens, S.M. Watson (1) 118-133

Investigation of Underwater Acoustic Networking Enabling the Cooperative Operation of Multiple Heterogeneous Vehicles, N.A. Cruz, B.M. Ferreira, O. Kebkal, A.C. Matos, C. Petrioli, R. Petroccia, D. Spaccini (2) 43-58

DeepStar 11304: Laying the Groundwork for AUV Standards for Deepwater Fields, J. Jacobson, P. Cohen, A. Nasr, A.J. Schroeder Jr., G. Kusinski (3) 13-18

DeepStar Metocean Studies: 15 years of Discovery, C. Cooper, T. Mitchell, G. Forristall, J. Stear (3) 19-26

Recent Development in IR Sensor Technology for Monitoring Subsea Methane Discharge, M. Schmidt, P. Linke, D. Esser (3) 27-36

Development of the *Jiaolong* Deep Manned Submersible, W. Cui (3) 37-54

Elements of Underwater Glider Performance and Stability, S. Fan, C. Woolsey (3) 81-98

Analysis of Underwater Acoustic Communication Channels, S. Ahmed, H. Arslan (3) 99-117

Wrecks on the Bottom: Useful, Ecological Sentinels?, A. Peirano (3) 118-127

Consideration of a Variable Frequency Energy Conversion System for Marine and Onshore Wind Energy Extraction, C.R. Merz (4) 218-225

U.S. IOOS: An Integrating Force for Good,
Z. Willis, L. Griesbauer (5) 19-25

Motivations and Methods for Modern
Maritime Communications: A Survey of
Recent and Emerging Trends, D.M. Kocak,
A.M. Clark (5) 7-18

Understanding the Planetary Life Support
System: Next-Generation Science in the
Ocean Basins, J.R. Delaney (5) 31-36

Verification of Wave Measurement Systems,
M.E. Luther, G. Meadows, E. Buckley,

S.A. Gilbert, H. Purcell, M.N. Tamburri
(5) 104-116

Long-Term Methods for High-Definition
Image Maps of Benthic Surveys, L. Penland,
B. Brooks, E. Ochoa (6) 7-15

A New Generation of ADS Capabilities,
J.F. Clark (6) 73-79

Ocean Pollution

Electrochemical Cell Applications for Ballast
Water Treatment, C.B. Güney, F. Yonsel
(1) 134-145

DeepStar Metocean Studies: 15 years of
Discovery, C. Cooper, T. Mitchell,
G. Forristall, J. Stear (3) 19-26

Analysis of Underwater Acoustic
Communication Channels, S. Ahmed,
H. Arslan (3) 99-117

The Future of Maritime Propulsion:
"Reading the Propulsion Crystal Ball",
M. Tangora (5) 51-55

2013 Reviewers for *MTS Journal*

- Robert Adey
Wessex Institute of Technology
- Emmanuel Agamloh
North Carolina State University
- Gabriel Alsenas
Florida Atlantic University
- Tim Arcano
NOAA
- William Arnold
NOAA/NMFS/Southeast Regional
Office
- Kenneth Baldwin
University of New Hampshire
- Steve Barrow
FMC Technologies
- Tommy Beals
Naval Sea Systems Command
- Clarissa Belloni
Oxford University
- Landry Bernard
NOAA/NDBC
- Eric Bibeau
University of Manitoba
- Remi Blokker
Bluerise
- Lotzi Boloni
University of Central Florida
- Peter Brickley
Horizon Marine, Inc.
- Massimo Caccia
Istituto di Studi sui Sistemi
Intelligenti per l'Automazione
- Todd Callaghan
Massachusetts Coastal Zone
Management
- Palmer Carlin
National Renewable Energy
Laboratory
- Jeffrey Cerquetti
JMT Engineering
- Joe Cichock
HARRIS Corporation
- Jonathan Colby
Verdant Power
- Andrea Copping
Pacific Northwest National
Laboratory
- Joe Crouch
Southwest Research Institute
- João Cruz
GL Garrad Hassan
- Herve de Naurois
Total
- Petar Denoble
Divers Alert Network USA
- Chris Dieterle
Portland General Electric
- Frederick Driscoll
National Renewable Energy
Laboratory
- Dave Driver
BP
- Jean-Francois Drogou
Ifremer
- Lindsay Dubbs
University of North Carolina
Coastal Studies Institute
- Alana Duerr
U.S. Department of Energy
- Brian Dzwonkowski
University of Maine
- Sören Ehlers
Norwegian University of Science
& Technology
- Dan Ensz
Timonium, MD
- Jennifer Ervin
Naval METOC Command
- Ralph Fehr
University of South Florida
- Bob Freeman
Office of the Oceanographer
of the Navy
- David Gaden
University of Manitoba
- Francesco Gasperoni
ENI Tecnomare
- Brooke Gintert
University of Miami
- Art Gleason
University of Miami
- Peter Gough
Harvey Mudd College
- Monty Graham
University of Southern Mississippi
- Pat Grandelli
Makai Ocean Engineering
- Kevin Haas
Georgia Institute of Technology
- Angelos Hannides
University of Cyprus
- Howard Hanson
Florida Atlantic University
- Michael Hayes
University of Canterbury
- John Hedgepeth
Tenerra Environment
- Douglas Helton
NOAA Office of Response &
Restoration
- Bobby Hodgkinson
University of Florida
- Tim Hogan
Alden Laboratories
- Stephan Howden
University of Southern Mississippi
- Brian Howes
University of Massachusetts at
Dartmouth
- Iqbal Husain
North Carolina State University
- Joe Imlach
Exocetus Development LLC
- Jules Jaffe
University of California, San Diego
- Tommy Jensen
University of Hawaii
- Mark Kaiser
Louisiana State University
- Sagar Kamarthi
Northeastern University
- D. Kirubakaran
St. Joseph Engineering College
- Donna Kocak
HARRIS Corporation
- Karen Kohanowich
Sea Space Initiative
- William Kohnen
Hydrospace Group
- Josh Kohut
Rutgers University
- David Kraemer
University of Wisconsin-Platteville
- Guido Kuiper
Shell International
- Havannes Kulhandjian
SUNY at Buffalo
- John Langan
St. Louis, MO
- Raymond Laoulache
University of Massachusetts at
Dartmouth

Michael Lombardi
Lombardi Undersea Resource
Center

Patrick Lorenz
Maine Maritime Academy

Jim Luby
University of Washington

Mark Luther
University of South Florida

Daniel MacDonald
University of Massachusetts at
Dartmouth

Stephen Maconi
U.S. Naval Academy Foundation

Bill Maddock
BP America

Rafael Mandujano
Vehicle Control Technologies, Inc.

Palaniappan Manickavasagam
Wartsila Ship Design Ltd.

Manikandan Mariappan
FMC Technologies

Greg McFall
NOAA National Marine Sanctuary

Sean McTavish
Carlton University

Maggie Merrill
New England Marine Renewable
Energy Center

Clifford Merz
University of South Florida

Michael Moran
Ohio State University

Cory Moore
Statoil

Paul Moorhouse

Ryan Morton
Anadarko

Linda Mullen
U.S. Navy

Mark Munro

K. Murali
Indian Institute of Technology
Madras

K.G. Nadeeshani Nanayakkara
University of Peradeniya

Vince Neary
Oak Ridge National Laboratory

Dong Trong Nguyen
Marine Cybernetics

Guy Noll
Esri

Phil Nuytten
Nuytco Research Ltd.

Edward O'Brien
Woods Hole Oceanographic
Institution

Reiner Onken
Center for Maritime Research &
Experimentation

Bill O'Reilly
Scripps Institution of Oceanography

Mark Patterson
Virginia Institute of Marine
Science

Dave Peters
ConocoPhillips

Roberto Petroccia
University of Rome

S.V.S. Phani Kumar
National Institute of Ocean
Technology

Jeff Pieper
University of Calgary

Brian Polagye
University of Washington

Omer Poroy
Bluefin Robotics

Joe Prudell
Columbia Power

Paul Raeymakers
rEvo Rebreathers

Anna Redden
Acadia Centre for Estuarine
Research

Steven Resler
InnerSpace Scientific Diving

Yanxia Rong

Kelley Ruehl
Sandia National Laboratories

Anatoly Sagalevich
P.P. Shirshov Institute of
Oceanology

A. Sankaranarayanan
GE Energy & Power Conversion

Dana Savage
Skidaway Institute of Oceanography

Martin Sayer
National Facility for Scientific
Diving

Daniel Schwartz
University of Washington

Thomas Sebastian
MIT Lincoln Laboratory

Marc Senders
University of Western Australia

Richard Seymour
Scripps Institution of Oceanography

S. Shankar
Kongu Engineering College

Richard Starr
Moss Landing Marine Laboratories

Miles Sundermeyer
University of Massachusetts at
Dartmouth

Robinson Swift
University of New Hampshire

Shinichi Takagawa
University of Tokyo

Chris Taylor
NOAA Applied Ecology &
Restoration Research Branch

Chung-Chu Teng
NOAA

Michael Triantafyllou
MIT

Igor Tsukrov
University of New Hampshire

Kurt Uetz
Woods Hole Oceanographic
Institution

Septimus van der Linden
Brolin Associates LLC

Luis Vega
University of Hawaii

Philip Vitale
Naval Facilities Engineering
Command

Annette von Jouanne
Oregon State University

Zoran Vukić
University of Zagreb

Anni K. Vuorenkoski
Harbor Branch Oceanographic
Institute

Robert Weller
Woods Hole Oceanographic
Institution

Robert Wernli
First Centurion Enterprises

Martin Wosnik
University of New Hampshire

Yanhua Wu
Nanyang Technological University

Zhaoqing Yang
Pacific Northwest National
Laboratory

Feitian Zhang
Michigan State University

Vincent Zintzen
Museum of New Zealand

UPCOMING MTS JOURNAL ISSUES

January/February 2014

General Issue

March/April 2014

Marine Technologies from Norway

May/June 2014

Marine Technology Developments in Asia

Guest editors: Dhugal Lindsay and Hiroyuki Nakahara



marine technology
SOCIETY

Opportunity runs deep™

Check the Society website for future *Journal* topics.
www.mtsociety.org

CALL FOR PAPERS

The *MTS Journal* includes technical papers, notes and commentaries of general interest in most issues.

Contact Managing Editor
Amy Morgante
(morganteeditorial@verizon.net)
if you have material you would like considered.

Specifications for submitting a manuscript are on the MTS website under the Publications menu.
www.mtsociety.org

E-mail:
morganteeditorial@verizon.net

Or visit our homepage at
www.mtsociety.org

STATEMENT OF OWNERSHIP

Statement of Ownership, Management, and Circulation (Required by 39 U.S.C. 3685)

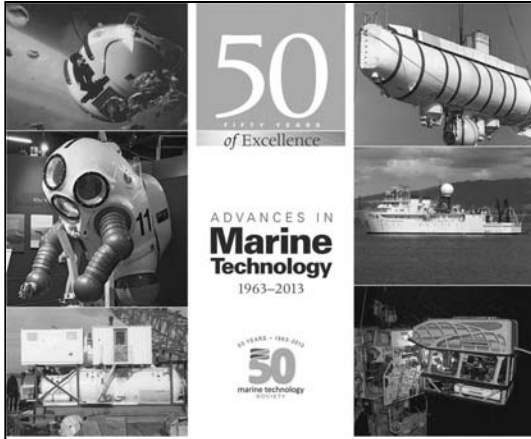
1. Publication Title: Marine Technology Society Journal
2. Publication Number: 0025-3324
3. Filing Date: 10/30/13
4. Issue Frequency: Bi-monthly
5. Number of Issues Published Annually: 6
6. Annual Subscription Price: \$135 Domestic; \$200 Foreign
7-8. Complete Mailing Address of Known Office of Publication and Headquarters or General Business Office of Publisher (Not printer): Marine Technology Society, 1100 H Street NW, LL-100, Washington, DC 20005
9. Publisher: Marine Technology Society, 1100 H Street NW, LL-100, Washington, DC 20005; Editor: Ann Jochens, MTS, 1100 H Street NW, LL-100, Washington, DC 20005; Managing Editor: Amy Morgante, 1100 H Street NW, LL-100, Washington, DC 20005
10. Owner: Marine Technology Society, 1100 H Street NW, LL-100, Washington, DC 20005
11. Known Bondholders, Mortgagees, and Other Security Holders Owning or Holding 1 Percent or More of Total Amount of Bonds, Mortgages, or Other Securities: None

12. Tax Status: Has Not Changed During Preceding 12 Months
13. Publication Title: Marine Technology Society Journal
14. Issue Date for Circulation Data Below: Nov/Dec 2013
15. Extent and Nature of Circulation

	Average No. Copies Each Issue During Preceding 12 Months	No. Copies of Single Issue Published Nearest to Filing Date
a. Total Number of Copies (Net Press Run)	650	650
b. Paid Circulation (By Mail and Outside the Mail)		
1. Mailed Outside-Country Paid Subscriptions Stated on PS Form 3541 (include paid distribution above normal rate, advertiser's proof copies, and exchange copies)	500	500
2. Mailed In-County Paid Subscriptions Stated On form 3541 (include advertiser's proof and exchange copies)	0	0
3. Sales Through Dealers and Carriers, Street Vendors, Counter Sales, and Other Non-USPS Distribution	0	0

4. Paid Distribution by Other Classes of Mail Through the USPS	50	50
c. Total Paid Distribution (sum of 15b, (1), (2), (3) and (4))	550	550
d. Free or Nominal Rate Distribution (By Mail and Outside the Mail)		
1. Outside-country as Stated on Form 3541	0	0
2. In-County as Stated on Form 3541	0	0
3. Other Classes Mailed Through the USPS	0	0
4. Free Distribution Outside the Mail	50	50
e. Total Free or Nominal Rate Distribution (Sum of 15d)	50	50
f. Total Distribution (Sum of 15c and 15e)	600	600
g. Copies not Distributed	50	50
h. Total (sum of 15f and g)	650	650
i. Percent Paid (15c divided by 15f times 100)	92%	92%

16. Publication Statement of Ownership will be printed in the Vol. 47, No. 6 issue of this publication, Nov/Dec 2013.
I certify that the statements above made by me are correct and complete.
Amy Morgante



**MTS' 50 Years of Excellence:
Advances in Marine Technology
is now available!
Be sure to order your copy
today for the perfect gift.**

See the ad on page 3, or call 202-717-8705, ext. 102.

**Hardbound edition is \$60, quality paperbound is \$45.
Shipping and handling is \$5/each.**

The MTS Top 10!

10. **Showcase your research** at Society-sponsored conferences
9. **Stay up-to-date** with our industry-leading peer-reviewed *MTS Journal*
8. **Join the network of professionals** in *your* local community
7. **Focus-in on your area of expertise** by joining one of over 25 highly specialized Professional Committees
6. **Expand your horizons** at the many MTS specialized workshops including the TechSurge program
5. **Grow your mentoring and leadership skills** by working with our Young Professionals and Students
4. **Gain national recognition** through the MTS Awards program
3. **Network with international businesses and members** in Europe, Asia and South America
2. **Take advantage of opportunity.** The MTS motto is "Opportunity Runs Deep"
1. **Enter the gateway to the international community** of scientists, ocean engineers, technologists and policy-makers.

Spread the word today about MTS Membership — and all the advantages for individuals, students, and companies!

**Call 202-717-8705
Visit: www.mtsociety.org**

Marine Technology Society Member Organizations

CORPORATE MEMBERS

ABCO Subsea
Houston, Texas

Aerojet Rocketdyne Extreme Engineering
Houston, Texas

AMETEK Sea Connect Products, Inc.
Westerly, Rhode Island

Bluefin Robotics
Quincy, MA

C & C Technologies, Inc.
Lafayette, Louisiana

CDL, Inc.
Houston, Texas

C-MAR Group
Houston, Texas

Compass Publications, Inc.
Arlington, Virginia

DOF Subsea USA
Houston, Texas

Dynacon, Inc.
Bryan, Texas

EMAS AMC
Houston, Texas

Fluor Offshore Solutions
Sugar Land, Texas

Forum Energy Technologies
Houston, Texas

Fugro Chance, Inc.
Lafayette, Louisiana

Fugro Geoservices, Inc.
Houston, Texas

Fugro-McClelland Marine Geosciences
Houston, Texas

Fugro Pelagos, Inc.
San Diego, California

Geospace Offshore Cables
Houston, Texas

GE Energy Power Conversion
Houston, Texas

GL Noble Denton
Houston, Texas

HARRIS CapRock Communications
Melbourne, Florida

Hydroid, LLC
Pocasset, Massachusetts

Innerspace Corporation
Covina, California

INTECSEA
Houston, Texas

InterMoor, Inc.
Houston, Texas

J P Kenny, Inc.
Houston, Texas

Kongsberg Maritime, Inc.
Houston, Texas

L-3 Communications
Houston, Texas

L-3 MariPro
Goleta, California

Lockheed Martin Sippican
Marion, Massachusetts

MacArtney, Inc.
Houston, Texas

Marine Cybernetics AS
Trondheim, Norway

Mitsui Engineering and Shipbuilding Co. Ltd.
Tokyo, Japan

Oceaneering Advanced Technologies
Hanover, Maryland

Oceaneering International, Inc.
Houston, Texas

OceanWorks International
Houston, Texas

Odyssey Marine Exploration
Tampa, Florida

Oil States Industries, Inc.
Arlington, Texas

Petrustech Oil & Gas
Houston, Texas

Phoenix International Holdings, Inc.
Largo, Maryland

QinetiQ North America – Technology Solutions Group
Slidell, Louisiana

Quest Offshore Resources
Sugar Land, Texas

Raytheon Technical Service Company, LLC

Saipem America, Inc.
Houston, Texas

SBM Atlantia
Houston, Texas

Schilling Robotics, LLC
Davis, California

SEA CON Brantner and Associates, Inc.
El Cajon, California

Siemens Energy, Inc.
Houston, Texas

SonTek/YSL, Inc.
San Diego, California

South Bay Cable Corp.
Idyllwild, California

Stress Engineering Services, Inc.
Houston, Texas

Subsea 7 (US), LLC
Houston, Texas

Technip
Houston, Texas

Teledyne Benthos
North Falmouth, Massachusetts

Teledyne Oil & Gas
Daytona Beach, Florida

Teledyne RD Instruments, Inc.
Poway, California

UniversalPegasus International, Inc.
Houston, Texas

Wachs Subsea LLC
Houston, Texas

Whitefield Plastics
Houston, Texas

BUSINESS MEMBERS

Ashtead Technology, Inc.
Houston, Texas

Baker Marine Solutions
Mandeville, Louisiana

Bastion Technologies, Inc.
Houston, Texas

BioSonics, Inc.
Seattle, Washington

Braemar Engineering
Houston, Texas

C.A. Richards and Associates, Inc.
Houston, Texas

CARIS
Alexandria, Virginia

Cochrane Technologies, Inc.
Lafayette, Louisiana

Contros Systems & Solutions GmbH
Kiel, Germany

DeepSea Power and Light
San Diego, California

Deepwater Rental and Supply
New Iberia, Louisiana

DPS Offshore Inc.
Houston, Texas

Embient GmbH
Halstenbek, Germany

Energy Sales, Inc.
Redmond, Washington

Falmat, Inc.
San Marcos, California

FASTORQ
New Caney, Texas

Fugro GeoSurveys, Inc., a division of Fugro
Canada Corp.
St. John's, Newfoundland and Labrador, Canada

Horizon Marine, Inc.
Marion, Massachusetts

HortonGMC
Houston, Texas

Huisman North America Services
Rosenberg, Texas

iXBlue, Inc.
Cambridge, Massachusetts

Knight, LLC
Lake Forest, California

Liquid Robotics, Inc.
Palo Alto, California

London Offshore Consultants, Inc.
Houston, Texas

Makai Ocean Engineering, Inc.
Kailua, Hawaii

Maritime Assurance & Consulting Ltd.
Aberdeen, United Kingdom

Matthews-Daniel Company
Houston, Texas

Oceanic Imaging Consultants, Inc.
Honolulu, Hawaii

Offshore Analysis & Research Solutions (OARS), LLC
Austin, Texas

Offshore Inspection Group, Inc.
Houston, TX

Poseidon Offshore Mining
Oslo, Norway

QPS
Portsmouth, New Hampshire

Remote Ocean Systems, Inc.
San Diego, California

RRC Robotica Submarina
Macaé, Brazil

SeaBotix
San Diego, California

SeaLandAire Technologies, Inc.
Jackson, Mississippi

SEATECHRIM
Moscow, Russia

SeaView Systems, Inc.
Dexter, Michigan

Sonardyne, Inc.
Houston, Texas

SIMCorp Marine Environmental, Inc.
St. Stephens, Canada

Sound Ocean Systems, Inc.
Redmond, Washington

Stress Subsea, Inc.
Houston, Texas

SURF Subsea, Inc.
Magnolia, Texas

Technip – Global Industries
Houston, Texas

Technology Systems Corporation
Palm City, Florida

Teledyne Impulse
San Diego, California

Tension Member Technology
Huntington Beach, California

VideoRay, LLC
Phoenixville, Pennsylvania

W2S2, LLC
Houston, Texas

WET Labs, Inc.
Philomath, Oregon

WFS Technologies Ltd
Livingston, United Kingdom

Xodus Group
Houston, Texas

INSTITUTIONAL MEMBERS

Canadian Coast Guard
St. John's, Newfoundland and Labrador, Canada

City of St. John's
Newfoundland and Labrador, Canada

CLS America, Inc.
Largo, Maryland

Consortium for Ocean Leadership
Washington, DC

Department of Innovation, Trade and Rural
Development
St. John's, Newfoundland and Labrador, Canada

Fundação Homem do Mar
Rio de Janeiro, Brazil

Harbor Branch Oceanographic Institute
Fort Pierce, Florida

International Seabed Authority
Kingston, Jamaica

Jeju Sea Grant Center
Jeju-City, South Korea

Marine Institute
Newfoundland and Labrador, Canada

Monterey Bay Aquarium Research Institute
Moss Landing, California

National Research Council Institute for Ocean Technology
St. John's, Newfoundland and Labrador, Canada

NAVFAC Atlantic
Norfolk, VA

NewcastleGateshead Initiative
Gateshead, United Kingdom

NOAA/PMEL
Seattle, Washington

Noblis
Falls Church, Virginia

OceanGate, LLC
Miami, Florida

Oregon State University College of Oceanic and
Atmospheric Sciences
Corvallis, Oregon

Richard Stockton College of New Jersey
Port Republic, New Jersey

Schmidt Ocean Institute
Lake Forest Park, Washington

U.S. Naval Academy Library
Annapolis, Maryland

University of Massachusetts–Dartmouth
New Bedford, Massachusetts

marine technology SOCIETY
1100 H Street NW, Suite LL-100
Washington, DC 20005

Postage for periodicals
is paid at Washington, DC
and additional mailing offices.

